Distribution Agreement

In presenting this thesis or dissertation as a partial fulfillment of the requirements for an advanced degree from Emory University, I hereby grant to Emory University and its agents the non-exclusive license to archive, make accessible, and display my thesis or dissertation in whole or in part in all forms of media, now or hereafter known, including display on the world wide web. I understand that I may select some access restrictions as part of the online submission of this thesis or dissertation. I retain all ownership rights to the copyright of the thesis or dissertation. I also retain the right to use in future works (such as articles or books) all or part of this thesis or dissertation.

Student's signature

_____ _____

Karen A. (Newell) Litwa Date

Hermansky-Pudlak Complexes, AP-3 and BLOC-1, Regulate the Molecular Architecture of the Synapse

By,

Karen A. (Newell) Litwa
Doctor of Philosophy

Graduate Division of Biological and Biomedical Sciences
Biochemistry, Cell, and Developmental Biology

_____

Victor Faundez, M.D., Ph.D.
Advisor

_____

Gary Bassell, Ph.D.
Committee Member

_____

Ping Chen, Ph.D.
Committee Member

_____

Andrew P. Kowalczyk, Ph.D.
Committee Member

_____

Steven L'Hernault, Ph.D.
Committee Member

_____

Winfield S. Sale, Ph.D.
Committee Member

Accepted:

_____

Lisa A. Tedesco, Ph.D.
Dean of the Graduate School

_____

Date

Hermansky-Pudlak Complexes, AP-3 and BLOC-1, Regulate the Molecular Architecture of the Synapse

Karen A. (Newell) Litwa

B.S., Grove City College, 2004

Advisor: Victor "Y" Faundez, M.D., Ph.D.

An Abstract of

A dissertation submitted to the Faculty of the Graduate School of Emory University in partial fulfillment of the requirements for the degree of Doctor of Philosophy

Graduate Division of Biological and Biomedical Sciences
Biochemistry, Cell, and Developmental Biology

2009

Abstract

Hermansky-Pudlak Complexes, AP-3 and BLOC-1, Regulate
the Molecular Architecture of the Synapse
By Karen A. (Newell) Litwa

Mechanisms that underlie pre-synaptic membrane composition are essential for proper neurotransmission. My thesis research examined how two endosomal sorting adaptors, AP-3 and BLOC-1, regulate synaptic vesicle biogenesis. Neurons express two AP-3 isoforms with distinct vesicle traffic functions: ubiquitous AP-3 in conjunction with BLOC-1 sorts membrane proteins (cargoes) to lysosomes, while neuronal AP-3 creates synaptic vesicles. However, recent proteomes of synaptic vesicles revealed the presence of AP-3-sorted lysosomal cargoes, leading me to hypothesize that these divergent endosomal sorting pathways coordinately regulate synaptic vesicle composition by sorting similar membrane proteins from a shared early endosome compartment. In support of this hypothesis, my dissertation demonstrates by both biochemical and immunomicroscopy techniques that synaptic vesicle and AP-3-sorted lysosomal cargoes co-localize in early endosomes and synaptic vesicles. Furthermore, AP-3 isoform-specific pathways competitively regulate synaptic vesicle content, with neuronal AP-3 deficiency decreasing and either ubiquitous AP-3 or BLOC-1 deficiencies increasing the content of similar cargoes in synaptic vesicle fractions. AP-3-dependent synaptic vesicle biogenesis mechanisms also contribute to brain region-specific differences in synaptic architecture through differential regulation of membrane protein content and synaptic vesicle size in pre-synaptic compartments of the striatum and dentate gyrus of the hippocampus. BLOC-1 selectively modifies AP-3-dependent traffic in the dentate gyrus, but not the striatum. Overall, my work leads me to propose the concept that rather than a unitary synaptic vesicle being produced by all neurons, as is currently believed, neurons assemble diverse pre-synaptic vesicles using lysosomal vesicle biogenesis mechanisms that contribute to pre-synaptic organelle biogenesis.

Hermansky-Pudlak Complexes, AP-3 and BLOC-1, Regulate the Molecular Architecture of the Synapse

Karen A. (Newell) Litwa

B.S., Grove City College, 2004

Advisor: Victor "Y" Faundez, M.D., Ph.D.

A dissertation submitted to the Faculty of the Graduate School of Emory University in partial fulfillment of the requirements for the degree of Doctor of Philosophy

Graduate Division of Biological and Biomedical Sciences
Biochemistry, Cell, and Developmental Biology

2009

ACKNOWLEDGEMENTS

I am particularly blessed to have so many people to thank for their contributions to my dissertation as well as my personal development as a scientist. The pre-eminent position on this list of acknowledgements belongs to my advisor, Dr. Victor "Yoda" Faundez. Since the first day that I entered the lab, his treatment of me as a colleague empowered me with enthusiasm for my scientific pursuits. Victor – I have particularly enjoyed (and will sorely miss) our many discussions about philosophy, religion, politics, and of course, science. I admire you both as a scientist and a human being. I am daily inspired by your love of knowledge, your encyclopedic memory, your humanitarian spirit, your generosity, and your positive outlook on life. I am truly indebted to you, and I know that any of my future scientific successes will be the result of having been your apprentice ("jedi") for these past five years.

I would also like to thank the rest of the Faundez lab for the joy it has been to work with each of them. Erica Werner and Gloria Salazar are my role models for women in science. I am awed by their commitment to both science and family. To the graduate students who came before me, Melanie Styers and Branch Craige - I am grateful for the high standards that you set for me. I wish to particularly thank Branch Craige for his tremendous patience as a teacher. All of the microscopy presented in this work stems from training on the Kalman microscope with Branch. Stephanie Zlatic, while two years behind me in graduate school, has also taught me so much, particularly about discipline in science. I am honored to have worked with you, and I will miss our time listening

to and discussing NPR in the lab, particularly during the presidential election year. And while my time with you was brief, I am also thankful to Jennifer Larimore, LeeAnne McGaha, Pearl Ryder, and Karine Tornieri, for their cheerfulness and their scientific curiosity.

For the last two years, the Smith lab has been generous enough to welcome me as part of their lab family. Their commitment to training me in immunohistochemistry and electron microscopy techniques is reflected in Chapter 3 of my dissertation. I am truly grateful to Dr. Yoland Smith for inviting me to take part in laboratory meetings and for his commitment to my training as a neuroscientist. Furthermore, Susan Jenkins and Jeff Pare were always willing to answer my numerous questions. Along with Susan and Jeff, Jim Bogenpohl, Darlene Mitrano, and Rosa Villalba all spent time training me in various techniques.

Each member of my thesis committee, Drs. Gary Bassell, Ping Chen, Andrew Kowalczyk, Steve L'Hernault, and Win Sale, contributed their own unique insights to this project. This project and my own scientific thinking were transformed by your challenging questions. I am especially grateful to Win for encouraging me to take the Woods Hole course in Physiology.

Finally, my family has provided the prerequisite support throughout my lifetime for me to achieve my academic goals. My dad and mom, David and Debbie Newell, instilled a love of nature in me from a very young age. Whether treasure-hunting for acorns with my mom or watching fish in the aquarium with my dad, my parents introduced me to the wonderful detail of biology. My

husband, Matthew David Litwa, is the true scholar of the family. I am daily inspired and challenged by your example to achieve more in my own studies. Although I may rarely acknowledge it, I am extremely fortunate to have a husband who sacrificed his own graduate studies so that we could be together. I love you and I am delighted that you now have the opportunity to begin your own PhD studies. And to all of my family (Newell and Litwa), thank you for your enduring love!

Table of Contents

Page Number

CHAPTER I

GENERAL INTRODUCTION*

*Significant portions of this introduction are reproduced from Newell-Litwa et al. JCS, 2007 with permission from The Company of Cell Biologists.

Summary

Vesicles selectively exchange lipids, membrane proteins and luminal content between organelles along the exocytic and endocytic routes (Figure 1). Membrane protein repertoire is critical for vesicle function, like the one in synaptic vesicles where membrane transporters determine the type of neurotransmitter stored in the vesicle lumen. Vesicles define their composition at the time of their biogenesis, a process controlled by cytosolic coat proteins. Among them, the heterotetrameric adaptor protein complex 3 (AP-3) participates in the generation of a diverse group of secretory organelles/lysosome-related organelles. This introduction will focus on recent developments in the mechanisms that regulate AP-3 and the phenotypic analysis of organisms carrying genetic deficiencies of the AP-3 pathway. These developments serve as a foundation for my own dissertation studies. These previous findings point toward a more complex picture of how AP-3 functions in multiple tissues, including neuronal tissue, and reveal potential links between endocytic sorting mechanisms and synaptic architecture. My own dissertation addresses questions that these studies raise about the role of AP-3-mediated endosomal sorting in neurons.

Introduction to Vesicle-Mediated Transport

Membrane-enclosed organelles possess distinctive protein compositions dynamically maintained by vesicle formation and vesicle fusion mechanisms (Bonifacino and Glick, 2004). These vesicles are generated by cytosolic coat proteins that selectively concentrate specific membrane proteins into departing vesicles (Bonifacino and Glick, 2004). Heterotetrameric coat protein complexes

known as adaptor protein complexes (AP-1, AP-2, AP-3 and AP-4) act as scaffolds bringing together membrane lipids, sorting signals present in the cytosolic domains of membrane proteins, components of the vesicle fusion machinery and additional components of the vesicle formation apparatus (Boehm and Bonifacino, 2001; Robinson, 2004; Sorkin, 2004). The function of these adaptors is linked to the donor organelle in which they perform their sorting function (Figure 1). AP-1 generates vesicles from the trans-Golgi network that transport cargoes bound for late-endosome and lysosome compartments, whereas AP-1 adaptors found in endosomes generate vesicles routed to the cell surface or back to the Golgi complex (Robinson, 2004; Ohno, 2006b). AP-2 resides exclusively in the plasma membrane, where it generates endocytic vesicles (Robinson, 2004; Ohno, 2006b). AP-3 is present in endosomes and delivers proteins to late endosomes and lysosomes (Robinson, 2004; Ohno, 2006b). In neurons, AP-3 generates synaptic vesicles or vesicles carrying synaptic vesicle membrane proteins (Faundez *et al.*, 1998). Finally, AP-4 is localized to the trans-Golgi network, where it produces vesicles that transport specific lysosomal proteins (Robinson, 2004; Ohno, 2006a). In each case, at the donor compartments, adaptors cycle between cytosolic and membrane-bound pools, and this process is controlled by inositol phospholipids (Balla and Balla, 2006; Di Paolo and De Camilli, 2006) and ARF GTPases (Robinson, 2004) (Figure 2).

My dissertation concentrates on the function, regulation and interactions of the vertebrate adaptor AP-3 from the perspective of neuronal membrane protein traffic. Recent studies offer the potential to further expand our understanding of effects associated with loss, dysfunction or subversion of the

AP-3 machinery – for example, in the generation of HIV particles (Dong *et al.*, 2005), and possibly in the pathogenesis of schizophrenia (Owen *et al.*, 2005; Norton *et al.*, 2006) and other psychiatric disorders (Breen *et al.*, 2006).

Genetics of the AP-3 pathway in vertebrates

Much of our knowledge about AP-3 function in metazoans comes from the phenotypic analysis of mouse and human AP-3 mutations as well as mutations in gene products that interact with this adaptor complex (Li, Rusiniak et al. 2004; Di Pietro and Dell'Angelica 2005). Deficiencies in at least 14 loci, including AP-3 gene defects, trigger a syndrome characterized by systemic and in some cases neurological phenotypes. The systemic defects include occulo-cutaneous pigment dilution, platelet dysfunction, pulmonary fibrosis (Li, Rusiniak et al. 2004; Di Pietro and Dell'Angelica 2005), recurrent infections due to defects of innate immunity (Fontana, Parolini et al. 2006; Jung, Bohn et al. 2006), cyclic neutropenia (Benson *et al.*, 2004) and cytotoxic T lymphocyte (CTL) defects (Clark, Stinchcombe et al. 2003). These systemic phenotypes define in humans the Hermansky-Pudlak Syndrome (HPS1 to HPS8, OMIM 203300), a disease generated by defects in at least eight genetic loci (Li, Rusiniak et al. 2004; Di Pietro and Dell'Angelica 2005). HPS disorder type 2 (HPS2) specifically results from altered AP-3 function in humans (Dell'Angelica, Shotelersuk et al. 1999; Sugita, Cao et al. 2002; Clark, Stinchcombe et al. 2003; Fontana, Parolini et al. 2006; Jung, Bohn et al. 2006). Epilepsy and hyperactivity characterize the neurological symptoms found in a group of these genetic deficiencies (Kantheti, Qiao et al. 1998; Kantheti, Diaz et al. 2003; Nakatsu, Okada et al. 2004; Seong,

Wainer et al. 2005) as well as arthrogryposis due to motor axon defects (Gissen, Johnson et al. 2004).

The majority of these 14 genes encode polypeptides that assemble into five protein complexes: AP-3 (Figure 3), BLOC-1 to BLOC-3 (Figure 4) (biogenesis of lysosome-related organelles complex), and HOPS (homotypic vacuolar protein sorting or VPS class C complex) (Di Pietro and Dell'Angelica, 2005). These complexes are present in endosomes, where they participate in membrane protein sorting and vesicle biogenesis (Peden *et al.*, 2004; Theos *et al.*, 2005; Di Pietro *et al.*, 2006; Setty *et al.*, 2008). Vesicles generated by the AP-3–BLOC machinery carry membrane proteins bound to a wide range of secretory organelles, such as lysosomes, lysosome-related organelles (e.g. melanosomes, platelet dense granules, azurophilic granules and surfactant granules) (Li, Rusiniak et al. 2004; Di Pietro and Dell'Angelica 2005; Wei 2006) and synaptic vesicles (Nakatsu, Okada et al. 2004; Salazar, Love et al. 2004; Seong, Wainer et al. 2005). This diversity of organelles regulated by AP-3–BLOC complexes explains the pleiotropic nature of the phenotypes already described.

Mutations affecting vertebrate AP-3 subunits

AP-3 consists of four subunits δ, β3, μ3 and σ3. β3, μ3 and σ3 each exist as two isoforms (A and B; Fig. 3A, B) (Boehm and Bonifacino 2001; Boehm and Bonifacino 2002; Robinson 2004). Two of these isoforms, β3B (Darnell, Furneaux et al. 1991; Newman, McKeever et al. 1995; Gurkan, Lapp et al. 2005) and μ3B (Pevsner, Volknandt et al. 1994; Gurkan, Lapp et al. 2005), are largely restricted to neuronal and neuroendocrine tissues, whereas both σ3A and σ3B are

ubiquitously expressed (Fig. 3A, B) (Dell'Angelica, Ohno et al. 1997; Gurkan, Lapp et al. 2005). β3B and μ3B are thought to assemble into neuronal isoform complexes containing δ and σ3A or σ3B subunits (Fig. 3B). By contrast, β3A, μ3A, δ, and σ3A or σ3B subunits are part of the ubiquitous AP-3 adaptor isoform present in all cells, including neurons (Fig. 3B). Murine deficiencies in four of these AP-3 subunits (δ, β3A, β3B and μ3B; Fig. 3A) (Kantheti, Qiao et al. 1998; Feng, Seymour et al. 1999; Yang, Li et al. 2000; Nakatsu, Okada et al. 2004; Seong, Wainer et al. 2005) recapitulate to different degrees the phenotypes that result from the most severe form of AP-3 deficiency, the *mocha* mutation (Lane and Deol 1974; Noebels and Sidman 1989; Kantheti, Qiao et al. 1998). Systemic phenotypes and neurological alterations characterize the *mocha* mouse mutant (Lane and Deol 1974; Rolfsen and Erway 1984; Noebels and Sidman 1989; Kantheti, Qiao et al. 1998; Miller, Burmeister et al. 1999; Kantheti, Diaz et al. 2003). *Mocha* mice lack the δ subunit of AP-3, a subunit common to all AP-3 complexes (Kantheti *et al.*, 1998). The consequence of the *mocha* defect is the degradation of all neuronal and ubiquitous AP-3 subunits (Kantheti, Qiao et al. 1998; Peden, Rudge et al. 2002). By contrast, β3A genetic deficiencies (*pearl* and *Ap3b1*$^{-/-}$ in mice; HPS2 in humans; Fig. 3A) elicit degradation of the ubiquitous AP-3 (Zhen, Jiang et al. 1999; Yang, Li et al. 2000; Peden, Rudge et al. 2002). β3A mutations lead to systemic phenotypes (Zhen, Jiang et al. 1999; Yang, Li et al. 2000).

Regulation of AP-3 function

The mechanisms controlling recruitment of AP-3 to membranes and AP-3-dependent membrane protein sorting include GTPases (Simpson, Bright et al. 1996; Dell'Angelica, Ohno et al. 1997; Faundez, Horng et al. 1997; Faundez, Horng et al. 1998; Ooi, Dell'Angelica et al. 1998), kinases (Faundez and Kelly 2000; Salazar, Craige et al. 2005; Craige, Salazar et al. 2008), intermediate filament proteins (Styers, Salazar et al. 2004; Styers, Kowalczyk et al. 2006), accessory proteins (Crump, Xiang et al. 2001), and clathrin (Dell'Angelica, Klumperman et al. 1998) (Fig. 2 and 5). Best understood is the regulated recruitment of AP-3 to membranes by Arf GTPases (Ooi *et al.*, 1998). These GTPases cycle between GTP- and GDP-bound forms, controlling recruitment and release of coat proteins from membranes. Brefeldin A interferes with this cycle, leading to accumulation of GDP-Arf1, and thus prevents the binding of coats such as AP-3 to membranes (Simpson, Bright et al. 1996; Dell'Angelica, Ohno et al. 1997; Drake, Zhu et al. 2000; Jackson and Casanova 2000; Zeghouf, Guibert et al. 2005). Similarly, Arf1 mutants locked in their GDP-bound form prevent the binding of AP-3 to organelles (Faundez, Horng et al. 1998; Ooi, Dell'Angelica et al. 1998). By contrast, an Arf1 mutant unable to hydrolyze GTP holds AP-3 on membranes (Faundez, Horng et al. 1998; Ooi, Dell'Angelica et al. 1998).

GTP-bound Arf1 directly interacts with the AP-3 complex (Austin, Boehm et al. 2002; Lefrancois, Janvier et al. 2004). The association involves the σ3 subunit or the δ-σ3 AP-3 subcomplex (Fig. 5) (Austin, Boehm et al. 2002; Lefrancois, Janvier et al. 2004). The crystal structure of the adaptor complexes AP-1 and AP-2 reveals that their σ subunits are buried in the tetramer (Collins,

McCoy et al. 2002; Heldwein, Macia et al. 2004). Thus, the σ3-Arf1 interaction suggests that, in AP-3, σ3 becomes exposed partially or transitorily to the cytosolic environment. Notably, the interaction is selective since Arf5 does not appear to interact with AP-3 (Austin, Boehm et al. 2002). Moreover, a GDP-locked Arf5 mutant does not affect recruitment of AP-3 to membranes (Ooi, Dell'Angelica et al. 1998). These results suggest that AP-3 directly discriminates between different Arf GTPases and/or that factors affecting Arf1 GTPase activity are selectively recognized by AP-3.

The intrinsic GTPase activity of Arf1 is very low and nucleotide hydrolysis only occurs in the presence of members of a diverse family of GTPase activating proteins (ArfGAPs) (Nie and Randazzo, 2006). AGAP1 is an ArfGAP that selectively affects Arf-dependent recruitment of AP-3 to membranes. AGAP1 contains four types of domain, among them Arf GAP and pleckstrin homology (PH) domains (Nie, Boehm et al. 2003). The latter can bind inositol phospholipids (Balla, 2005) and in AGAP1 it binds to the AP-3 δ-σ3 subcomplex (Nie, Boehm et al. 2003) (Fig. 5). The AGAP1 PH domain could thus functionally link inositol phospholipids with adaptor complexes. AGAP1 GAP activity is stimulated by phosphatidylinositol (4,5)-bisphosphate [PtdIns(4,5)*P*2] and phosphatidylinositol (3,4,5)-trisphosphate [PtdIns(3,4,5)*P*3] in vitro (Nie, Stanley et al. 2002). Thus, AGAP1 could regulate the levels of membrane-bound AP-3 by sensing membrane concentrations of PtdIns(4,5)*P*2 and/or PtdIns(3,4,5)*P*3. Key to understanding Arf1-AGAP1-mediated regulation of AP-3 recruitment is, therefore, the identification of the enzymes that generate inositol

phospholipid species and the mechanisms by which such enzymes reach and/or define domains of AP-3 vesicle formation.

One such potential enzyme, phosphatidylinositol 4-kinase type II alpha (PI4KIIα), phosphorylates phosphatidylinositol (PtdIns) to generate phosphatidylinositol (4)-phosphate, a precursor of PtdIns(4,5)*P*2 and PtdIns(3,4,5)*P*3 (Balla and Balla, 2006). PI4KIIα is present in endosomes (Balla, Tuymetova et al. 2002; Guo, Wenk et al. 2003; Salazar, Craige et al. 2005; Minogue, Waugh et al. 2006) and is a major component of AP-3-derived vesicles (Salazar *et al.*, 2005b). The kinase serves as an AP-3 cargo, but PI4KIIα is not limited to acting as a passive cargo (Craige, Salazar et al. 2008). Its expression affects the subcellular localization of AP-3 to endosomes: downregulation of the kinase leads to a redistribution of endosomal AP-3 to cytosol (Salazar, Craige et al. 2005; Craige, Salazar et al. 2008); conversely, overexpression of the kinase increases AP-3-dependent vesicle generation (Salazar *et al.*, 2005b).

How are PI4KIIa, Arf1, AGAP1, and AP-3 integrated to generate vesicles? GTP-Arf1-dependent recruitment of AP-3 to membranes should be one of the primary events. We envisage that, once on membranes, AP-3 binds PI4KIIα and concentrates this enzyme into endosomal domains able to generate vesicles. In these domains, inositol phospholipids generated by PI4KIIα should further recruit AP-3 and increase the activity of AGAP1. Accumulation of coat and cargo in a nascent vesicle depends on recruitment of an inactive AGAP1 by AP-3. Thus, only when PI4KIIα lipid products reach a particular threshold level, would AGAP1 be activated and coat recruitment finish. This model assumes that binding AP-3 to AGAP1 decreases its Arf1GAP activity and holds it in an inactive state

until enough lipid species have been produced to activate its GAP activity. This is the case for the closely related ArfGAP AGAP2, whose GAP activity towards Arf1 is inhibited by the presence of the adaptor complex AP-1, to which AGAP2 selectively binds (Nie, Fei et al. 2005).

PI4KIIα and AGAP1 represent extrinsic factors capable of regulating recruitment of AP-3 to membranes. However, AP-3 has an intrinsic mechanism that can regulate its recruitment to membranes. The AP-3 δ ear domain (see Fig. 3C) binds to the σ3 subunit of AP-3 (Fig. 5), preventing the binding of GTPArf1 to AP-3 and recruitment of the adaptor to membranes (Lefrancois, Janvier et al. 2004). An intramolecular regulatory mechanism could thus couple binding of AP-3 to membranes with Arf1 levels and nucleotide status. Feedback mechanisms involving the enzymatic activities of Arf1 and PI4KIIα may further control the type of cargo and the coat content in nascent AP-3 vesicles; these remain to be explored.

The elusive role of clathrin in AP-3 vesiculation

Arf1 has an indisputable function in the early stages of formation of AP-3 vesicles. However, clathrin's role at later stages remains unclear. Clathrin provides a scaffold to bind adaptors, and accessory factors involved in cargo recognition, membrane curvature and uncoating (Kirchhausen 2000; Conner and Schmid 2003; Traub 2005). Formation of AP-1 and AP-2 vesicles requires clathrin both in vivo and in vitro (Kirchhausen 2000; Conner and Schmid 2003; Miwako, Schroter et al. 2003; Pagano, Crottet et al. 2004; Traub 2005;

Hinrichsen, Meyerholz et al. 2006). By contrast, in vivo and in vitro data on the role of clathrin in AP-3 vesicle formation are conflicting.

In vitro AP-3-dependent sorting proceeds in the absence of clathrin (Faundez, Horng et al. 1997; Faundez, Horng et al. 1998) and in the presence of clathrin-perturbing reagents (Shi, Faundez et al. 1998), which indicates that clathrin may not be necessary for formation of AP-3 vesicles. Indeed, AP-3 is absent from purified clathrin-coated vesicles from brain (Simpson, Bright et al. 1996; Dell'Angelica, Ooi et al. 1997; Blondeau, Ritter et al. 2004), and vesicles partially coated with AP-3 lack detectable levels of clathrin (Salazar *et al.*, 2005b). Collectively, this evidence suggests that clathrin is dispensable for AP-3 vesicle formation. However, it could also indicate that clathrin plays cargo-selective roles in AP-3-dependent sorting rather than vesicle formation. In addition, the absence of AP-3 in clathrin-coated vesicles may just reflect labile clathrin–AP-3 interactions that do not withstand the purification procedure or the relative levels of clathrin–AP-3 coated vesicles in different cell types. In fact, immunoelectron microscopy identifies clathrin-decorated, AP-3 budding profiles on endosomes (Dell'Angelica, Klumperman et al. 1998; Peden, Oorschot et al. 2004; Theos, Tenza et al. 2005), and AP-3 is present in clathrin-coated vesicles isolated from HeLa (Borner *et al.*, 2006) and PC12 cells (Salazar *et al.*, 2009). Furthermore, clathrin binds to AP-3 in cell-free conditions through the β3 subunit of AP-3 (Dell'Angelica, Klumperman et al. 1998) (Fig. 5). The crystal structure of the β3 clathrin-binding motif bound to the N-terminal domain of clathrin shows that the binding mechanism is similar to that of other clathrin-binding proteins (ter Haar, Harrison et al. 2000) and uses a conserved ‘clathrin-

box' motif (ter Haar, Harrison et al. 2000; Dell'Angelica 2001). However, β3 mutants lacking the clathrin-box motif still rescue a characteristic missorting phenotype in β3-deficient fibroblasts (Peden, Rudge et al. 2002), which challenges the idea that clathrin has a role in AP-3 function.

A caveat of such studies is that they only assess the effects on one cargo protein (Shi, Faundez et al. 1998; Peden, Rudge et al. 2002). Lack of the clathrin box could lead, for example, to selective sorting alterations rather than defective vesicle formation itself. Alternatively, the clathrin box in β3 subunits may recruit clathrin in vitro but not be necessary for clathrin recruitment in vivo. Indeed, only half of all endosomal AP-3 budding profiles are decorated with clathrin in immunoelectron microscopy experiments (Dell'Angelica, Klumperman et al. 1998; Peden, Oorschot et al. 2004; Theos, Tenza et al. 2005). Thus, the clathrin box may not be functional in some AP-3 complexes, or an AP-3-interacting protein may selectively recruit clathrin to certain AP-3 vesicle buds. Irrespective of the mechanism, this suggests that AP-3 complexes generate vesicles that have different compositions.

Not all AP-3s are created equal: neuronal versus ubiquitous adaptors

AP-3 complexes assembled by neuronal AP-3 adaptin isoforms could generate vesicles with different cargo composition. This idea is strengthened by the observation that μ3A and μ3B subunits present in ubiquitous and neuronal AP-3 complexes recognize different tyrosine-based sorting motifs (Ohno, Aguilar et al. 1998). Because of their restricted expression in brain tissue, β3B and μ3B subunits are assumed to assemble exclusively into neuronal AP-3 complexes,

whereas β3A and μ3A assemble into a ubiquitously expressed complex (Fig. 3B). This notion is supported by the observation that β3B protein levels are reduced in μ3B-deficient mouse brain (Nakatsu *et al.*, 2004). However, analysis of the neuronal phenotypes observed in β3B-deficient (*Ap3b2*$^{-/-}$) and μ3B-deficient (*Ap3m2*$^{-/-}$) mice suggests a more complex picture. If neuronal AP-3 subunit isoforms were to assemble exclusively into neuronal complexes, then targeted disruption of either the *Ap3b2* or the *Ap3m2* locus in the same background should lead to identical brain phenotypes. In fact, although both mouse mutants display juvenile spontaneous epilepsy (Nakatsu, Okada et al. 2004; Seong, Wainer et al. 2005), they have different zinc transporter (ZnT3) phenotypes.

ZnT3 is a metal transporter exclusively targeted to synaptic vesicles and is necessary for luminal storage of ionic zinc in synaptic vesicles (Palmiter, Cole et al. 1996; Cole, Wenzel et al. 1999; Salazar, Love et al. 2004). Synaptic vesicle ZnT3 levels are normal in μ3B-deficient mice but reduced in β3B-deficient mice (Nakatsu, Okada et al. 2004; Seong, Wainer et al. 2005). This suggests partially divergent functions of AP-3 complexes assembled with β3B or μ3B. Differences in the phenotypes of β3B-deficient and μ3B-deficient mice may be due to partially overlapping expression of these gene products in different brain regions – as suggested by EST expression profiles in UNIGENE and the membrome database (Pevsner, Volknandt et al. 1994; Gurkan, Lapp et al. 2005) (http://symatlas.gnf.org/SymAtlas/). Alternatively, the remaining β3B in *Ap3m2*$^{-/-}$ mice could form δ-σ3-β3B-μ3A tetramers, which could account for their lack of a zinc transporter phenotype.

Heterologous expression of neuronal AP-3 adaptin isoforms in non-neuronal cells indicates that neuronal subunits can assemble into complexes containing ubiquitous AP-3 isoforms (Peden, Rudge et al. 2002). β3A and the neuronal β3B isoform effectively rescue the phenotypes observed in β3A-deficient fibroblasts, which demonstrates that the endogenous μ3A isoforms present in these non-neuronal cells forms complexes with both β3 subunits (Peden, Rudge et al. 2002). Therefore, the spectrum of AP-3 complexes assembled in neuronal tissue could even be more diverse than presumed. These considerations are important in the interpretation of the phenotypes caused by loss of AP-3 in the brain. Because neuronal phenotypes, such as zinc storage, appear to be more penetrant in *Ap3b2*$^{-/-}$ than *Ap3m2*$^{-/-}$ mice, the following dissertation research will use *Ap3b2*$^{-/-}$ mice to investigate the role of neuronal AP-3 in synaptic vesicle composition. Furthermore, both *Ap3b2*$^{-/-}$ and *Ap3b1*$^{-/-}$ mice are genetic knockouts within a C57 wild type background, allowing me to compare the relative contributions of these isoforms to neuronal phenotypes.

The function(s) of AP-3 complexes in neuronal cells

The hypothesis that AP-3 adaptors are involved in the sorting of synaptic membrane proteins emerged after the identification of AP-3 μ transcripts in the electric lobe of the ray *Discopyge ommata*, a tissue rich in synaptic terminals (Pevsner *et al.*, 1994). The staining of synaptic terminals by human anti-β3B autoimmune antibodies supported this idea (Newman, McKeever et al. 1995). However, it was not until the development of cell-free vesicle biogenesis assays that definitive evidence implicated AP-3 in targeting of synaptic vesicle

membrane proteins (Faundez, Horng et al. 1998; Shi, Faundez et al. 1998; Blumstein, Faundez et al. 2001). In these assays targeting of proteins requires either AP-3-containing brain cytosol or purified brain AP-3 and ARF1 (Faundez, Horng et al. 1998; Shi, Faundez et al. 1998; Blumstein, Faundez et al. 2001).

The sorting of synaptic vesicle membrane proteins is controlled by AP-3 in vivo (Fig. 6), as illustrated by the cellular phenotypes of the *Ap3d*$^{-/-}$ (*mocha*), *Ap3b2*$^{-/-}$, and *Ap3m2*$^{-/-}$ mice. The *mocha* strain is characterized by epilepsy and hyperactivity (Lane and Deol 1974; Rolfsen and Erway 1984; Noebels and Sidman 1989; Kantheti, Qiao et al. 1998; Miller, Burmeister et al. 1999; Kantheti, Diaz et al. 2003). Their nerve terminals lack ionic zinc owing to defective sorting of ZnT3 (Kantheti, Qiao et al. 1998; Kantheti, Diaz et al. 2003; Salazar, Love et al. 2004; Stoltenberg, Nejsum et al. 2004), which binds directly and selectively to AP-3 (Salazar, Love et al. 2004). The defective targeting of ZnT3 in *mocha* and *Ap3b2*$^{-/-}$ (Seong *et al.*, 2005) mouse models as well as the defective GABAergic neurotransmission in *Ap3m2*$^{-/-}$ mice (Nakatsu *et al.*, 2004) provide conclusive evidence that synaptic vesicle targeting defects are part of the AP-3-deficient neuronal phenotype.

Several other synaptic vesicle membrane proteins are mistargeted in AP-3-deficient brains. These include synaptic vesicle chloride channel 3 (ClC-3) (Salazar, Love et al. 2004), vesicular glutamate transporter 1 (VGLUT1) (Salazar, Craige et al. 2005), PI4KIIα (Salazar *et al.*, 2005b), the vesicular GABA transporter (VGAT) (Nakatsu *et al.*, 2004), and the synaptobrevin-1-like SNARE VAMP7-TI (also known as Sybl1, VAMP7 or TI-VAMP) (Salazar, Craige et al. 2006; Scheuber, Rudge et al. 2006). Defective targeting of VAMP7 in *mocha*

brain affects spontaneous and evoked release at hippocampal mossy fiber synapses (Scheuber, Rudge et al. 2006). Similarly to ZnT3, several of these membrane proteins are sorted by AP-3 into endosome-derived microvesicles when expressed in PC12 cells. An important consideration is that these synaptic vesicle protein targeting defects are selective as evidenced by the normal levels of ubiquitous synaptic vesicle membrane proteins such as synaptophysin, the116-kDa subunit of the vacuolar ATPase, and SV2 in vesicles (Salazar, Love et al. 2004; Salazar, Love et al. 2004; Salazar, Craige et al. 2005; Salazar, Craige et al. 2005; Seong, Wainer et al. 2005; Salazar, Craige et al. 2006).

Despite the defective targeting of selected synaptic vesicle proteins, electrophysiological analysis of *mocha* brain hippocampus reveals that short-term synaptic plasticity and synaptic vesicle recycling remain unaffected (Vogt *et al.*, 2000), although this involves only low-frequency stimulation. These observations are consistent with the preponderant role that AP-2 plays in synaptic vesicle biogenesis at the synapse (Fig. 6B) (Murthy and De Camilli, 2003). However, recent electrophysiological and neuronal imaging evidence indicate that AP-3 contributes to synaptic vesicle (Voglmaier, Kam et al. 2006) and large dense core vesicle biogenesis (Grabner, Price et al. 2006). In contrast to the AP-2 pathway, AP-3-dependent synaptic vesicle sorting mechanisms contribute to synaptic vesicle recycling only under high-frequency stimulation (Voglmaier, Kam et al. 2006). High frequency stimulation of motoneurons induces the formation of endosomes in pre-synaptic terminals (Heuser and Reese, 1973), a compartment from where AP-3 forms vesicles in other neuronal and non-neuronal cell types (Fig.6B).

The neuronal phenotypes of AP-3-deficient animals already discussed point to a synaptic defect (Fig. 6). However, it is important to consider that the synaptic defects observed in *mocha* neurons may also reflect defective trafficking processes outside pre-synaptic terminals. Three observations are consistent with the hypothesis that AP-3 performs extrasynaptic functions in neurons. First, AP-3 exists in the cell body as well as the processes of neurons (Seong *et al.*, 2005). Second, immature amphibian motor neurons display a constitutive axonal vesicle recycling mechanism sensitive to brefeldin A (Zakharenko, Chang et al. 1999), much like the biogenesis of AP-3-bearing vesicles from endosomes in PC12 cells (Faundez, Horng et al. 1997). This brefeldin-A-sensitive recycling mechanism, although present in axons, is absent at the site of contact between the motor neuron and myoblasts in cultured preparations (Zakharenko, Chang et al. 1999). Moreover, *mocha* hippocampal neurons, despite their dramatic reduction in PI4KIIα levels in nerve terminals, have normal or increased levels of this kinase in cell bodies (Salazar *et al.*, 2005b). Similar observations have been made of BLOC-1 complex subunits (see below) (Salazar *et al.*, 2006) and VAMP7 (Scheuber, Rudge et al. 2006). These results suggest that vesicles containing synaptic vesicle proteins may be generated by AP-3 from endosomes either in the axon or in the cell body (Fig. 6A), before targeting to pre-synaptic terminals. The idea is explored in Chapter 3 of my dissertation, where I describe the distribution of AP-3 among pre-terminal and terminal axons from perfusion-fixed brain tissue. My findings are consistent with both synaptic and extrasynaptic roles for AP-3.

Neuronal functions for the 'non-neuronal' AP-3 complexes

Because of the absence of all AP-3 isoforms in *mocha* mutants, the contribution of neuronal and ubiquitous AP-3 isoforms to the neuronal phenotypes observed cannot be discerned. In a simple model, AP-3 isoforms perform different sorting functions: ubiquitous AP-3 regulates the biogenesis of neuronal lysosomes whereas neuronal AP-3 exclusively traffics synaptic vesicle proteins. This hypothesis was founded on the observation that mice selectively lacking neuronal AP-3 (*Ap3b2*$^{-/-}$ or *Ap3m2*$^{-/-}$) (Nakatsu, Okada et al. 2004; Seong, Wainer et al. 2005) exhibit an epileptic phenotype but mice lacking the ubiquitous AP-3 isoform (*Ap3b1*$^{-/-}$ or *pearl*) do not show this defect (Feng, Seymour et al. 1999; Yang, Li et al. 2000). However, closer inspection of the Ap3b1$^{-/-}$ brains reveals a selective increase in the content of synaptic vesicle AP-3 cargoes (ZnT3, and ClC-3) in synaptic vesicle fractions (Seong *et al.*, 2005). These changes are paralleled by an increase in histochemically reactive zinc in *Ap3b1*$^{-/-}$ hippocampus and cortex (Seong *et al.*, 2005). To a certain extent, AP-3 complexes assembled with β3A or β3B may thus recognize similar cargoes. Moreover, these findings suggest that subtle neurological and behavioral phenotypes previously not appreciated may occur in β3A-deficient and BLOC-1-null mice. Answers to these questions will be presented in Chapters 2 and 3, where I describe alterations to synaptic composition and behavioral motor coordination in β3A-deficient and BLOC-1-null mice.

How can β3A- or β3B-containing complexes generate different phenotypes if both contribute to the recognition of overlapping synaptic vesicle proteins? This could be explained by differences in the spectrum of synaptic vesicle

proteins recognized by complexes carrying β3A or β3B, the subcellular localization of adaptor complexes carrying β3A and β3B, and/or the fate of the vesicles generated by these adaptor complexes. Vesicles generated by β3A-containing complexes could target synaptic vesicle membrane proteins to degradative compartments (Fig. 6A). This hypothesis is consistent with the increased content of synaptic vesicle AP-3 cargoes in *Ap3b1*$^{-/-}$ mice (Seong *et al.*, 2005) and predicts the existence of an AP-3-derived vesicle population bound for lysosomal compartments that contains both synaptic vesicle proteins and lysosomal AP-3 cargoes. Proteomic analysis of organelle fractions enriched in AP-3-derived microvesicles suggests that lysosomal and synaptic vesicle AP-3 cargoes coexist in these fractions (Salazar *et al.*, 2005b) as well as in purified brain synaptic vesicles (Takamori, Holt et al. 2006). The lysosomal proteins present in AP-3 microvesicles include LAMP1, vps33b, the R-(v)-SNARE VAMP7-TI, and four subunits of the octameric BLOC-1 complex (pallidin, dysbindin/sandy, snapin and muted). Importantly, these proteins either directly and/or genetically interact with AP-3 (Di Pietro and Dell'Angelica, 2005).

My dissertation will address whether AP-3 complexes assembled with either β3A or β3B converge in the sorting of cargo proteins, or whether they diverge in order to regulate two separate cargo populations. Convergence of these two AP-3 mechanisms would provide a regulatory mechanism for determining synaptic vesicle content by lysosomal vesicle traffic.

Interactions between AP-3 and other Hermansky-Pudlak gene products

BLOC-1 and AP-3 complexes are both thought to participate in the transport of membrane proteins destined for lysosomes and lysosomes-related organelles (Li, Rusiniak et al. 2004; Di Pietro and Dell'Angelica 2005). Genetic and cell biological evidence support two models of AP-3 and BLOC-1 function. In the first, AP-3 and BLOC-1 complexes act together and interact to sort components into the same vesicle transport mechanism (vesicle A in Fig.7). In a second non-exclusive mechanism, AP-3 and BLOC-1 act independently, at different locations in endosomes, sharing overlapping but distinct sets of cargo proteins and generating two different types of vesicle (vesicles A and B in Fig. 7). Both mechanisms are likely to exist in mammalian cells but operate to different extents depending on the cell type (Di Pietro *et al.*, 2006; Gautam *et al.*, 2006; Salazar *et al.*, 2006; Setty *et al.*, 2008).

The notion that AP-3 and BLOC-1 act together is supported by the observed similarity of the cellular phenotypes of BLOC-1-deficient and AP-3-deficient skin fibroblasts. These phenotypes include: missorting of lysosomal proteins to the cell surface (CD63 and LAMP1) (Di Pietro *et al.*, 2006; Salazar *et al.*, 2006; Salazar *et al.*, 2009), mistargeting of PI4KIIα, and reduced levels of the R-(v)-SNARE VAMP7-TI (Salazar *et al.*, 2006; Salazar *et al.*, 2009). Furthermore, cell biological studies reveal the presence of both complexes on the same AP-3 vesicle (Salazar *et al.*, 2006) and interactions between AP-3 and BLOC-1 can be demonstrated by immunoprecipitation of an AP-3–BLOC-1 supra-

complex either from isolated membranes (Di Pietro, Falcon-Perez et al. 2006) or whole cells (Salazar *et al.*, 2009) (Fig. 5).

The precise mechanism(s) by which the BLOC-1–AP-3 supra-complex regulates sorting into the same vesicle remains unknown (Fig. 7). BLOC-1 might play a role in recruitment of AP-3 to membranes (Di Pietro *et al.*, 2006); however, this is unlikely to be at a rate-limiting step because the steady-state levels of membrane-bound AP-3 remain unaffected in BLOC-1-deficient cells (Salazar *et al.*, 2006; Setty *et al.*, 2007). Alternatively, BLOC-1 could recognize specific cargoes, such as SNAREs (Fig. 7A). Two subunits of the BLOC-1 complex, pallidin and snapin, can interact with the endocytic SNAREs syntaxin 13 (Huang *et al.*, 1999; Moriyama and Bonifacino, 2002) and SNAP23-25 (Ilardi *et al.*, 1999; Ruder *et al.*, 2005; Tian *et al.*, 2005), respectively (Fig. 8). Furthermore, downregulation of another BLOC-1 subunit, dysbindin, decreases the levels of a subset of synaptic vesicle proteins, including the SNARE, SNAP25 (Numakawa *et al.*, 2004). Consistent with these observations is the observation that the levels of the SNARE VAMP7-TI, an AP-3-interacting protein (Alberts *et al.*, 2003; Martinez-Arca *et al.*, 2003), are selectively reduced in AP-3-null and BLOC1$^{-/-}$ cells (Salazar *et al.*, 2006).

It is likely, however, that BLOC-1 also functions in sorting independently of AP-3 (Fig. 7B). For example, BLOC-1, but not AP-3, deficiencies lead to reduced colocalization of the VAMP-7-binding cognate SNAREs syntaxin 7 and syntaxin 8 (Salazar *et al.*, 2006), which allow VAMP-7-containing vesicles to fuse with late endosomes/lysosomes (Mullock *et al.*, 2000; Ward *et al.*, 2000; Bogdanovic *et al.*, 2002; Pryor *et al.*, 2004). The hypothesis that AP-3 and

BLOC-1 act independently at different subcellular locations yet recognizing overlapping but distinct sets of cargo proteins is strongly supported by the observation that AP-3-null and BLOC-1-null double-knockout mice have phenotypes more pronounced than those observed in single-complex-deficient mice (Gautam *et al.*, 2006).

In spite of these recent research advancements that demonstrate a molecular interaction between AP-3 and BLOC-1 and similar sorting phenotypes, my dissertation provides the first evidence of their coordinated regulation of synaptic composition. In Chapter 2, subcellular fractionation of *Ap3b1*$^{-/-}$ and BLOC-1$^{-/-}$ brains demonstrates that these two complexes regulate the synaptic vesicle levels of similar cargo proteins. In Chapter 3, I demonstrate that BLOC-1 controls the subcellular distribution of AP-3 within the dentate gyrus of the hippocampus. This BLOC-1-mediated redistribution of AP-3 affects the molecular composition of these synaptic terminals similar to the loss of AP-3.

The BLOC-1–AP-3 über-complex: a possible connection to schizophrenia

Despite similar functions of AP-3 and BLOC-1 in nonneuronal tissue, an important question is whether BLOC-1 and its interaction with AP-3 play a role in synaptic vesicle protein trafficking. Three lines of evidence implicate BLOC-1 in synaptic mechanisms. First, BLOC-1, like AP-3 complexes, is present in neuronal microvesicles containing synaptic vesicle markers as well as in hippocampal mossy fiber nerve terminals (Salazar *et al.*, 2006; Talbot *et al.*, 2006). Second, targeted disruption of snapin, a BLOC-1 subunit, leads to defective secretion of

neurotransmitters in mice (Tian *et al.*, 2005) (Fig. 8). Finally, human genetic polymorphisms in the genes encoding the BLOC-1 subunits dysbindin, more commonly known in humans as dystrobrevin-binding protein 1 (DTNBP1) (Benson *et al.*, 2004; Funke *et al.*, 2004; Bray *et al.*, 2005; Norton *et al.*, 2006) and muted (Straub *et al.*, 2005) may be associated with schizophrenia. However, the single patient deficient in dysbindin showed Hermansky-Pudlak syndrome without any reported mental illness (Li *et al.*, 2003). However, the *sandy* mouse lacking this protein has been recently reported to exhibit schizophrenia-related behaviors, including social withdrawal and cognitive deficits (Feng *et al.*, 2008).

Defective pre-synaptic vesicle fusion has been hypothesized to be a pathogenic mechanism in schizophrenia (Mirnics *et al.*, 2000; Honer and Young, 2004; Camargo *et al.*, 2007). Schizophrenic brain possesses reduced levels of mRNA and/or proteins involved in synaptic vesicle fusion, such as NSF, VAMP2 and SNAP-25 (Mukaetova-Ladinska *et al.*, 2002; Halim *et al.*, 2003; Knable *et al.*, 2004). In common with schizophrenia, AP-3 and BLOC-1 have been linked with the fusion machinery involved in synaptic vesicle secretion (Fig. 5 and 8). Indeed, loss of AP-3 in the *mocha* mice affects spontaneous and evoked release at hippocampal mossy fiber synapses (Scheuber *et al.*, 2006). Furthermore, recruitment of AP-3 to neuroendocrine microvesicles is sensitive to tetanus neurotoxin (Salem *et al.*, 1998). This agent selectively cleaves VAMP2 on synaptic vesicles and effectively halts synaptic vesicle fusion (Lalli *et al.*, 2003). Furthermore, the BLOC-1 subunit snapin binds to SNAP-25, a Q-(t)-SNARE that forms a complex with VAMP2 (Tian *et al.*, 2005) or VAMP7-TI (Alberts *et al.*, 2003; Martinez-Arca *et al.*, 2003) (Fig. 8).

A role of AP-3 and BLOC-1 complexes in proper targeting of the synaptic vesicle fusion machinery is supported by the reduced levels of R-(v)-SNARE VAMP7-TI in both AP-3-deficient and BLOC-1-deficient mice (Salazar *et al.*, 2006), its defective targeting to *mocha* nerve terminals (Scheuber *et al.*, 2006), and the neurological phenotype of mice lacking the BLOC-1 subunit snapin. These mice possess impaired neurotransmitter secretion by mechanisms involving the SNARE SNAP-25 (Tian *et al.*, 2005). The most compelling connection between the AP-3–BLOC-1 machinery and schizophrenia is the finding that brain tissue from schizophrenia patients has reduced levels of the BLOC-1 subunit dysbindin in hippocampal mossy fibers (Talbot *et al.*, 2004). This phenotype is also found in AP-3-deficient *mocha* brain (Salazar *et al.*, 2006). Finally, the pre-synaptic levels of the synaptic vesicle protein VGLUT1, which is sorted in part by AP-3 (Salazar *et al.*, 2005a) (Fig. 8), increase in hippocampal nerve terminals of schizophrenic patients (Talbot *et al.*, 2004). A potential explanation for this observation is that the targeting of VGlut1 to degradative compartments is impaired by the decreased levels of dysbindin.

Conclusions and Perspectives

Although AP-3 mutations have helped us to identify multiple AP-3-dependent cellular functions, our understanding of the mechanisms that regulate AP-3 still lacks the molecular and structural detail of its predecessors, AP-1 and AP-2. The identification of the whole network of AP-3 interactors, regulators and adaptor accessory proteins remains a challenge. However, a potential list of these AP-3 interacting proteins has recently been obtained (Salazar *et al.*, 2005b;

Salazar *et al.*, 2009). Definition of structural-functional modules in these proteins, as in many AP-1- and AP-2- interacting proteins, will greatly facilitate the dissection of the precise mechanisms that lead to the formation of AP-3 vesicles. Some of the components may assist AP-3 function, rather than be required for AP-3 function. This concept is particularly relevant considering that AP-3 might generate vesicles that have different compositions in the same cell.

A particularly intriguing problem that is common to several coat protein complexes is how isoforms contribute to the functional diversity of adaptors. We have begun to unravel this problem in the analysis of AP-1 (Folsch *et al.*, 1999; Ohno *et al.*, 1999; Folsch *et al.*, 2001; Sugimoto *et al.*, 2002; Folsch *et al.*, 2003) and AP-3 adaptors (Nakatsu *et al.*, 2004; Seong *et al.*, 2005). However, the presence of two adaptor isoforms expressed in the same cell still leaves several unanswered questions regarding the regulation of assembly and function. Adaptors are assembled from shared polypeptides and tissue specific isoforms. For example, δ is common to neuronal and ubiquitous AP-3 (Fig. 3B). Thus, adaptors carrying a common subunit probably partially overlap and/or compete at the level of biosynthetic assembly, cargo or accessory polypeptide selection and subcellular distribution. In the search for common molecular mechanisms governing adaptor function, we have ignored the contribution that tissue-specific components may play in adaptor function. This is particularly clear in AP-3 and BLOC complex deficiencies, in which the phenotypes of double mutants are more pronounced than those of single mutants. However, the penetrance of the genetic interactions among AP-3 and BLOC complexes varies among tissues (Gautam *et al.*, 2006). Furthermore, the δ subunit deficiencies *mocha* and the milder

mocha(2J) differ in their zinc transporter phenotypes. *Mocha* mice show a severe reduction of vesicular zinc in hippocampus and cortex. By contrast, *mocha(2J)* mice exhibit normal expression in hippocampal mossy fibers, but abnormal patterns in the neocortex (Kantheti *et al.*, 1998; Kantheti *et al.*, 2003). This indicates that unknown tissue-specific and brain-region-specific modifiers affect the function of sorting complexes.

My research compares how BLOC-1 and AP-3 contribute to synaptic composition within the hippocampus versus the striatum, by examining AP-3 cargo expression and synaptic vesicle morphology. Interestingly, these studies reveal that BLOC-1 serves as a brain-region-specific modifier of AP-3 expression and sub-synaptic distribution in the dentate gyrus of the hippocampus, but not the striatum.

Challenging Prevailing Paradigms: How this Dissertation Research Contributes to our Understanding of Endosomal Sorting in Neurons.

As stated above, the prevailing paradigm for understanding AP-3 isoform-specific endosomal sorting in neurons conceives of these two mechanisms as mutually exclusive. This is due largely to the segregation of systemic phenotypes with *Ap3b1*$^{-/-}$ mice and neurological phenotypes with *Ap3b2*$^{-/-}$ mice. However, the majority of neurological phenotypes have been assessed in either *mocha* mice, which lack all AP-3, or in neuronal AP-3-deficient mice (*Ap3b2*$^{-/-}$ or *Ap3m2*$^{-/-}$), not in ubiquitous AP-3-deficient (*Ap3b1*$^{-/-}$) mice. Therefore, it is unclear whether AP3b1 contributes to *mocha* neuronal pathology. Additionally, molecular alterations of synaptic vesicle proteins in *Ap3b1*$^{-/-}$ mice suggest that

AP3b1 may play a previously unappreciated role in neuronal function. The contributions of AP3b1 to neuronal function could be underappreciated because they only appear during particular neuronal challenges, such as high frequency stimulation, or because they result in subtle neuronal defects that either increase with age, such as the accumulation and aggregation of synaptic vesicle proteins, or that result in psychiatric disorders, such as schizophrenia, which are difficult to diagnose in mouse models. My dissertation will test a hypothesis that proposes a neuronal-specific role for ubiquitously-expressed protein complexes that mediate endosomal to lysosomal vesicle traffic, including AP-3 and BLOC-1.

Specifically, I hypothesize that neuronal AP-3 and ubiquitous AP-3 compete for similar cargo proteins on shared donor early endosomes, sorting both synaptic vesicle and lysosomal cargo to either a synaptic vesicle or lysosomal fate. This hypothesis diverges from the traditional model, which superimposes the organization of endosomal sorting in non-neuronal cells, where recycling and lysosomal sorting pathways are both molecularly and spatially distinct, onto endosomal sorting in neurons (see Figure 9 for comparison of traditional model with my alternative hypothesis). The predictions of this traditional model for endosomal sorting in neurons are the following:

1) Synaptic vesicle and lysosomal cargoes are sorted from distinct donor early endosomes or distinct sites on donor early endosomes.
2) Synaptic vesicle and lysosomal cargoes are restricted in their interactions with AP-3, such that synaptic vesicle cargoes interact solely with neuronal AP-3 and are sorted to synaptic vesicles, while lysosomal cargoes are sorted by ubiquitous AP-3 to lysosomes.

3) Based on predictions 1 and 2, synaptic vesicle and AP-3-sorted lysosomal cargoes should not significantly co-localize in neuronal cells.
4) Only neuronal AP-3 should significantly regulate synaptic vesicle composition and the molecular composition of the synapse.

However, my results refute each of these predictions and lead to an alternative view for how endosomal sorting in neurons functions to regulate the molecular composition of the synapse. In response to the predictions of the traditional model, my results demonstrate that:

1) Synaptic vesicle and AP-3-sorted lysosomal cargoes co-reside in shared early endosomes, where they co-localize in 'sorting patches' of the limiting membrane.
2) Ubiquitous and neuronal AP-3 are capable of sorting shared cargoes, both synaptic vesicle and lysosomal. I can biochemically isolate a synaptic vesicle population that contains both synaptic vesicle proteins and AP-3-sorted lysosomal proteins.
3) Synaptic vesicle and AP-3-sorted lysosomal cargoes significantly co-localize in neuronal cells.
4) Both ubiquitous AP-3 and BLOC-1 regulate synaptic vesicle composition. Furthermore, deficiencies of AP-3, as well as BLOC-1, impact the molecular composition of the synapse.

These results demonstrate the existence of shared donor early endosomes from which synaptic vesicle and AP-3-sorted lysosomal cargoes can be similarly sorted to either a synaptic vesicle or lysosomal fate.

Summary and General Overview

My dissertation focuses on how Hermansky-Pudlak complexes, AP-3 and BLOC-1, regulate synaptic architecture through endosomal sorting of shared cargoes to either lysosomes or synaptic vesicles. Specifically, this work tests the hypothesis that both AP-3-sorted lysosomal and synaptic vesicle cargoes are competitively sorted from shared early endosomes by two AP-3-dependent sorting pathways, either ubiquitous AP-3 and BLOC-1-mediated lysosomal sorting or neuronal AP-3-mediated synaptic vesicle biogenesis. By deconvolution microscopy of neuronal cell lines and mouse primary neurons, I demonstrate that AP-3-sorted lysosomal and synaptic vesicle cargoes significantly co-localize, and that this co-localization originates with 'sorting patches' of shared early endosomes. Furthermore, these two cargo populations are co-sorted to either lysosomes or synaptic vesicles. Biochemical isolation of mouse brain synaptic vesicles reveals that some of these vesicles also contain AP-3-sorted lysosomal cargoes. Additionally, glycerol gradient fractionation of AP-3-isoform specific knockout and BLOC-1 null mouse brains demonstrates that these complexes sort overlapping cargoes, and that ubiquitous AP-3 and BLOC-1, which sort cargoes to lysosomes, also regulate synaptic vesicle composition. These results demonstrate the existence of a competitive endosomal sorting

mechanism by which both lysosomal and synaptic vesicle sorting pathways are necessary for proper synaptic vesicle composition.

This competitive sorting mechanism predicts that both AP-3 and BLOC-1 will alter the molecular architecture of the synapse. Using light and electron microscopy of AP-3- and BLOC-1-deficient mouse brains, I discovered that these complexes coordinately regulate synaptic architecture, particularly within the dentate gyrus of the hippocampus. By light microscopy, AP-3 is expressed throughout the brain, with strong expression in both the striatum and hippocampus. Loss of either AP-3 or BLOC-1 selectively reduces expression of the AP-3 cargo, VAMP7-TI, within the dentate gyrus, without affecting another synaptic vesicle marker, synaptophysin. Furthermore, loss of BLOC-1 reduces AP-3 expression in the dentate gyrus, by reducing the amount of AP-3 in axons. AP-3 predominantly localizes to axons, where it closely associates with synaptic vesicles. In the majority of cases, AP-3 only partially labels axonal structures. Thus synaptic vesicles differentially associate with AP-3, suggesting that AP-3 generates a unique pre-synaptic vesicle population. Furthermore, loss of AP-3 results in smaller synaptic vesicles within the striatum, but larger synaptic vesicles within the dentate gyrus. These results demonstrate that endosomal sorting mechanisms contribute to differences in synaptic vesicle composition and synaptic architecture by regulating both the molecular content and size of synaptic vesicles.

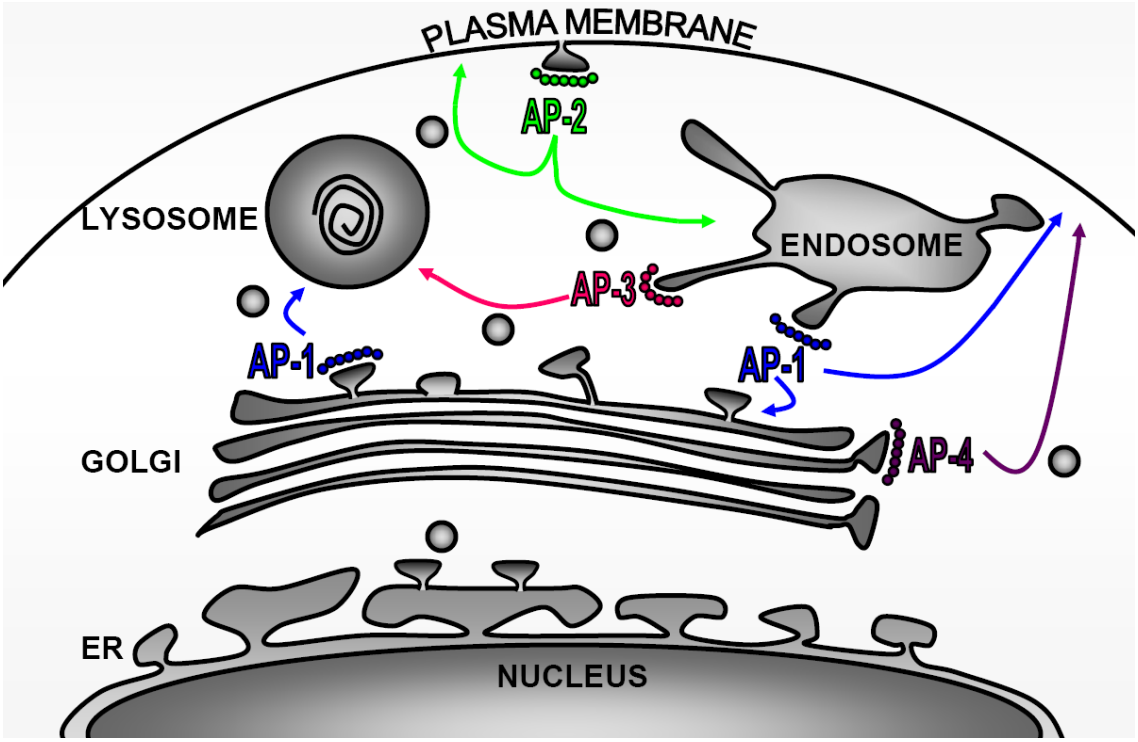

Figure 1: Adaptor-Mediated Vesicle Transport. Four heterotetrameric adaptor protein complexes (AP-1, 2, 3 and 4) create vesicles at discrete intracellular donor organelles. These vesicles carry lipids and proteins to specific target organelles. My dissertation focuses on AP-3, which creates vesicles at endosomes to be delivered to the lysosome.

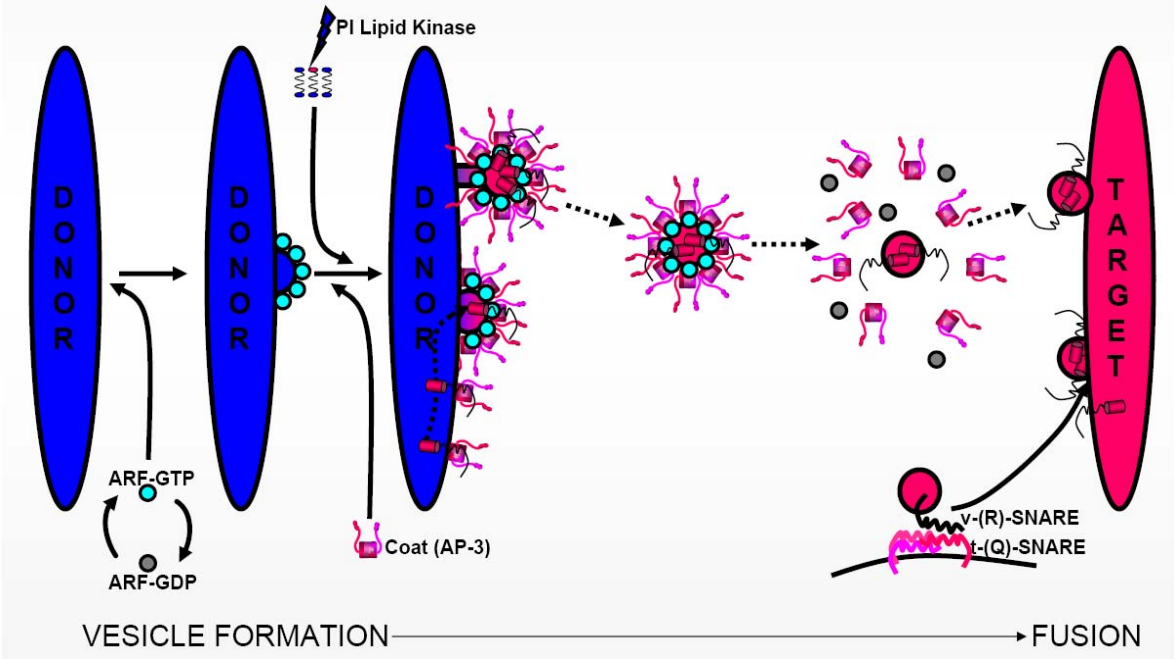

Figure 2: Regulators of Vesicle Formation and Fusion. Vesicle formation begins at a donor organelle, when ARF-GTP nucleates a vesicle formation site that recruits an adaptor protein complex, such as AP-3, from a cytosolic pool to a membrane-bound pool. The lipid composition of the donor membrane can also help to recruit the adaptor coat. The adaptor coat interacts with sorting sequences within the cytosolic tail of transmembrane proteins to cluster them into the vesicle. Once it is released from the donor organelle, the vesicle uncoats to reveal fusion machinery. A vesicle SNARE protein (v-(R)-SNARE) interacts with target SNAREs (t-(Q)-SNAREs) to mediate vesicle fusion.

A

Gene Name	Protein Name	Expression	Mutants
Ap3d	δ	Ubiquitous	*mocha*
Ap3b1	β3A	Ubiquitous	HPS2, *pearl*, *Ap3b1-/-*
Ap3b2	β3B	Neuronal	*Ap3b2-/-*
Ap3m1	μ3A	Ubiquitous	
Ap3m2	μ3B	Neuronal	*Ap3m2-/-*
Ap3s1	σ3A	Ubiquitous	
Ap3s2	σ3B	Ubiquitous	

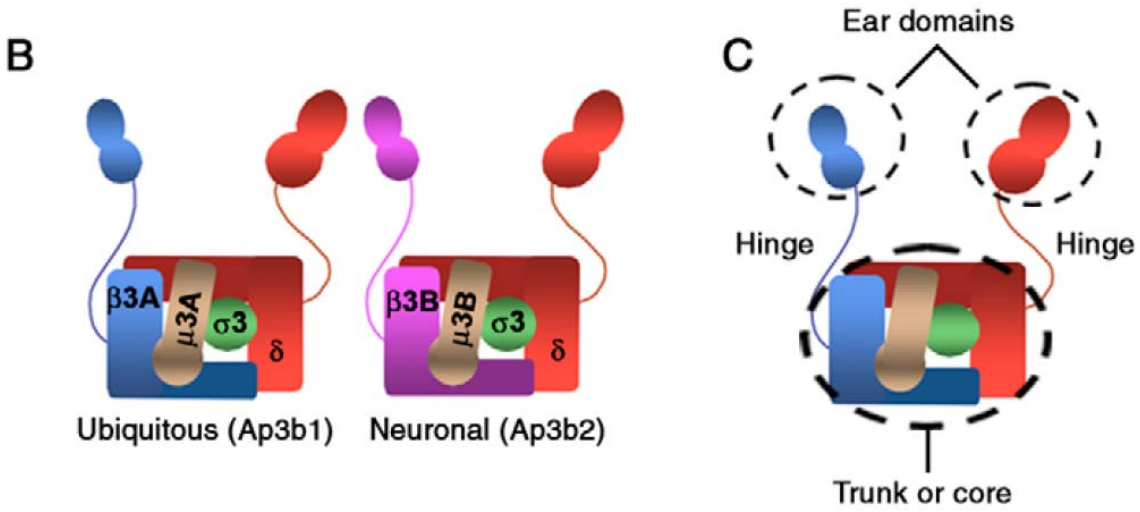

Figure 3: Nomenclature and structure of AP-3 subunit isoforms. (A) AP-3 subunit genes and their corresponding gene products. The pattern of expression of each subunit is described as neuronal, corresponding to neurons and neuro-endocrine tissue, or ubiquitous, for subunits expressed in all cells including neuronal tissues. Mice carrying natural or engineered AP-3 subunit deficiencies are listed. (B) Proposed subunit composition of the neuronal and ubiquitous AP-3 isoforms. Both AP-3 complexes can carry either a σ3A or B subunit. (C) Adaptor complexes possess three defined domains. The ears correspond to the C-terminal domains of δ and β3. The trunk or core is composed of a protease-resistant core formed by fragments of β3 and δ as well as full-length μ3 and σ3 subunits. The ears and trunk are connected by hinges.

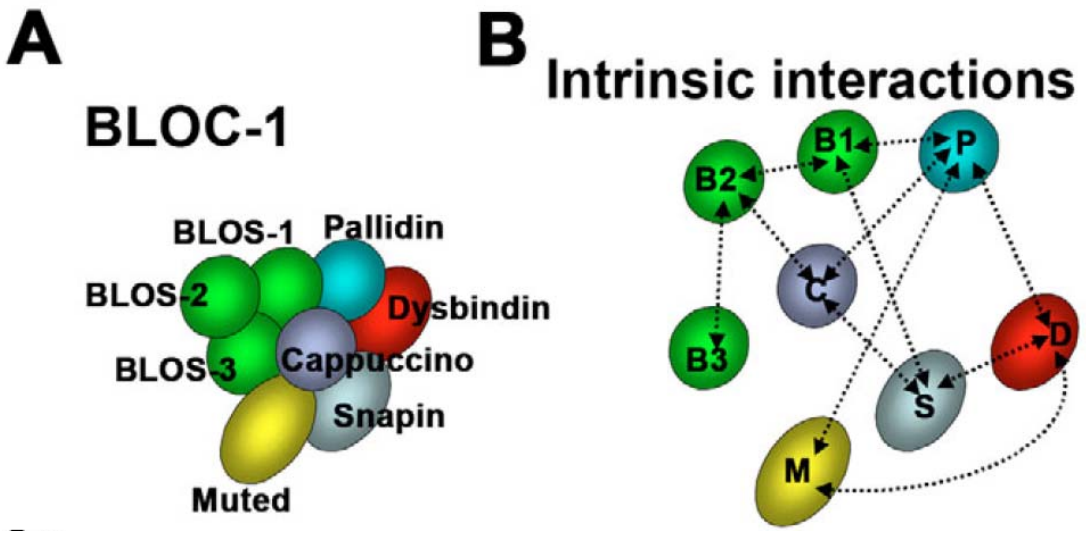

Figure 4: Subunit composition and intramolecular interactions of the BLOC-1 complex. (A) The model depicts the known subunit structure of the BLOC-1 complex. (B) The name of each subunit is denoted by the initial letter of the protein name. The diagram describes the intramolecular interactions between subunits of the BLOC-1 complex, here referred to as intrinsic interactions. For details see (Di Pietro and Dell'Angelica, 2005).

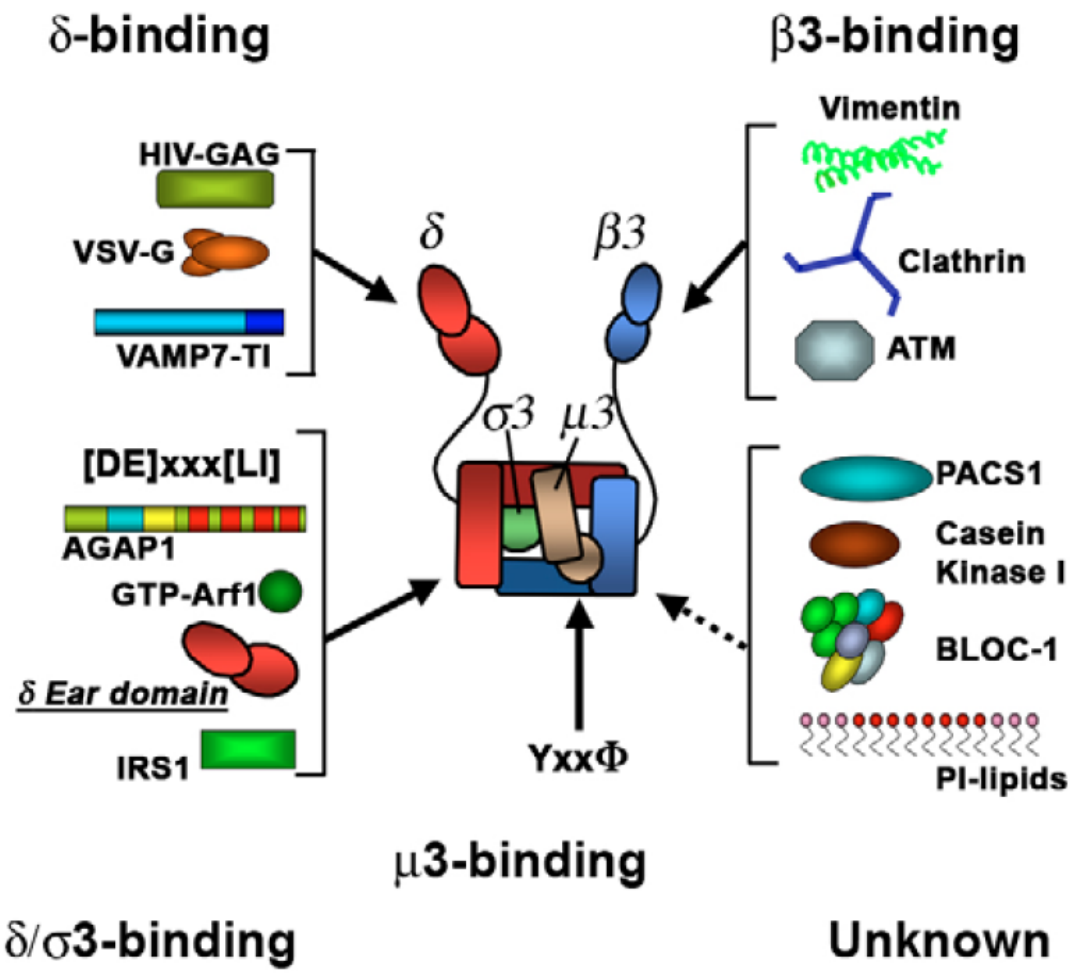

Figure 5: Molecular interactions of the adaptor complex AP-3. The diagram depicts AP-3 subunits. δ is shown in red, σ3 is shown in green, μ3 is shown in brown and β3 is shown in blue. Known interactions with a particular AP-3 subunit are indicated by a solid arrow. Interactions with AP-3 where the subunit is not known are depicted by a dashed arrow. These interactions correspond to PACS-1 (Crump, Xiang et al. 2001), a casein kinase (Faundez and Kelly 2000), BLOC-1 (Di Pietro, Falcon-Perez et al. 2006) and inositol phospholipids (PI-Lipids). Vimentin (Styers *et al.*, 2004; Salazar *et al.*, 2009), clathrin (Dell'Angelica, Klumperman et al. 1998) and the ataxia telangiectasia

gene product (ATM) (Lim, Kirsch et al. 1998) directly associate with the β3 subunit. The δ subunit provides a platform sufficient to bind HIV Gag protein (Dong, Li et al. 2005), protein G of the vesicular stomatitis virus (VSV-G) (Nishimura, Plutner et al. 2002) or the R-(v)-SNARE VAMP7-TI (Martinez-Arca, Rudge et al. 2003). Alternatively δ adaptin in a complex with σ3 or σ3 by itself binds di-leucine sorting motifs ([DE]xxx[LI]) (Janvier, Kato et al. 2003), AGAP1 (Nie, Boehm et al. 2003), the Arf1 GTPase (Lefrancois, Janvier et al. 2004), the δ ear domain (Lefrancois, Janvier et al. 2004), and the insulin receptor substrate 1 (IRS1) (VanRenterghem, Morin et al. 1998). Tyrosine sorting motifs (YxxΦ) bind to the μ3 subunits (Ohno, Stewart et al. 1995).

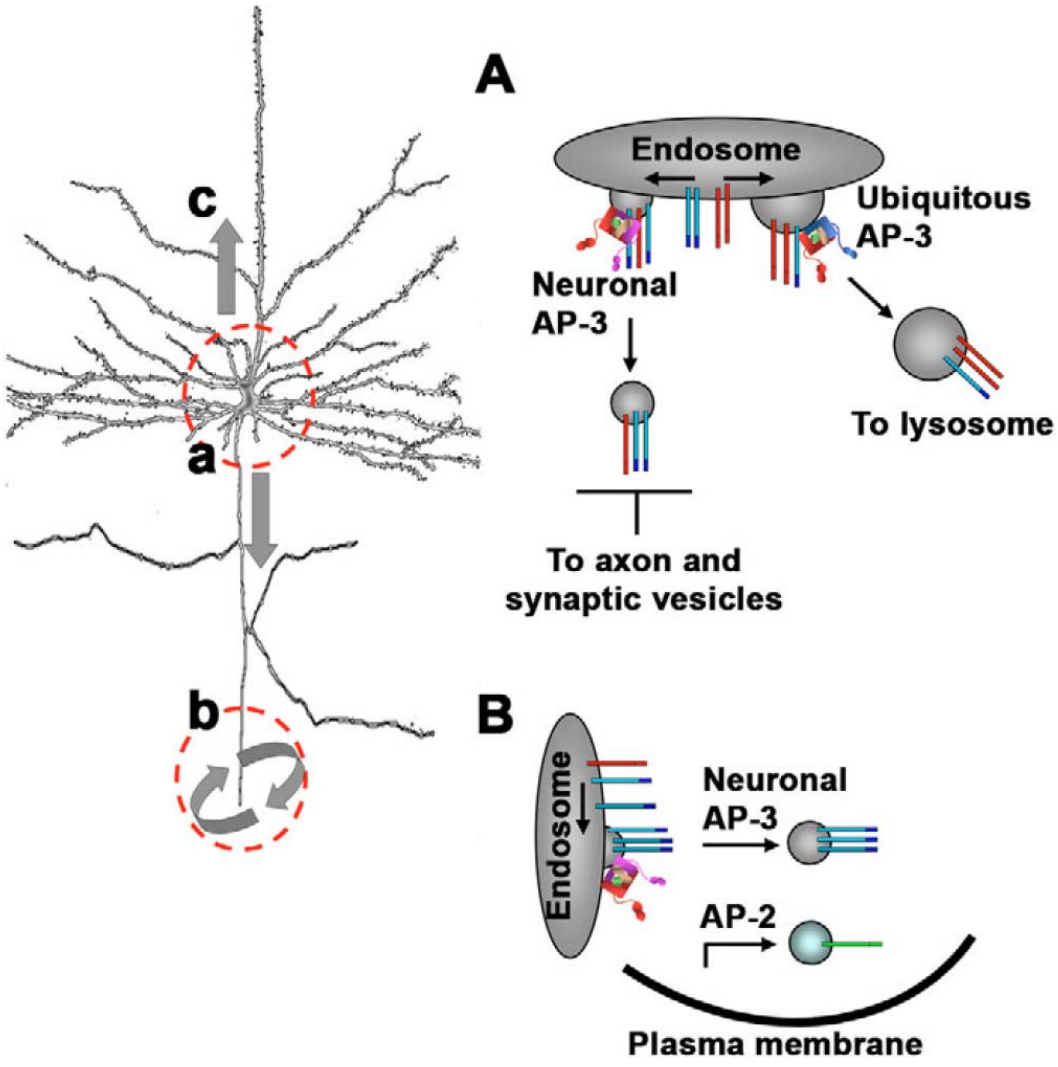

Figure 6: AP-3 sorting mechanisms in neuronal cells. A neuron possesses neuronal and ubiquitous AP-3 complexes in the cell body (a) but only neuronal AP-3 in axons (b) and dendrites (c) (Seong *et al.*, 2005). (A) Proposed functions of the neuronal and ubiquitous AP-3 in cell bodies. Both AP-3 forms reside in the same endosome. Neuronal AP-3 sorts proteins into the axon or a synaptic vesicle pathway. Ubiquitous AP-3 sorts proteins to the lysosomal pathway. Model A explains the changes in ZnT3 levels observed in *Ap3b1*$^{-/-}$ and *Ap3b2*$^{-/-}$ mice (Seong *et al.*, 2005; Salazar *et al.*, 2009). In this model AP-3-

sorted proteins, like ZnT3, are recognized by both AP-3 isoforms and therefore routed to either a synaptic vesicle-axonal or a lysosomal pathway. Thus, in the absence of one AP-3 isoform, membrane proteins are targeted to the other pathway. The amount of ZnT3 in synaptic vesicles is reduced in the absence of neuronal AP-3 (*Ap3b2*$^{-/-}$) and ZnT3 is instead routed to lysosomes for degradation. Similarly, the amount of ZnT3 targeted to lysosomes is reduced in the absence of ubiquitous AP-3 (*Ap3b1*$^{-/-}$) and it is then routed by the neuronal AP-3 (encoded by *Ap3b2*) to synaptic vesicles, thus triggering increased levels of ZnT3 in synaptic vesicles. Model B shows the proposed role of neuronal AP-3 in synaptic vesicle biogenesis in pre-synaptic terminals. AP-3 generates synaptic vesicles from pre-synaptic endosomes. This route is parallel to the AP-2 route, which generates synaptic vesicles from the plasma membrane. A role for AP-3 in sorting to dendrites (c) has not been documented yet.

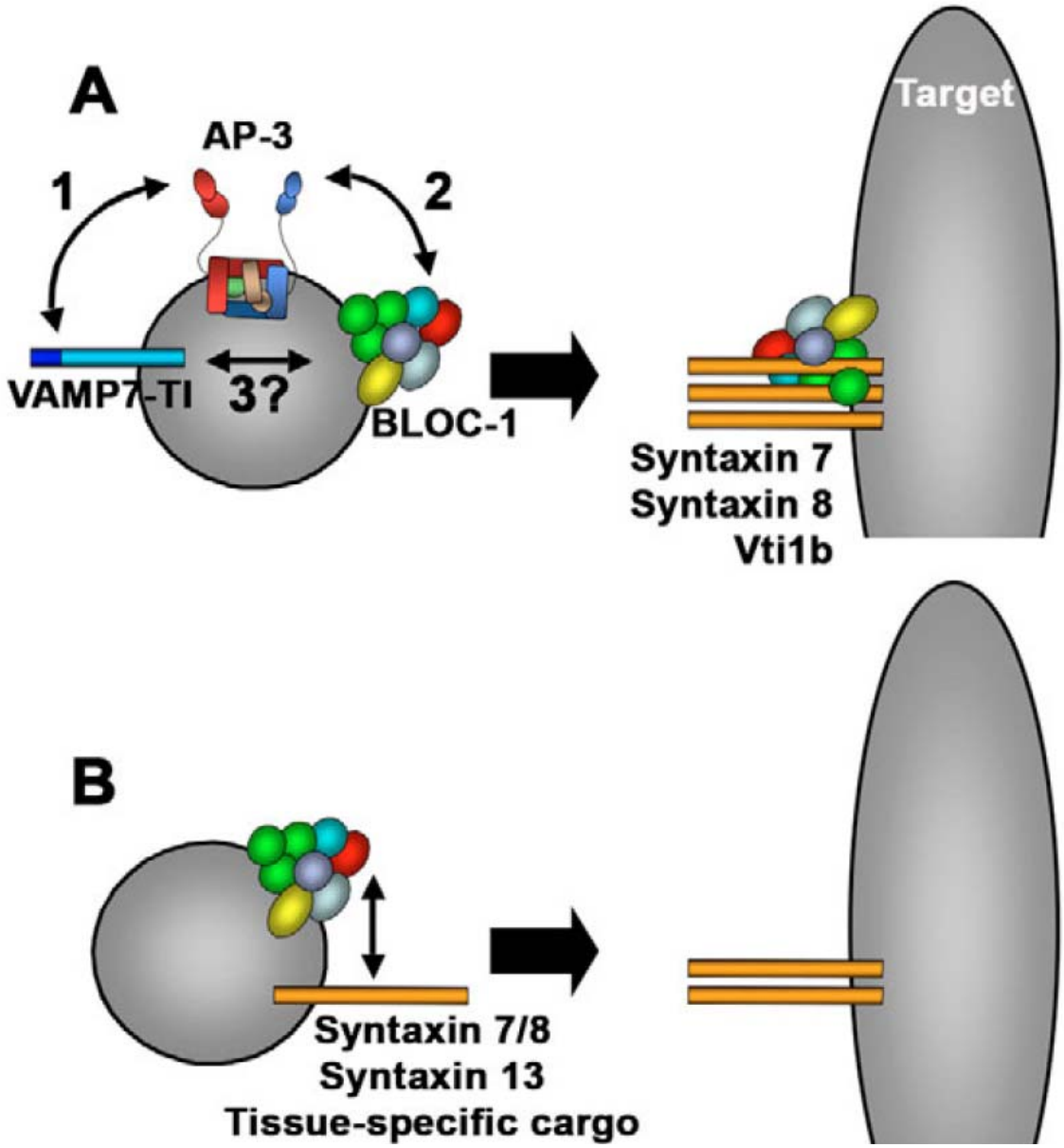

Figure 7: Models of BLOC-1–AP-3 sorting functions. (A,B) Two different vesicles, A and B, fuse with a target organelle (right). VAMP7-TI is present in vesicle A (blue cylinder). Its cognate Q-(t)-SNAREs (syntaxin 7, 8 and Vti1b; orange cylinders) are present in the target organelle. Model A depicts AP-3 and BLOC-1 complexes coresiding in vesicle A (Salazar *et al.*, 2006). In this vesicle, BLOC-1 may regulate the recognition of specific cargoes, like the SNARE VAMP7-

TI, either by bridging AP-3 and a selected membrane protein (interactions 2 and 3) or by stabilizing specific AP-3–cargo interactions (interactions 1 and 2). Interactions 1 (Martinez-Arca *et al.*, 2003) and 2 have been documented (Di Pietro *et al.*, 2006; Salazar *et al.*, 2009). Interaction 3 is speculative. On the target membrane a tripartite Q-(t)-SNARE complex of syntaxin 7, syntaxin 8, and Vti1b is maintained by BLOC-1, independently of AP-3. Model B depicts the selective sorting of SNAREs or tissue-specific cargo into vesicle B by the BLOC-1 complex. Vesicle B represents a vesicle population distinct from vesicle A. Sorting into and/or biogenesis of vesicle B requires BLOC-1 but not AP-3 function. Model A and model B are non-exclusive. Either Model A alone or a combination of models A and B explain both the convergent sorting phenotypes of BLOC-1 and AP-3 deficiencies as well as the altered colocalization between syntaxins 7 and 8, which is unique to BLOC-1–mutant cells (Salazar *et al.*, 2006).

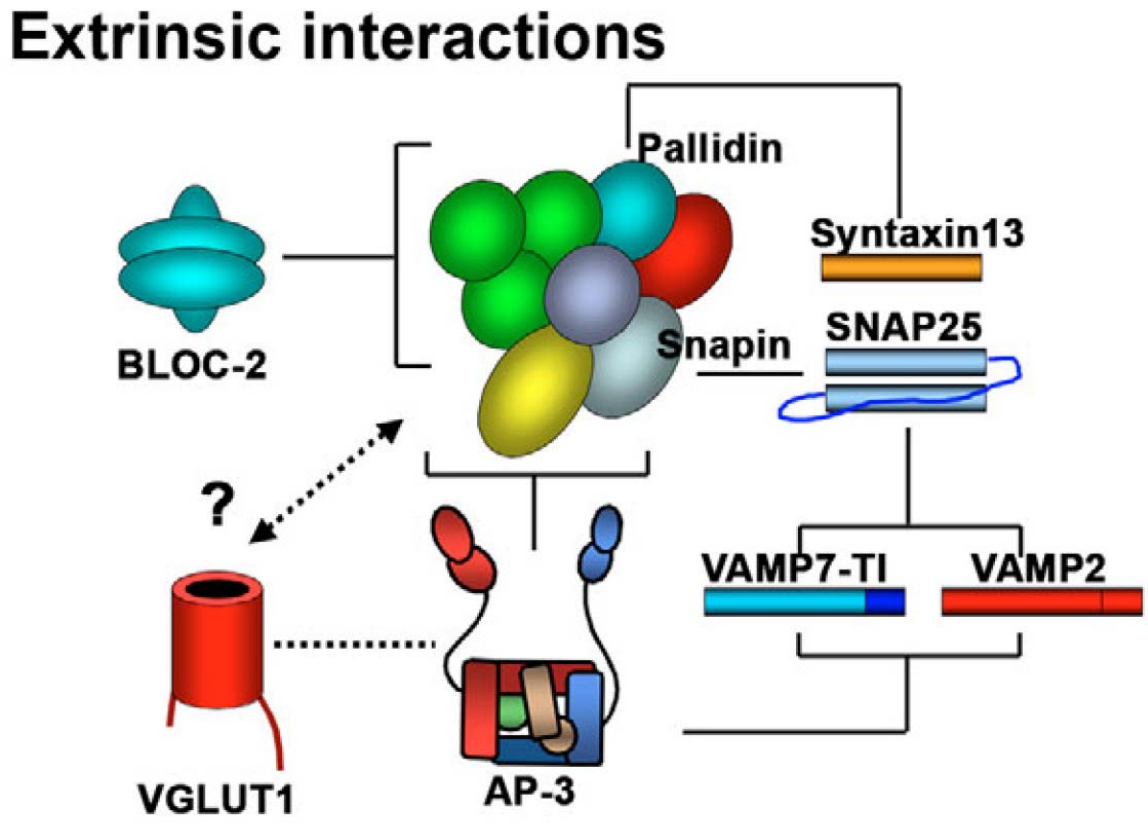

Figure 8: Intermolecular Interactions of the BLOC-1 Complex. The diagram represents a partial list of interactions (solid lines), functional relationships (dashed line), or potential relationships (double-headed arrow with question mark) relevant to vesicle generation, fusion, and the pathogenesis of schizophrenia. A detailed list of interactions is described in (Di Pietro and Dell'Angelica, 2005).

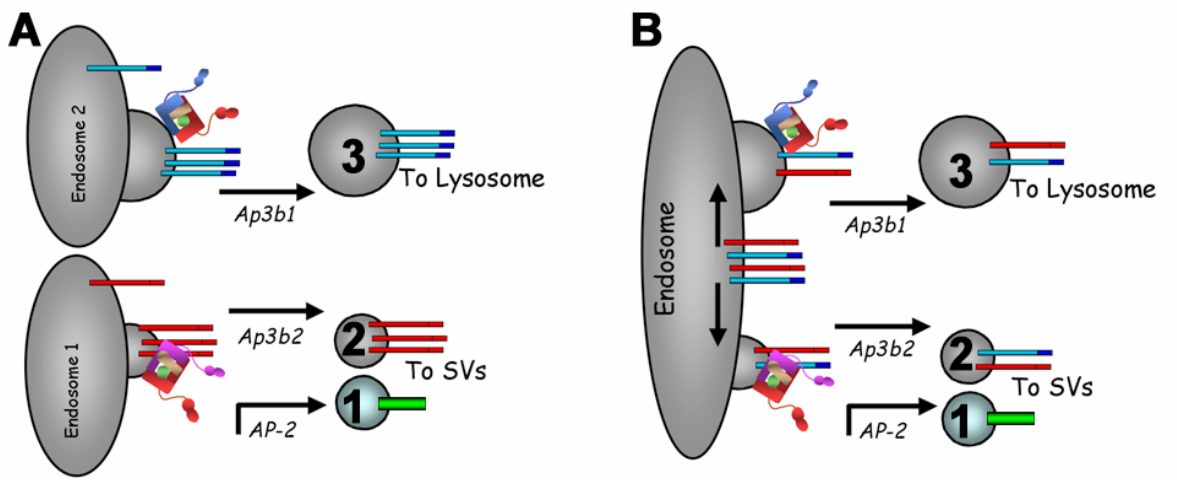

Figure 9: Models of Endosomal Sorting in Neurons. A) Traditional Model In a traditional model of endosomal sorting, synaptic vesicle and lysosomal cargoes are sorted from distinct endosomes or distinct endosomal sites into segregated vesicle traffic pathways, either lysosomal or synaptic vesicle. Only neuronal AP-3-derived (*Ap3b2*) synaptic vesicles, which do not contain lysosomal proteins, will be transported to the synapse. Note, AP-2 mediates another synaptic vesicle biogenesis pathway from the plasma membrane. **B) Alternative Model** Data from my dissertation supports an alternative model for endosomal sorting in neurons. In this model, synaptic vesicle and AP-3-sorted lysosomal cargoes co-localize in 'sorting patches' of shared donor early endosomes, from which they are similarly sorted to either synaptic vesicle or lysosomal fates. In this model, neuronal AP-3 would create synaptic vesicles with AP-3-sorted lysosomal cargoes. Furthermore, ubiquitous AP-3 and BLOC-1 (not shown) would influence synaptic vesicle content and the molecular composition of the synapse by antagonizing the neuronal-AP-3-mediated synaptic vesicle biogenesis pathway. Figure is courtesy of Victor Faundez.

CHAPTER II

Roles of BLOC-1 and Adaptor Protein-3 Complexes in Cargo Sorting to Synaptic Vesicles

Karen Newell-Litwa,*† Gloria Salazar,† Yoland Smith,‡ and Victor Faundez†§

*Graduate Program in Biochemistry, Cell, and Developmental Biology;
†Department of Cell Biology; §Center for Neurodegenerative Diseases; and
‡Department of Neurology, Emory University, Atlanta, GA 30322

Molecular Biology of the Cell
Vol. 20, 1441–1453, March 1, 2009

Abstract

Neuronal lysosomes and their biogenesis mechanisms are primarily thought to clear metabolites and proteins whose abnormal accumulation leads to neurodegenerative disease pathology. However, it remains unknown whether lysosomal sorting mechanisms regulate the levels of membrane proteins within synaptic vesicles. Using high-resolution deconvolution microscopy, we identified early endosomal compartments where both selected synaptic vesicle and lysosomal membrane proteins coexist with the *a*daptor *p*rotein complex 3 (AP-3) in neuronal cells. From these early endosomes, both synaptic vesicle membrane proteins and characteristic AP-3 lysosomal cargoes can be similarly sorted to brain synaptic vesicles and PC12 synaptic-like microvesicles. Mouse knockouts for two Hermansky–Pudlak complexes involved in lysosomal biogenesis from early endosomes, the ubiquitous isoform of AP-3 (*Ap3b1*$^{-/-}$) and *muted*, defective in the *b*iogenesis of *l*ysosome-related *o*rganelles *c*omplex *1* (BLOC-1), increased the content of characteristic synaptic vesicle proteins and known AP-3 lysosomal proteins in isolated synaptic vesicle fractions. These phenotypes contrast with those of the mouse knockout for the neuronal AP-3 isoform involved in synaptic vesicle biogenesis (*Ap3b2*$^{-/-}$), in which the content of select proteins was reduced in synaptic vesicles. Our results demonstrate that lysosomal and lysosome-related organelle biogenesis mechanisms regulate steady-state synaptic vesicle protein composition from shared early endosomes.

Introduction

Endosomes are sorting hubs that receive proteins and lipids from the cell surface or the *trans*-Golgi network and further deliver them to either downstream endocytic compartments, the exocytic pathway, or back to the cell surface. In addition to these functions, neurons possess endosomes that participate in specialized sorting mechanisms, such as retrograde delivery of neurotrophic signals to the cell body through signaling endosomes (Howe and Mobley, 2005); or in the biogenesis of synaptic vesicles (Murthy and De Camilli, 2003). Signaling endosomes and synaptic vesicles originate at the nerve terminal, a cell domain lacking ultrastructurally identifiable lysosomes. These lytic organelles and their components are thought to be restricted to neuronal cell bodies (Parton *et al.*, 1992). Because of this spatial segregation, the biogenesis of signaling endosomes and synaptic vesicles is thought to be independent from traditional lysosome biogenesis. However, recent evidence indicates that diverse lysosomal proteins, either those resident in lysosomes or involved in traffic to lysosomes, are also found in signaling endosomes, nerve terminals, and synaptic vesicles (Overly and Hollenbeck, 1996; Stobrawa *et al.*, 2001; Salazar *et al.*, 2005b; Saxena *et al.*, 2005; Arantes and Andrews, 2006; Deinhardt *et al.*, 2006; Karten *et al.*, 2006; Salazar *et al.*, 2006; Scheuber *et al.*, 2006; Takamori *et al.*, 2006; Talbot *et al.*, 2006; Burre and Volknandt, 2007).

The mechanism to account for the presence of lysosomal proteins in organelles generated at the nerve terminal remains unknown. The presence of lysosomal proteins in synaptic vesicles challenges a conventional view where neuronal early endosomes function in a pathway for sorting synaptic vesicle

proteins and lysosomal cargoes away from each other into different vesicles bound to the cell surface or lysosomal compartments, respectively.

Here, we propose that sorting machineries specialized in lysosome biogenesis in nonneuronal cells contribute to the generation of pre-synaptic compartments by regulating the targeting of synaptic vesicle and lysosomal membrane proteins to synaptic vesicles. We tested this hypothesis by using genetic deficiencies of Hermansky–Pudlak lysosomal sorting complexes that localize to early endosomes. These deficiencies include *Ap3b1*$^{-/-}$, a mouse lacking the ubiquitous *a*daptor *p*rotein complex *3* (AP-3) and *muted*$^{mu/mu}$, a mouse defective in the *b*iogenesis of *l*ysosome-related *o*rganelles *c*omplex *1* (BLOC-1).

AP-3 and BLOC-1 possess well-established roles in the sorting of membrane proteins into vesicles bound to lysosomes, lysosome-related organelles, and synaptic vesicle fates (for reviews, see (Di Pietro and Dell'Angelica, 2005; Ohno, 2006b; Danglot and Galli, 2007; Newell-Litwa *et al.*, 2007)). AP-3 exists as two isoforms defined by their subunit composition. The subunits δ and σ3 are common to all AP-3 isoforms, yet β3 and μ3 subunits exist as two differentially expressed gene products each (A and B). The expression of β3B and μ3B subunits is restricted to neuronal cells (Nakatsu *et al.*, 2004; Seong *et al.*, 2005). These subunits are believed to assemble into the neuronal isoform complex together with δ and σ3. In contrast, β3A, μ3A, δ, and σ3 subunits generate the ubiquitous AP-3 adaptor present in all cells. Mice deficient for both AP-3 complexes due to a mutation in δ adaptin (*mocha*), shared by both AP-3 isoforms, are characterized by defective targeting of proteins to synaptic vesicles, lysosomes, and lysosome-related organelles (Kantheti *et al.*, 1998). These

phenotypes are recapitulated in part by isoform specific AP-3 deficiencies. Thus, β3A loss-of-function alleles, such as *Ap3b1*$^{-/-}$, which abrogate ubiquitous AP-3 complex expression, possess defective assembly of lysosomes and lysosome-related organelles (Feng *et al.*, 1999; Yang *et al.*, 2000; Seong *et al.*, 2005). These phenotypes are also found in mice lacking any one of the eight subunits found in the BLOC-1 complex, a complex that genetically and biochemically interacts at least with ubiquitous AP-3. Mutations in genes encoding individual BLOC-1 subunits, such as *muted*$^{mu/mu}$, lead to down-regulation of the whole BLOC-1 complex (Di Pietro and Dell'Angelica, 2005; Di Pietro *et al.*, 2006; Gautam *et al.*, 2006; Salazar *et al.*, 2009).

In humans, genetic deficiencies in loci encoding for proteins of either the ubiquitous AP-3 or BLOC-1 complex trigger a disease known as Hermansky–Pudlak syndrome (OMIM: 203300) (Di Pietro and Dell'Angelica, 2005; Raposo and Marks, 2007). In contrast, β3B alleles (*Ap3b2*$^{-/-}$) abolish the expression of neuronal AP-3. Neuronal AP-3 mutants recapitulate synaptic vesicle targeting and neurological phenotypes found in the *mocha* allele but lack their systemic lysosomal phenotypes (Nakatsu *et al.*, 2004; Seong *et al.*, 2005). These findings have led to the notion that AP-3 isoforms perform segregated sorting functions in mammals. However, this view fails to consider that both AP-3 adaptor isoforms (Seong *et al.*, 2005; Salazar *et al.*, 2006), as well as BLOC-1, are present in neuronal cell bodies and that AP-3 adaptor isoforms share their ability to recognize similar sorting motifs in membrane proteins (Bonifacino and Traub, 2003). This raises the question of whether membrane proteins targeted to the synapse could be regulated by both AP-3 adaptor isoforms.

Based on this evidence, we hypothesize that divergent endocytic sorting routes, synaptic vesicle biogenesis mediated by the neuronal AP-3 isoform and lysosomal transport mediated by the ubiquitously expressed AP-3 isoform and BLOC-1 complex, regulate synaptic vesicle composition by sorting similar cargo from shared early endosomes. This mechanism would operate as a "seesaw" from a common early endosome. From this endosome, AP-3 adaptor isoforms would behave as branches of a seesaw. Thus, neuronal AP-3 would sort both synaptic vesicle and lysosomal AP-3 cargoes into synaptic vesicles, whereas ubiquitous AP-3 would compete for both types of cargoes and deliver them to lysosomal compartments. In the absence of ubiquitous AP-3, cargoes that normally would have been sorted to lysosomes would instead be routed to synaptic vesicles and vice versa. The seesaw model is consistent with the increased targeting of zinc transporter 3 (ZnT3) to ubiquitous AP-3-null brain synaptic vesicles (Seong *et al.*, 2005). The seesaw mechanism leads to the following predictions: 1) Donor early endosomes in neurons will contain both lysosomal and synaptic vesicle cargoes so that these cargoes can be subsequently targeted to either a lysosomal or synaptic vesicle destination. 2) Both synaptic vesicle and lysosomal AP-3 cargoes are sorted to a common synaptic-like microvesicle in PC12 cells and synaptic vesicle in neurons. 3) Finally, a balance between lysosomal and synaptic vesicle targeting branches of the seesaw will define synaptic vesicle composition. In the absence of either targeting mechanism, cargoes will be more available to enter the alternate route, thereby disrupting the balance of synaptic vesicle cargoes. Therefore, genetic deficiencies of Hermansky–Pudlak complexes involved in the biogenesis of lysosomes or lysosome-related organelles (ubiquitous AP-3/*Ap3b1*$^{-}$

$^{/-}$ and BLOC-1/$muted^{mu/mu}$) would increase synaptic vesicle content of synaptic vesicle and lysosomal AP-3 cargoes, whereas genetic deficiencies in synaptic vesicle sorting machinery (neuronal AP-3/$Ap3b2^{-/-}$) would reduce the levels of lysosomal and synaptic vesicle cargo proteins in synaptic vesicles. The following experiments address these predictions and provide evidence supporting our hypothesis that lysosomal and synaptic vesicle targeting mechanisms recognize similar proteins and deliver them to alternate destinations, either synaptic vesicles or lysosomes. Ultimately, our findings demonstrate a novel role for lysosomal sorting machineries in regulating the fate of synaptic vesicle membrane proteins and composition of synaptic vesicle fractions.

Materials and Methods

Antibodies

The following antibodies were used in this study: Monoclonal antibodies against GM130, TGN38, CD63, Vti1B, Syntaxin 8, and clathrin heavy chain were from BD Biosciences (Franklin Lakes, NJ); monoclonal antibodies (mAbs) against VGlut1, vesicular GABA transporter (VGAT), and vesicle-associated membrane protein (VAMP) 2 (69.1) and polyclonal antibodies against green fluorescent protein (GFP) and VAMP2 were from Synaptic Systems (Goettingen, Germany); polyclonal antibody against pallidin was from Proteintech Group (Chicago, IL); mAb against synaptophysin (SY38) and polyclonal antibody against microtubule-associated protein 2 were from Millipore Bioscience Research Reagents (Billerica, MA); mAb against transferrin receptor (H68.4) was from Zymed Laboratories/Invitrogen (Carlsbad, CA); mAb against tubulin was from Sigma-

Aldrich (St. Louis, MO); monoclonal antibodies against AP3-δ (SA4), synaptic vesicle (SV) 2 (10H4), mouse lysosomal membrane protein (LAMP) 1 (1D4B), and human LAMP1 (H4A3) were from Developmental Studies Hybridoma Bank (University of Iowa, Iowa City, IA); and polyclonal antibody against myc were from Bethyl Laboratories (Montgomery, TX). A mAb against lysobisphosphatidic acid (LBPA) (6CY) was the kind gift of Dr. Jean Gruenberg (University of Geneva, Geneva, Switzerland; (Kobayashi *et al.*, 1998)), whereas polyclonal antibodies against Syntaxin 13 and Sialin were the gifts of Drs. A. Peden (University of Cambridge, Cambridge, United Kingdom) and R. Reimer (Stanford University, Stanford, CA) respectively. The mAb against VAMP7-TI has been described in (Advani *et al.*, 1999) and is further characterized in Supplemental Figure 1. The polyclonal antibody against phosphatidylinositol-4-kinase type IIα (PI4KIIα) has been described in (Guo *et al.*, 2003). KF4 mAb against AP-3δ was developed by Dr. A. Peden and is described in (Craige *et al.*, 2008). Polyclonal antibodies against AP-3 σ3 and ZnT3 have been described in (Faundez *et al.*, 1998) and (Salazar *et al.*, 2004a), respectively.

DNA Constructs

VAMP2N49A-glutathione transferase (GST) is described in (Salem *et al.*, 1998). VAMP7-GST was a gift of Dr. A. Peden. Recombinant proteins were prepared as described previously (Roos and Kelly, 1998). Rab5Q79L-GFP plasmid and PC12 cell transfections were described previously (Craige *et al.*, 2008).

Oligonucleotide-mediated Small Interfering RNA (siRNA)

All siRNA constructs were obtained from Dharmacon RNA Technologies/Thermo Fisher Scientific (Lafayette, CO). The following oligonucleotide sequences were used to silence expression of human VAMP7-TI (Dharmacon siGENOME SMARTpool reagent M-020864-00-0005; human SYBL1, NM_005638): sense sequence (1): G.G.A.G.A.A.A.G.A.U.U.G.G.A.A.U.U.A.U.U.U and antisense sequence (1): 5'-P.A.U.A.A.U.U.C.C.A.A.U.C.U.U.U.C.U.C.C.U.U; sense sequence (2): G.U.A.C.U.C.A.C.A.U.G.G.C.A.A.U.U.A.U.U.U and antisense sequence (2): 5'-P.A.U.A.A.U.U.G.C.C.A.U.G.U.G.A.G.U.A.C.U.U; sense sequence (3): A.A.G.A.A.G.A.G.G.U.U.C.C.A.G.A.C.U.A.U.U and antisense sequence (3): 5'-P.U.A.G.U.C.U.G.G.A.A.C.C.U.C.U.U.C.U.U.U.U; and sense sequence (4): G.C.U.A.A.G.A.U.A.C.C.U.U.C.U.G.A.A.A.U.U and antisense sequence (4): 5'-P.U.U.U.C.A.G.A.A.G.G.U.A.U.C.U.U.A.G.C.U.U. As a control, we used Dharmacon siCONTROL NonTargeting siRNA Pool #1 D-001206-13-05.

Human embryonic kidney (HEK) or HeLa ATCC cells plated in six-well plates were grown to ~85% confluence and treated with a final concentration of 25 nM double-stranded VAMP7-TI along with 5 μl of Lipofectamine 2000 (Invitrogen) and 1 ml of Opti-MEM (Invitrogen). Control cells were treated in parallel with the same concentration of control siRNA. After 4-h incubation at 37°C and 10%CO2, 1 ml of 10% fetal bovine serum (FBS) DMEM was added to the cells. The following day, the cells were either left alone or grown in regular 10% FBS DMEM. After 24 h, the same transfection procedure was repeated again. The next day, cells were once again split into maintenance media, and after 24 h they were used for experimentation.

Animals

The *Ap3b1*$^{-/-}$ mouse strain was obtained from Dr. S. Mansour (University of Utah, Salt Lake City, UT) (Yang *et al.*, 2000). The *Ap3b2*$^{-/-}$ mouse strain was generated as described in (Seong *et al.*, 2005). *Ap3b1*$^{-/-}$, *Ap3b2*$^{-/-}$, and wild-type C57BL mice were all bred in-house at Emory University. *Muted*$^{mu/mu}$ (Zhang *et al.*, 2002) mice were obtained from Dr. R. Swank (Roswell Park Cancer Institute, Buffalo, NY) and bred in-house.

Cell Culture

PC12 cells were cultured in DMEM containing 10% horse serum, 5% fetal bovine serum, and 100 U/ml penicillin and 100 μg/ml streptomycin at 10% CO2 and 37°C. PC12 cells stably expressing ZnT3 were maintained with the addition of 0.2 mg/ml G418 (Salazar *et al.*, 2004b). HeLa ATCC cells were grown in DMEM containing 10% fetal bovine serum and 100 U/ml penicillin and 100 μg/ml streptomycin at 10% CO2 and 37°C (Craige *et al.*, 2008).

Mouse neocortical neurons were harvested from E18.5 embryos and prepared similarly to (Tippens and Lee, 2007). Briefly, neocortical tissue was dissociated by incubation with papain (Worthington Biochemicals, Lakewood, NJ) for 1 h at 37°C and 5% CO2, followed by tituration in 10% FBS minimal essential medium (MEM) inactivation solution. Cells were plated at an average density of 75,000 –100,000 cells/12-mm coverslip pre-coated with polylysine HBr (Sigma-Aldrich) in growth media containing 1 mM pyruvate, 0.6% dextrose, 5% fetal bovine serum, B-27 supplement (Invitrogen), 0.5 mM penicillin/streptomycin/glutamine, and 0.001% mito-serum extender (BD

Biosciences) and incubated at 5% CO2 and 37°C. After 72 h, 5 μM 1-β-D-arabinofuranosylcytosine was added. After 2 wk (days in vitro [DIV] = 14), cells were used for immunofluorescence.

Microscopy

Immunofluorescence was preformed as described in (Salazar *et al.*, 2004b) and (Craige *et al.*, 2008). Briefly, PC12 cells were plated on Matrigel (BD Biosciences)-coated coverslips, whereas primary neurons were cultured on polylysine HBr (Sigma-Aldrich)-coated coverslips. Images were acquired with a scientific-grade cooled charge-coupled device (CoolSNAP HQ with ORCAERchip) on a multiwavelength, wide-field, three-dimensional microscopy system (Intelligent Imaging Innovations, Denver, CO), based on a 200M inverted microscope using a 63X numerical aperture 1.4 lens (Carl Zeiss, Thornwood, NY). Immunofluorescent samples were imaged at room temperature using a Sedat filter set (Chroma Technology, Rockingham, UT), in successive 0.20-μm focal planes. Out-of-focus light was removed with a constrained iterative deconvolution algorithm (Swedlow *et al.*, 1997). Images were processed and analyzed using MetaMorph software version 3.0 (Molecular Devices, Sunnyvale, CA). Three consecutive z-series were analyzed per image by thresholding to similar levels and determining colocalization as the percentage of pixel area overlap for the respective channels.

Labeled Epidermal Growth Factor (EGF) Internalization

PC12 cells plated on Matrigel coated-coverslips were serum deprived overnight with 0.1% FBS DMEM. Cells were labeled on ice with 100 nM fluorescein-conjugated EGF (E-3478; Invitrogen). After labeling, cells were washed with cold phosphate-buffered saline (PBS). EGF fluorescein was internalized by adding warm DMEM for 5, 15, or 30 min, and incubating the cells at 37°C. After internalization, cells were fixed, immunostained, and imaged as described in the microscopy section.

Subcellular Fractionation

Brains from 12 C57B, eight *Ap3b2*$^{-/-}$, nine *Ap3b1*$^{-/-}$, eight *Muted*$^{mu/mu}$, and eight *Muted*$^{+/mu}$ mice aged 7–12 wk were fractionated according to (Craige *et al.*, 2004) and (Salazar *et al.*, 2004a). Synaptic vesicle fractions were resolved by 5–25% glycerol gradient velocity sedimentation. All brains from the same genotype were processed together. Purified rat brain synaptic vesicles were prepared as described previously (Clift-O'Grady *et al.*, 1990; Craige *et al.*, 2004).

Subcellular Fractionation of PC12 cells and PC12 cells expressing ZnT3 (Salazar *et al.*, 2004b) was performed according to the Clift–O'Grady method as described in (Clift-O'Grady *et al.*, 1990), (Craige *et al.*, 2004), and (Salazar *et al.*, 2004a). Synaptic-like microvesicle (SLMV) fractions were resolved by 5–25% glycerol gradient velocity sedimentation. Immunomagnetic vesicular isolation of PC12 vesicles and mouse brain synaptic vesicles was performed as detailed in (Craige *et al.*, 2004) and (Salazar *et al.*, 2004a). Quantification of immunoreactive bands on glycerol gradient Western blots was done using NIH Image 1.63f (Grote *et al.*, 1995; Salazar *et al.*, 2004b).

Dithiobis(succinimidyl Propionate) (DSP) Cross-Linking of AP-3 Immunocomplexes

DSP Cross-linking of AP-3 immunocomplexes and their isolation has been described in (Craige *et al.*, 2008) and (Salazar *et al.*, 2009).

Statistics

All data are expressed as average ± SE. Experimental conditions were compared with the one-way analysis of variance followed by Student–Newman–Keuls multiple comparison as a post hoc test by using KaleidaGraph version 3.6.2 (Synergy, Reading, PA). Kolmogorov–Smirnov test was performed using the engine http://www.physics.csbsju.edu/stats/KS-test.n.plot_form.html.

Results

AP-3–sorted Lysosomal Cargoes and Synaptic Vesicle Membrane Proteins Colocalize in Early Endosomes

Purified PC12 cell synaptic-like microvesicles and rat brain synaptic vesicles copurify with proteins either targeted to or involved in the biogenesis of lysosomes. These include AP-3 and BLOC-1 subunits as well as AP-3 cargo membrane proteins such as PI4KIIα, the lysosomal vesicle-(R)-soluble *N*-ethylmaleimide-sensitive factor attachment protein receptor (SNARE) VAMP7-TI, LAMP-1, and chloride channel-3 (Salazar *et al.*, 2005b; Takamori *et al.*, 2006). A conventional view of the organization of endosomes in neurons would predict that synaptic vesicle proteins would recycle back to the cell surface. Thus,

synaptic vesicle proteins would be segregated from lysosomal cargoes, which are bound to late endosome and lysosome compartments. In contrast, our seesaw model predicts that synaptic vesicle proteins and lysosomal AP-3 cargoes will coexist in the same donor endosomes as well as in synaptic vesicles. To discriminate between these models, we explored whether 1) lysosomal and synaptic vesicle cargoes are sorted from shared donor endocytic compartments, and 2) whether they are targeted into the same synaptic vesicle.

As a first step, we determined whether synaptic vesicle and AP-3–sorted lysosomal membrane proteins colocalize at steady state in PC12 cells and cultured mouse primary neurons by immunomicroscopy. This approach does not distinguish between whether this colocalization occurs in either a donor early endosome, synaptic vesicles, or both types of organelle. We used quantitative wide-field deconvolution immunofluorescence microscopy of cells labeled with combinations of antibodies against AP-3–sorted lysosomal membrane proteins (PI4KIIα, cd63, LAMP1, and VAMP7-TI), bona fide synaptic vesicle membrane proteins (the SNARE synaptobrevin 2/VAMP2 and ZnT3), and/or late endosomal markers (syntaxin 8, Vti1b, and LBPA) (Baumert *et al.*, 1989; Le Borgne *et al.*, 1998; Cole *et al.*, 1999; Dell'Angelica *et al.*, 1999; Rous *et al.*, 2002; Martinez-Arca *et al.*, 2003; Peden *et al.*, 2004; Salazar *et al.*, 2004b; Salazar *et al.*, 2005b; Salazar *et al.*, 2006; Craige *et al.*, 2008). If synaptic vesicle proteins are segregated from lysosomal cargoes, a basic prediction is that colocalization of either ZnT3 or VAMP2 with AP-3 lysosomal cargoes should be negligible at steady state. In contrast, if SV and lysosomal cargoes are sorted from shared early endosomes into synaptic vesicles then the colocalization between synaptic vesicle

proteins and AP-3 lysosomal cargo will exceed the colocalization between synaptic vesicle proteins and late endosomal markers. However, this does not exclude that AP-3 lysosomal cargoes, like VAMP7-TI, will significantly colocalize with traditional late endosomal-lysosomal markers. We tested this latter prediction by using the late endosomal SNAREs syntaxin 8 and Vti1b, which form cognate SNARE pairs with VAMP7-TI, but not VAMP2 (Antonin *et al.*, 2000; Wade *et al.*, 2001; Bogdanovic *et al.*, 2002; Pryor *et al.*, 2004). Predictably, ~30% of late endosomes immunoreactive for vti1b or syntaxin 8 also possessed VAMP7-TI (Figure 1B and Supplemental Figure 3). Yet, VAMP2 was present in only ~10% of vti1b- or syntaxin 8-positive late endosomes (Figure 1B, and Supplemental Figure 3). This

colocalization value is similar to a background colocalization of 3–7% defined by the overlap of either VAMP2 or VAMP7-TI with Golgi markers (Figure 1B and Supplemental Figure 4, GM130 and TGN38). These results, obtained in PC12 cells, indicate that synaptic vesicle SNARE VAMP2 is below detection level in late endosome compartments at steady state.

In contrast with a conventional model where synaptic vesicle and lysosomal AP-3 cargoes are segregated into distinct organelles, our model predicts that AP-3–sorted lysosomal membrane proteins should colocalize with synaptic vesicle membrane markers in endosomes and synaptic vesicles. Although synaptobrevin/VAMP2 is not detectable in late endosomes, 36.6 ± 5% of VAMP2 colocalized with VAMP7-TI (Figure 1, A and B, and Supplemental Figure 2). Antibodies against VAMP2 and VAMP7-TI did not cross-react (Supplemental Figure 1). Similarly, VAMP7-TI colocalized extensively with the

synaptic vesicle protein ZnT3 (Figure 1, A and B). The colocalization between the synaptic vesicle SNARE VAMP2 and the AP-3 lysosomal cargo VAMP-7-TI was also observed with other AP-3 lysosomal cargoes. In fact, ~30–40% of VAMP2-positive compartments were also positive for the lysosomal AP-3 cargoes PI4KIIα and CD63 (Figure 1, A and B, and Supplemental Figure 2). The colocalization of VAMP2 with AP-3 lysosomal cargoes (cd63, PI4KIIα, and VAMP7-TI) exceeds by approximately two- to threefold VAMP2 colocalization with diverse late endosomal markers (syntaxin 8, vti1b, and LBPA) (Kobayashi *et al.*, 1998; Lebrand *et al.*, 2002) (Figure 1B and Supplemental Figures 3 and 4). These results suggest that the synaptic vesicle SNARE VAMP2 and AP-3 lysosomal cargoes coexist in an endosome upstream of late endosomal compartments.

We used three strategies to define whether synaptic vesicle proteins and AP-3 lysosomal cargoes occupy the same early endosome donor compartment. First, we assessed whether VAMP2 and the AP-3 lysosomal cargoes VAMP7-TI and PI4KIIα were present in endosomes positive for the adaptor complex AP-3. This adaptor complex has been localized to early endosomes in diverse cell types, including PC12 cells (Dell'Angelica *et al.*, 1997; Peden *et al.*, 2004; Theos *et al.*, 2005; Craige *et al.*, 2008). AP-3 was present in 25–50% of those structures immunoreactive for the synaptic vesicle membrane protein VAMP2 or AP-3 lysosomal cargoes (VAMP7-TI and PI4KIIα, Figure 1B and Supplemental Figure 2). Second, we transfected PC12 cells with rab5Q79L-GFP to enlarge early endosomes. The limiting membrane of these enlarged endosomes is highlighted by the GFP signal, allowing the identification of membrane proteins present in these endosomes (Raiborg *et al.*, 2002; Raiborg *et al.*, 2006; Craige *et al.*, 2008).

VAMP2 colocalized with AP-3 lysosomal cargoes (VAMP7-TI and PI4KIIα) and AP-3 in the limiting membrane of enlarged early endosomes (Figure 2A). This colocalization was above the level observed between VAMP2 and transferrin receptor, a receptor not trafficked by AP-3 (Figure 2B) (Dell'Angelica *et al.*, 1999). Additional controls revealed that PC12 rab5Q79L-enlarged endosomes are almost devoid of the adaptor complex AP-1 (Craige *et al.*, 2008). Third, we labeled endosomes with surface internalized fluorescently labeled-EGF (Figure 3). Fluorescein-EGF was bound at 4°C, and unbound ligand was washed away. EGF internalization was resumed at 37°C for either 5–15 min to label early endosomes or 30 min to label late endosomes (de Wit *et al.*, 1999). EGF reached compartments positive for VAMP2 and the lysosome AP-3 cargoes (VAMP7-TI and CD63) between 5 and 15 min (Figure 3A). However, EGF moved away from VAMP2-positive endosomes after 30 min, yet progressively accumulated in late endosomal compartments also positive for VAMP7-TI and CD63 (Figure 3, A and B). This is consistent with the steady-state colocalization analysis of PC12 cells, in which VAMP7-TI, but not VAMP2, significantly colocalizes with late-endosomal markers. These combined results from steady-state colocalizations, rab5Q79L-enlarged early endosomes, and pulse-chase with fluorescently labeled internalized EGF demonstrate that synaptic vesicle proteins and AP-3 lysosomal cargoes coexist in early endosome donor compartments but not late endosomes.

We further explored the extent of overlap between synaptic vesicle membrane proteins and lysosomal AP-3 cargoes in mouse primary neocortical neurons. Mouse primary neurons recapitulate our central findings in PC12 cells. For example, within the cell body of mouse primary neurons VAMP2 colocalizes

with AP-3–sorted lysosomal proteins VAMP7-TI and LAMP1 to the same extent that these two lysosomal proteins colocalize together (Figure 4 and Supplemental Figure 5). Immunoreactivity for VAMP2 or VAMP7-TI is present in cell body compartments also positive for AP-3 (Figure 4 and Supplemental Figure 5). Furthermore, the signal overlap between VAMP2 and lysosomal AP-3 cargoes in neuronal cell bodies was significantly above the colocalization of either VAMP2 or VAMP7-TI with the late endosomal marker LBPA (Supplemental Figure 5). The low colocalization of VAMP7-TI with LBPA in primary cultures of neurons and PC12 cells may be due to the fact that LBPA labels a limited set of late endosomes in other cell types (White *et al.*, 2006). In contrast with cell bodies, although we were still able to resolve distinct punctae in which synaptic vesicle proteins and lysosomal AP-3 cargoes colocalize, the overlap between VAMP2 and VAMP7-TI in neuronal processes was similar to the overlap of either one of these markers with LBPA (Supplemental Figure 5). This finding was the same regardless of whether processes where further classified as dendrites or axons (Supplemental Figure 5). The constrained architecture of slender cellular processes likely contributes to the overlap of VAMP2 and VAMP7-TI with LBPA. However, the entry of VAMP2 and VAMP7 into a shared synaptic vesicle compartment was also addressed by biochemical vesicular isolation (see below).

Collectively, our results in PC12 cells and primary cultured neurons favor a model in which at steady-state synaptic vesicle proteins and AP-3 lysosomal cargoes reside in shared early endosomes. From this donor compartment, synaptic vesicle and AP-3 lysosomal cargoes may be sorted to a common synaptic

vesicle if they interact with synaptic vesicle biogenesis machinery on early endosomes, which includes the neuronal AP-3 complex.

Lysosomal AP-3 Cargoes and Synaptic Vesicle Membrane Proteins Are Sorted to Common Synaptic-like Microvesicles and Synaptic Vesicles

We tested whether synaptic vesicle proteins and AP-3 lysosomal cargoes are sorted into a common vesicle by analyzing the composition of synaptic-like microvesicles and brain synaptic vesicles. PC12 synaptic-like microvesicles are generated from early endosomes (Faundez *et al.*, 1998; Lichtenstein *et al.*, 1998; de Wit *et al.*, 1999). PC12 synaptic-like microvesicles were isolated by differential centrifugation and size fractionated in glycerol gradients (Figure 5A). VAMP2 and AP-3–sorted lysosomal proteins (PI4KIIα and VAMP7-TI) comigrated in similarly sized vesicles (~40 nm; (Schmidt *et al.*, 1997; Salazar *et al.*, 2005b)). To determine whether these proteins reside on the same vesicle, glycerol gradient peak fractions (Figure 5A, underlined fractions) were used for immunomagnetic vesicle isolation. Synaptic-like microvesicles were immunoisolated using monoclonal antibodies that recognize cytosolic epitopes in the synaptic vesicle protein VAMP2 or the AP-3 lysosomal cargo VAMP7-TI (Figure 5B, lanes 3 and 4 and 6 and 7). Antibodies against late endosome SNARE Vti1b were used as controls (Figure 5B, lanes 2 and 5). Late endosomes are virtually absent from synaptic-like microvesicles and brain synaptic vesicle fractions (Supplemental Figure 6). Thus, no bound vesicles were expected with vti1b-beads, equating this control to a nonspecific antibody control. Synaptic-like microvesicles bound by

antibodies against either VAMP2 or VAMP7-TI contained AP-3–sorted lysosomal proteins PI4KIIα and VAMP7-TI in addition to known synaptic vesicle proteins VAMP2 and ZnT3 (Salazar *et al.*, 2004b). No vesicle binding was observed with magnetic beads decorated with Vti1b antibodies (Figure 5B, lanes 2 and 5). Similarly, VAMP2 and AP-3–sorted lysosomal proteins (VAMP7-TI, PI4KIIα, and LAMP1) comigrated in mouse brain synaptic vesicles resolved by glycerol sedimentation (Figure 5C). Brain synaptic vesicles immunoisolated with monoclonal antibodies against VAMP2 contained AP-3–sorted lysosomal proteins (VAMP7-TI, PI4KIIα, and LAMP1; Figure 5D, lanes 3 and 5) as well as known synaptic vesicle proteins (ZnT3 and SV2). Synaptic vesicle binding to control beads was negligible (Figure 5D, lanes 2 and 4). Similar results were obtained when synaptic vesicles were purified from rat brain by a different procedure (data not shown; (Clift-O'Grady *et al.*, 1990)). Thus, biochemical characterization of both PC12 cell synaptic-like microvesicles and mouse brain synaptic vesicles demonstrates that synaptic vesicle proteins and lysosomal AP-3 cargoes are sorted into a common organelle.

Hermansky–Pudlak Gene Products Involved in Lysosome and Lysosome-related Organelle Biogenesis Control the Composition of Synaptic Vesicle Fractions

Synaptic vesicle and lysosomal membrane proteins are present in a common donor early endosome that is positive for the adaptor complex AP-3. This raises the question as to which adaptor(s) sort(s) lysosomal proteins into synaptic vesicle fractions. We analyzed the content of synaptic vesicle and

lysosomal AP-3 cargoes in synaptic vesicle fractions isolated from control, *Ap3b1*$^{-/-}$ and *muted*$^{mu/mu}$ mouse brains. These two mutants disrupt subunits of the ubiquitous AP-3 and BLOC-1 complexes, which are affected in Hermansky–Pudlak syndrome, a disorder that affects the biogenesis of lysosomes and lysosome-related organelles (Di Pietro and Dell'Angelica, 2005; Raposo and Marks, 2007). We contrasted the effects of these mutations with *Ap3b2*$^{-/-}$, a mutant that affects the neuronal AP-3 complex and is involved in synaptic vesicle biogenesis (Nakatsu *et al.*, 2004; Seong *et al.*, 2005).

We first determined whether the interaction between AP-3 and BLOC-1 complexes observed in nonneuronal cells (Di Pietro *et al.*, 2006; Salazar *et al.*, 2009) is recapitulated in PC12 cells and mouse primary cultured neurons (Figure 6, A and B, respectively). We used in vivo DSP cross-linking to stabilize AP-3 interactors (Craige *et al.*, 2008). Cross-linked AP-3 complexes from PC12 cells and neurons were immunoprecipitated with antibodies against the AP-3 δ subunit and immunocomplexes analyzed by Western blot. We identified the following cargoes: PI4KIIα in AP-3 precipitates from cross-linked PC12 and mouse primary neurons (Figure 6A, compare lanes 3 and 4; Figure 6B, compare lanes 3 and 4) and PI4KIIα and ZnT3 in AP-3 precipitates from cross-linked PC12-ZnT3 cells (Figure 6A, compare lanes 5 and 6). Importantly, cross-linked AP-3 complexes from all these cells contained BLOC-1 detected with antibodies against the BLOC-1 subunit pallidin (Falcon-Perez *et al.*, 2002; Ciciotte *et al.*, 2003). The specificity of these interactions was confirmed in immunoprecipitations with transferrin receptor antibodies, which were free of AP-3 subunits, pallidin, PI4KIIα, and ZnT3 (Figure 6, A and B, lanes 1 and 2).

Moreover, transferrin receptor and synaptophysin, two proteins whose targeting is not affected by AP-3 deficiencies were absent from AP-3 immunocomplexes (Figure 6, A and B) (Dell'Angelica *et al.*, 1999; Salazar *et al.*, 2004b). The presence of PI4KIIα and BLOC-1 in cross-linked AP-3 complexes predicts that the targeting of PI4KIIα to synaptic vesicle fractions should be perturbed in AP-3 and BLOC-1 deficiencies. In contrast, synaptophysin, which is absent from cross-linked complexes, should remain unaffected.

To assess sorting of synaptic vesicle proteins and lysosomal AP-3 cargoes to synaptic vesicles, synaptic vesicle fractions were isolated by glycerol sedimentation of high-speed brain supernatants. In these gradients, synaptic vesicles migrate in the middle of the gradient as a symmetric peak. Defective sorting of a defined protein is assessed either by changes in its distribution and/or content in the gradient (Grote *et al.*, 1995; Schmidt *et al.*, 1997; Clift-O'Grady *et al.*, 1998; Thiele *et al.*, 2000; Craige *et al.*, 2004; Salazar *et al.*, 2004b). Synaptic vesicle membrane protein contents were analyzed by SDS-polyacrylamide gel electrophoresis (PAGE) and Western blotting for specific synaptic vesicle proteins (ZnT3, VGAT, synaptophysin, VAMP2, Vglut1, and SV2; (Takamori *et al.*, 2006)) and AP-3 lysosomal cargoes (PI4KIIα and VAMP7-TI). For lysosomal cargo, we focused on PI4KIIα and VAMP7-TI because these proteins are reliably detected in synaptic vesicles fractions (Salazar *et al.*, 2005b; Salazar *et al.*, 2006). Moreover, PI4KIIα and VAMP7-TI accumulate in the cell body and are depleted from nerve terminals of neurons lacking both AP-3 isoforms (*mocha*) (Salazar *et al.*, 2005b; Scheuber *et al.*, 2006).

Consistent with the presence of PI4KIIα and BLOC-1 in cross-linked AP-3 complexes (Figure 6), the distribution of PI4KIIα in glycerol gradients was modified in all AP-3 and BLOC-1 deficiencies tested (Figures 7 and 8). In contrast, neither the glycerol gradient distribution nor content of synaptophysin, a protein absent from cross-linked AP-3 complexes, was altered in AP-3 or BLOC-1-null brain synaptic vesicle fractions (Figures 7 and 8). These results indicate that glycerol velocity sedimentation of vesicles isolated from wild-type and mutant brains discriminates the sorting phenotypes of membrane proteins predicted from AP-3 cross-linked complexes (Figure 6).

We explored two seesaw model predictions by using this experimental paradigm. First, we asked whether the targeting of characteristic synaptic vesicle proteins to synaptic vesicle fractions was altered by deficiencies in transport to lysosomes and/or lysosome-related organelles (*Ap3b1*$^{-/-}$, *muted*$^{mu/mu}$). The seesaw model predicts that in the absence of ubiquitous AP-3 (*Ap3b1*$^{-/-}$) or BLOC-1 (*muted*$^{mu/mu}$), AP-3 cargoes that normally would have been sorted to lysosomes would instead be routed to synaptic vesicles. The content of the synaptic vesicle proteins ZnT3, VGAT, VAMP2, and the lysosomal AP-3 cargo VAMP7-TI was increased in *Ap3b1*$^{-/-}$ synaptic vesicle fractions. In addition, the synaptic vesicle proteins Vglut1 and the lysosomal AP-3 cargo PI4KIIα sedimented faster in fractions isolated from *Ap3b1*$^{-/-}$ (Figure 7). Vglut1 and PI4KIIα sedimentation in *Ap3b1*$^{-/-}$ is consistent with a potential mistargeting into larger vesicles. In contrast with the pleiotropic effects of *Ap3b1*$^{-/-}$ in synaptic vesicle composition, *muted*$^{mu/mu}$ only affected the targeting of VAMP7 and PI4KIIα (Figure 8). Much like *Ap3b1*$^{-/-}$, the content of VAMP7-TI was increased

in synaptic vesicle fractions, whereas PI4KIIα sedimented faster in synaptic vesicle fractions isolated from *muted*$^{mu/mu}$ brains (Figure 8). These changes in the targeting of synaptic vesicle proteins and AP-3 lysosomal cargoes observed in *Ap3b1*$^{-/-}$ and *muted*$^{mu/mu}$ were not due to the presence of contaminant recycling or late endosome markers comigrating with synaptic vesicles (Supplemental Figure 6, (Sagne and Gasnier, 2008)). Furthermore, these changes in vesicle composition were not attributable to overall changes in the expression of these proteins in mutant brains (Supplemental Figure 9). Nor are our results attributable to global changes in synaptic vesicle protein fractionation, as indicated by the normal content and distribution of synaptophysin and SV2 in *Ap3b1*$^{-/-}$ vesicle fractions, or ZnT3, VGAT, synaptophysin, VAMP2, Vglut1, and SV2 in vesicles isolated from *muted*$^{mu/mu}$ brains (Figures 7 and 8). Second, we asked whether neuronal AP-3 directs the incorporation of AP-3 lysosomal cargo into synaptic vesicle fractions by examining synaptic vesicles isolated from the neuronal AP-3–deficient, *Ap3b2*$^{-/-}$, mouse brain. The seesaw model predicts that in the absence of neuronal AP-3, lysosomal AP-3 cargoes that normally would have been targeted to synaptic vesicles would be reduced in synaptic vesicles because of their increased routing to lysosome compartments. The content of the lysosomal cargo VAMP7-TI was decreased in synaptic vesicle fractions from *Ap3b2*$^{-/-}$ (Figure 7). In addition, PI4KIIα glycerol sedimentation pattern was altered by the absence of neuronal AP-3 (Figure 7). This altered distribution could reflect the dual role for PI4KIIα as both an AP-3 recruitment factor and AP-3 cargo (Craige *et al.*, 2008). As reported previously and consistent with neuronal AP-3's role in synaptic vesicle biogenesis, ZnT3 and VGAT targeting to

synaptic vesicle fractions was decreased in *Ap3b2*$^{-/-}$ mouse brain vesicles (Figure 7) (Nakatsu *et al.*, 2004; Seong *et al.*, 2005). These results indicate that lysosomal (ubiquitous AP-3 and BLOC-1) and synaptic vesicle targeting mechanisms (neuronal AP-3) control the delivery of characteristic synaptic vesicle and AP-3–sorted lysosomal membrane proteins to a common synaptic vesicle. Moreover, our data indicate that cargoes sorted by neuronal AP-3, ubiquitous AP-3, or BLOC-1 are partially overlapping.

Discussion

Synapses depend on vesicle biogenesis mechanisms to deliver membrane proteins from the cell body to nerve terminals. Current models that account for membrane protein delivery to synaptic compartments do not consider the contribution of lysosome biogenesis mechanisms. In fact, lysosomal sorting and synaptic vesicle biogenesis machinery are thought to regulate mutually exclusive cargo proteins. However, our work challenges this model by presenting evidence for a mechanism where both lysosomal sorting and synaptic vesicle biogenesis machinery jointly regulate both synaptic vesicle and lysosomal cargo proteins from shared early endosome donor compartments. We have referred to this mechanism as the seesaw model, because both sorting machineries are necessary for a properly balanced synaptic vesicle composition. First, we provide high-resolution microscopy evidence, indicating that lysosomal and synaptic vesicle membrane proteins coexist with AP-3 in early endosomes. From these endosomes, synaptic vesicle and AP-3 lysosomal cargoes are sorted into synaptic-like microvesicles of PC12 cells and synaptic vesicles of mouse brain. Second, we

demonstrate that deficiencies in an AP-3 adaptor isoform involved in lysosome biogenesis (ubiquitous AP-3, *Ap3b1*$^{-/-}$) lead to changes in the targeting of characteristic synaptic vesicle membrane proteins (ZnT3, VGAT, VAMP2, and Vglut1) to synaptic vesicle fractions. Third, we demonstrate that mutant mice lacking an adaptor involved in the sorting of synaptic vesicle proteins (neuronal AP-3, *Ap3b2*$^{-/-}$) exhibit decreased targeting of several membrane proteins to synaptic vesicle fractions (Figure 7). Predictably, a group of synaptic vesicle membrane proteins is affected in *Ap3b2*$^{-/-}$ brains (ZnT3, VGAT, and SV2) (Figure 7). However, a more significant finding is the perturbed targeting of lysosomal proteins (VAMP7-TI and PI4KIIα) by a deficiency in a synaptic vesicle-sorting mechanism (Figure 7). Fourth, we show that mouse models defective in protein complexes involved in the biogenesis of lysosomes and lysosome-related organelles (ubiquitous AP-3, *Ap3b1*$^{-/-}$, and BLOC-1, *muted*$^{mu/mu}$) possess increased levels of membrane proteins found in lysosomes (VAMP7-TI and PI4KIIα) in their synaptic vesicle fractions.

How do ubiquitous and neuronal AP-3 regulate membrane protein content in synaptic vesicle fractions? A model ought to account for both the opposite effects that deficiencies in these adaptor complexes have in the targeting of ZnT3, VAMP7-TI, or VGAT to synaptic vesicle fractions. Although ubiquitous AP-3 deficiency in *Ap3b1*$^{-/-}$ mice increases the content of these proteins in synaptic vesicle fractions (Figure 7), in contrast, the absence of neuronal AP-3 in *Ap3b2*$^{-/-}$ mice decreases their content in synaptic vesicle fractions (Figure 7). The simplest explanation is that ubiquitous and neuronal AP-3 complexes compete for these cargoes to deliver them to two alternative fates. Neuronal AP-3 would deliver

these proteins into vesicles bound to nerve terminals and away from the lysosomal route controlled by the ubiquitous AP-3 complex (Dell'Angelica *et al.*, 1999; Robinson, 2004; Newell-Litwa *et al.*, 2007). Thus, both adaptors would behave as branches of a seesaw, such that in the absence of one AP-3 isoform the other sorting route would experience an increased availability of membrane proteins for delivery. For example, in the absence of ubiquitous AP-3, membrane proteins that otherwise would have been destined for late endosomes-lysosomes are rerouted to synaptic vesicle fractions by neuronal AP-3.

This seesaw mechanism would define the composition of synaptic vesicle precursors leaving the cell body. This model, which integrates divergent AP-3 sorting routes at the level of cell body endosomes, provides a conceptual framework to understand: 1) the coexistence of both AP-3 isoforms in neuronal cell bodies (Seong *et al.*, 2005); 2) the convergence of AP-3, synaptic vesicle, and lysosomal membrane proteins in early endocytic compartments in PC12 and primary cultured neurons (Figures 1–4); 3) the observation that the absence of both AP-3 isoforms in *mocha* (*Ap3d*$^{mh/mh}$) leads to a depletion of ZnT3, VAMP7-TI and PI4KIIα from nerve terminals concomitantly with their accumulation in cell bodies (Kantheti *et al.*, 1998; Salazar *et al.*, 2004b; Salazar *et al.*, 2005b; Scheuber *et al.*, 2006); 4) the previously puzzling identification of diverse late endosomal/lysosomal proteins, such as Npc1, dysbindin, vps33b, rab7, ClC-3, VAMP7-TI, LAMP-1, and PI4KIIα, in either developing axonal projections, nerve terminals, synaptic-like microvesicles, and/or synaptic vesicles (Overly and Hollenbeck, 1996; Stobrawa *et al.*, 2001; Guo *et al.*, 2003; Talbot *et al.*, 2004; Salazar *et al.*, 2005b; Saxena *et al.*, 2005; Arantes and Andrews, 2006; Deinhardt

et al., 2006; Karten *et al.*, 2006; Salazar *et al.*, 2006; Takamori *et al.*, 2006; Talbot *et al.*, 2006). Consistent with a role for AP-3–dependent targeting of lysosomal proteins to a synaptic vesicle fate, all of these lysosomal proteins found in axonal-synaptic compartments are either present in AP-3–derived vesicles or they genetically and/or biochemically interact with AP-3 (Stepp *et al.*, 1997; Le Borgne *et al.*, 1998; Dell'Angelica *et al.*, 1999; Martinez-Arca *et al.*, 2003; Salazar *et al.*, 2004a; Salazar *et al.*, 2005b; Newell-Litwa *et al.*, 2007). Despite the fact that competitive AP-3 sorting would be limited to the cell body, in which both AP-3 isoforms are present, the seesaw model does not preclude an individualized role for neuronal AP-3 directly in pre-synaptic terminals.

How do our results illuminate the sorting mechanisms controlled by AP-3 isoforms and the BLOC-1 complex? Membrane transport pathways are typically explored by analyzing a single cargo reporter. However, key concepts in membrane protein sorting have emerged from a collective view of the behavior of multiple cargoes in a trafficking route (Motley *et al.*, 2003; Traub, 2003). Therefore, to comprehensively assess the role of AP-3 isoforms and BLOC-1 in membrane protein sorting, we simultaneously analyzed the targeting of multiple synaptic vesicle and/or lysosomal membrane proteins. We took advantage of the defined composition of synaptic vesicles, the availability of multiple AP-3 cargoes, as well as mouse deficiencies in AP-3 isoforms and BLOC-1. The picture that emerges from our studies is that deficiencies in neuronal AP-3, ubiquitous AP-3 and BLOC-1 affect the targeting of a core group of membrane proteins constituted at least by VAMP7-TI and PI4KIIα. PI4KIIα is found in a complex with AP-3 and BLOC-1 subunits in neurons and the inclusion of PI4KIIα into

crosslinked AP-3 complexes is decreased in BLOC-1–deficient fibroblasts (Figure 6; (Salazar *et al.*, 2009)). These results could be interpreted as BLOC-1 acting as a factor that facilitates AP-3 recognition of cargoes such as VAMP7-TI and PI4KIIα (Di Pietro *et al.*, 2006; Salazar *et al.*, 2006). However, how can we understand the difference in affected cargoes between synaptic vesicle fractions from ubiquitous AP-3 deficient (*Ap3b1*$^{-/-}$) BLOC-1 deficient (*muted*$^{mu/mu}$) mouse brain? On one hand, BLOC-1 could serve as a cargo-specific adaptor, similar to β-arrestin, epsins, or autosomal recessive hypercholesterolemia protein, which bind selected membrane proteins and bring them into nascent AP-2–derived clathrin-coated vesicles (Traub, 2003). Our observations resemble these findings in that AP-3 and BLOC-1 are found in a complex (Figure 6), and BLOC-1 affects the targeting of a restricted subset of AP-3 cargoes (Figure 8). Alternatively, BLOC-1 could participate in a sorting mechanism independent of AP-3 isoforms, as is the case for ATP7A and Tyrp1, whose sorting to melanosomes, a lysosome related organelle, is independent of AP-3 (Setty *et al.*, 2007; Setty *et al.*, 2008).

In addition to PI4KIIα and VAMP7-TI, neuronal and ubiquitous AP-3 deficiencies also regulate synaptic vesicle targeting of membrane proteins not affected by BLOC-1 (ZnT3 and VGAT) (compare gradients in Figures 7 and 8). Yet, other synaptic vesicle membrane proteins (VAMP2, Vglut1, and SV2) are affected by a deficiency in just one of the AP-3 isoforms (Figure 7). These results support the notion that both AP-3 isoforms recognize distinct, as well as overlapping, membrane protein cargoes independently of BLOC-1. Furthermore, our results indicate that not all synaptic vesicle proteins reach synaptic vesicle pools through an AP-3–BLOC-1 route. A clear example is synaptophysin. This

protein does not interact with AP-3; rather, it associates with the AP-1 adaptor or components of the AP-2 vesicle biogenesis machinery (Figure 6) (Daly and Ziff, 2002; Horikawa *et al.*, 2002). Predictably, neither AP-3 nor BLOC-1 deficiencies explored here, nor *Ap3d*$^{mh/mh}$ and *Ap3m2*$^{-/-}$ deficiencies, affect synaptophysin targeting to nerve terminals/synaptic vesicle fractions (Figures 7 and 8) (Nakatsu *et al.*, 2004; Salazar *et al.*, 2004b).

Our research reveals significant alterations in the content of critical neurotransmitter and ionic transporters within synaptic vesicle fractions of mice deficient for AP-3 and BLOC-1 endocytic transport (Figures 7 and 8). Whereas neuronal AP-3 deficiencies selectively affect the inhibitory neurotransmitter transporter VGAT, ubiquitous AP-3 deficiencies modulate the synaptic vesicle levels of VGAT as well as the excitatory neurotransmitter transporter, VGlut1 (Figure 7). In *Ap3m2*$^{-/-}$ mouse brain, just a partial reduction of VGAT in synaptic vesicles directly correlates with decreased inhibitory neurotransmission (Ohno *et al.*, 1999). Therefore, the up-regulation of both VGlut1 and VGAT could affect both inhibitory and excitatory neurotransmission, especially with increasing evidence that pre-synaptic mechanisms, such as the content of neurotransmitter transporters in synaptic vesicles, modulate quantal size (Edwards, 2007). Diverting neurotransmitter transporters to synaptic vesicles by a seesaw mechanism could change the luminal content of neurotransmitters. Consistent with this idea, brefeldin A inhibition of AP-3–dependent sorting restores not only VGlut1 recycling but also excitatory neurotransmission, under high-frequency stimulation (Voglmaier *et al.*, 2006). Similarly, increased levels of ZnT3 in ubiquitous AP-3 null (*Ap3b1*$^{-/-}$) brain synaptic vesicles correlate with enhanced

histochemically reactive zinc in brain tissue (Seong *et al.*, 2005). Thus, a seesaw mechanism defining synaptic vesicle composition could regulate quantal size independent of transcriptional regulation. Finally, our model may provide a complementary view to understand the association of deficiencies affecting lysosomes or lysosome trafficking mechanisms with synaptic defects. This association is illustrated in *Drosophila*, *Caenorhabditis elegans*, as well as neurodegenerative disorders in humans (Narayanan *et al.*, 2000; Nixon *et al.*, 2000; Bahr and Bendiske, 2002; Skibinski *et al.*, 2005; Ramirez *et al.*, 2006; Rubinsztein, 2006; Sweeney *et al.*, 2006; Grill *et al.*, 2007). In these abnormal states, perturbed synaptic function follows cell and/or synapse loss due to product buildup. Thus, late endosomes and lysosomes are thought to just dispose of unwanted molecules preventing product amassment. However, our findings offer a mechanism that expands the function of lysosome trafficking by linking lysosomes with synaptic vesicle composition.

Acknowledgements

We are indebted to the Faundez laboratory members, Dr. Erica Werner, and anonymous reviewer 2 for helpful comments. This work was supported by National Institutes of Health grants NS-42599 and GM-077569 (to V. F.) and F31NS058163 (to K.N.-L.). K.N.-L. was supported by a grant-in-aid of research from the National Academy of Sciences, administered by Sigma Xi, The Scientific Research Society.

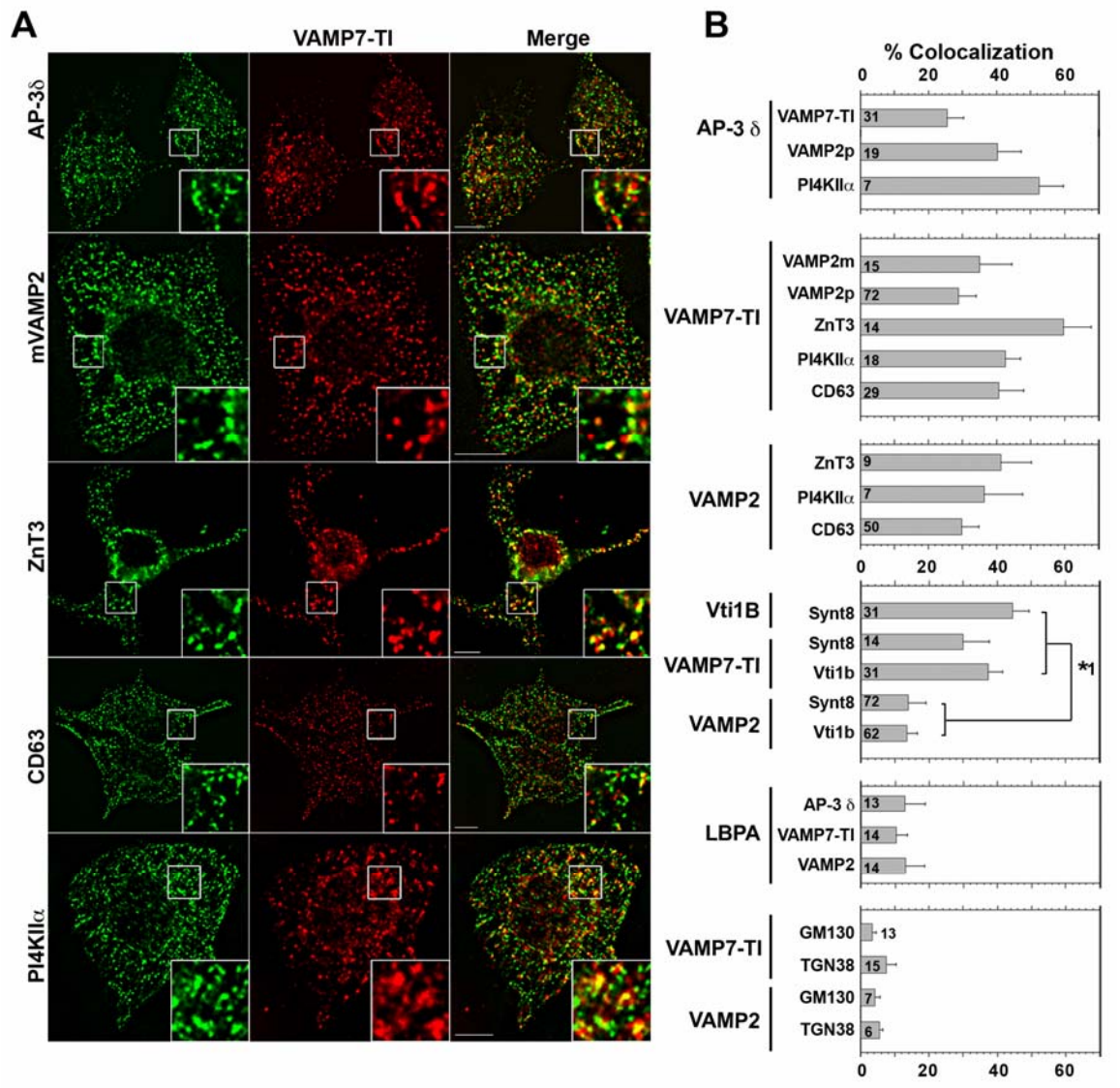

Figure 1: AP-3 synaptic vesicle and lysosomal cargoes selectively colocalize in PC12 Cells. (A) Fixed PC12 cells immunostained for VAMP7-TI and indicated protein. Cells were imaged by wide-field deconvolution microscopy. Bar, 5 μm. (B) Quantification of colocalization between AP-3 and synaptic vesicle (VAMP2) or lysosomal cargo (VAMP7-TI and PI4KIIα); VAMP7-TI and synaptic vesicle (VAMP2 and ZnT3) or lysosomal cargo (PI4KIIα and CD63); VAMP2 and synaptic vesicle or lysosomal cargo. Cognate SNARE

interactions and late endosomal marker LBPA illustrate the minimal contribution of late endosomes to the observed synaptic vesicle/lysosomal cargo colocalization. Golgi markers GM130 and TGN38 were used as negative controls to assess background levels of colocalization. Number of analyzed cells is indicated at the bottom of each bar graph. Asterisk represents p values for comparison of colocalization between either Vti1b or VAMP7-TI and either Syntaxin 8 or Vti1b, with colocalization between VAMP2 and Syntaxin 8 or Vti1b. All $p<0.0001$. One-way analysis of variance (ANOVA) Student–Newman–Keuls multiple comparison. Representative images of these quantifications are presented in Supplemental Figures 2–4.

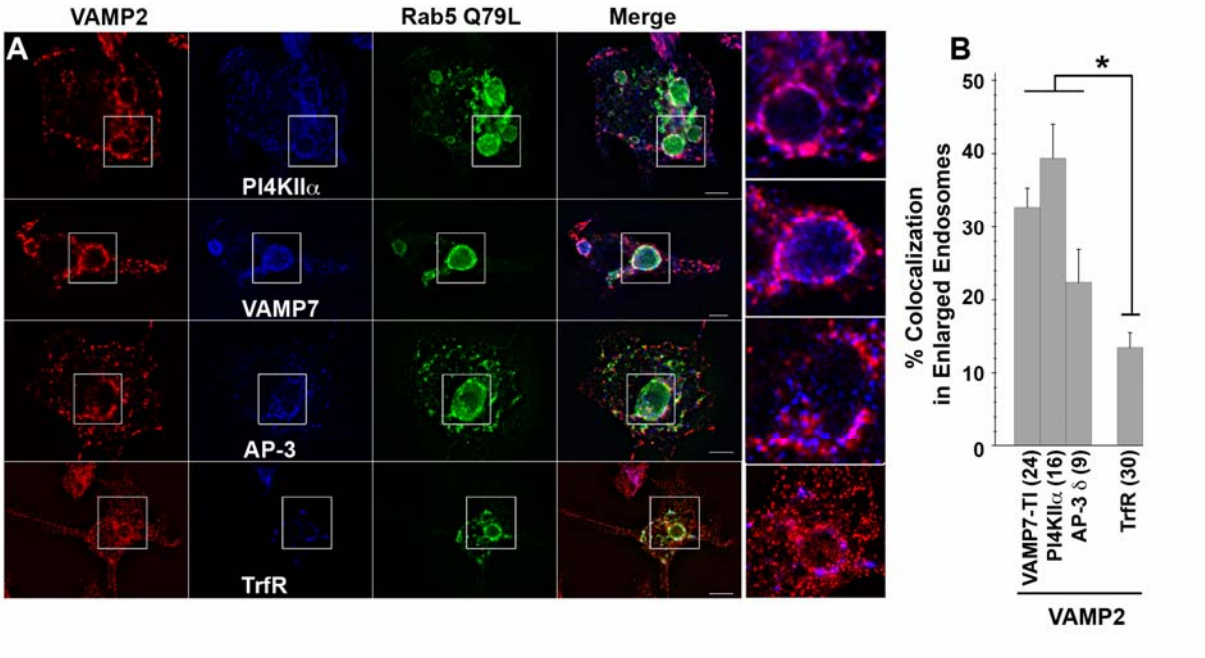

Figure 2: Synaptic Vesicle and AP-3 lysosomal cargoes are present in rab5Q79L early endosomes. (A) PC12 cells were transfected with the GFP-tagged rab5 GTP mutant Q79L. Fixed cells were double labeled for VAMP2 with either PI4KIIα, VAMP7-TI, AP-3 δ, or transferrin receptor (TrfR). Cells were imaged by wide-field deconvolution microscopy. (B) Colocalization quantification at the limiting membrane of enlarged endosomes. All $p<0.003$. One-way ANOVA Student–Newman–Keuls multiple comparison. Number in parentheses represent the number of enlarged endosomes analyzed.

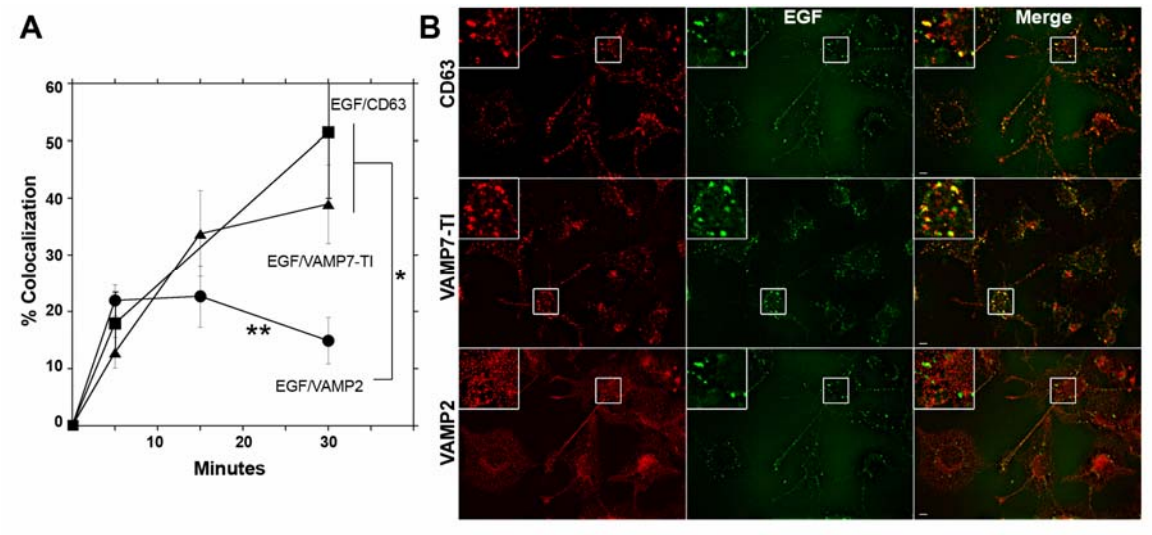

Figure 3: Internalized EGF labels early endosomes positive for VAMP2 and AP-3 lysosomal cargoes. PC12 cells endosomes were labeled with surface-bound fluorescein-EGF. Ligand was bound at 4°C, and excess ligand washed away. EGF internalization was resumed at 37°C for different times from 0 to 30 min. Cells were fixed and stained with antibodies against the synaptic vesicle protein VAMP2 and the AP-3 lysosomal cargoes VAMP7-TI and/or CD63. Cells were imaged by wide-field deconvolution microscopy and the extent of colocalization determined using MetaMorph software (A). In A, EGF reached compartments positive for VAMP2 and the AP-3 lysosomal cargoes (VAMP7-TI and CD63) between 5 and 15 min, but at 30 min, only AP-3 lysosomal cargoes localize to EGF-labeled late endosomes. Asterisk, $p<0.001$. Double asterisk compares the colocalization extent of EGF and VAMP2 at 15 and 30 min, $p<0.005$. One-way ANOVA Student–Newman–Keuls multiple comparison. Thirty to 145 cells collected per point from three to four independent experiments were analyzed. (B) Depicts images of cells after 30 min of EGF internalization.

Cells were double or triple labeled with EGF and either CD63, VAMP2, or VAMP7-TI antibodies. Bar, 5 μm.

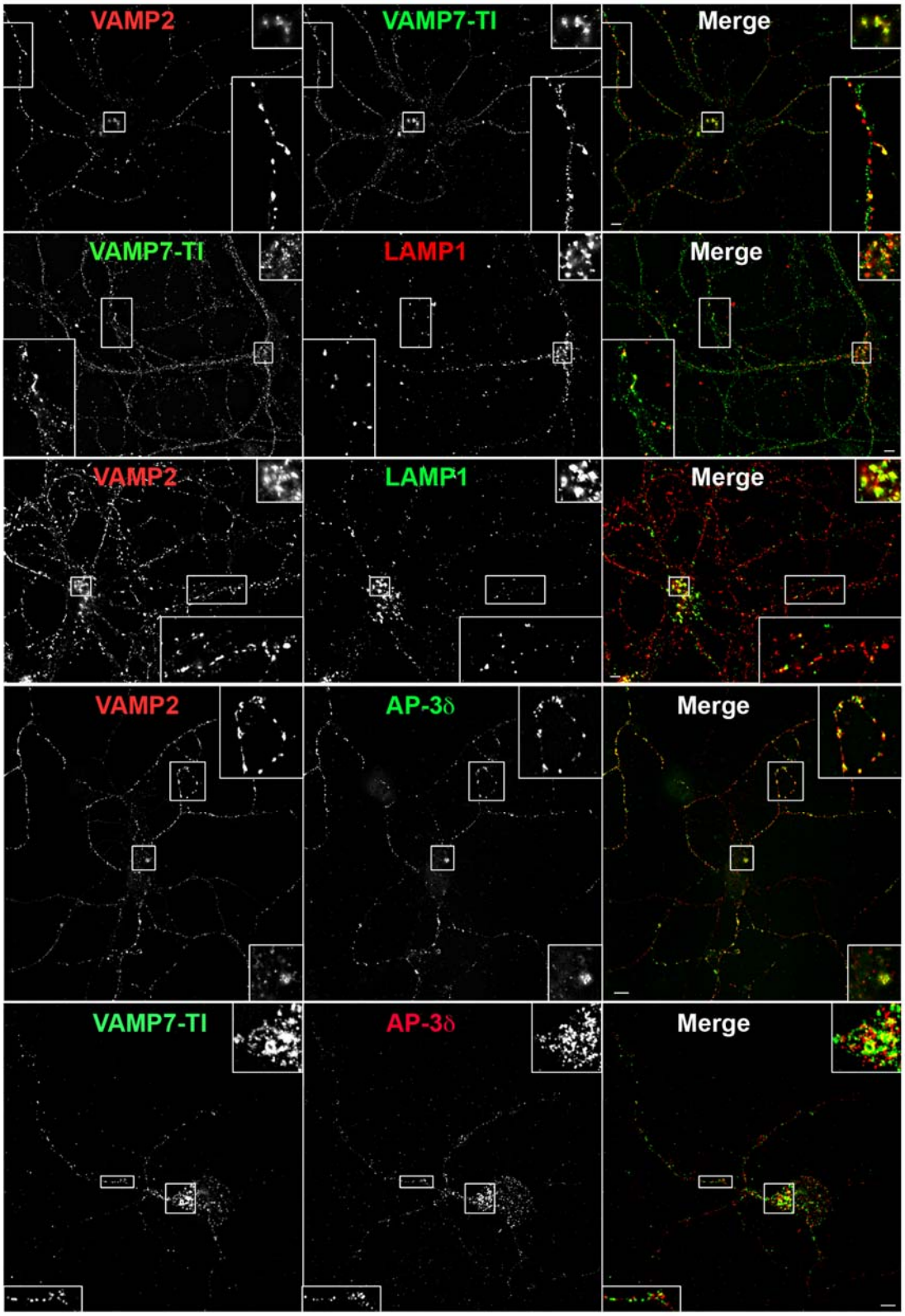
VAMP2
VAMP7-TI
Merge
VAMP7-TI
LAMP1
Merge
VAMP2
LAMP1
Merge
VAMP2
AP-3δ
Merge
VAMP7-TI
AP-3δ
Merge

Figure 4: Synaptic vesicle and lysosomal AP-3 cargoes colocalization in mouse primary neocortical neurons. Fixed E18.5 mouse primary neurons (DIV 14) from wild-type C57B or heterozygous controls immunostained for indicated proteins: VAMP2, VAMP7-TI, LAMP1, and AP-3 δ. Enlarged insets allow for comparison of colocalization in cell body and processes. Bar, 5 μm.

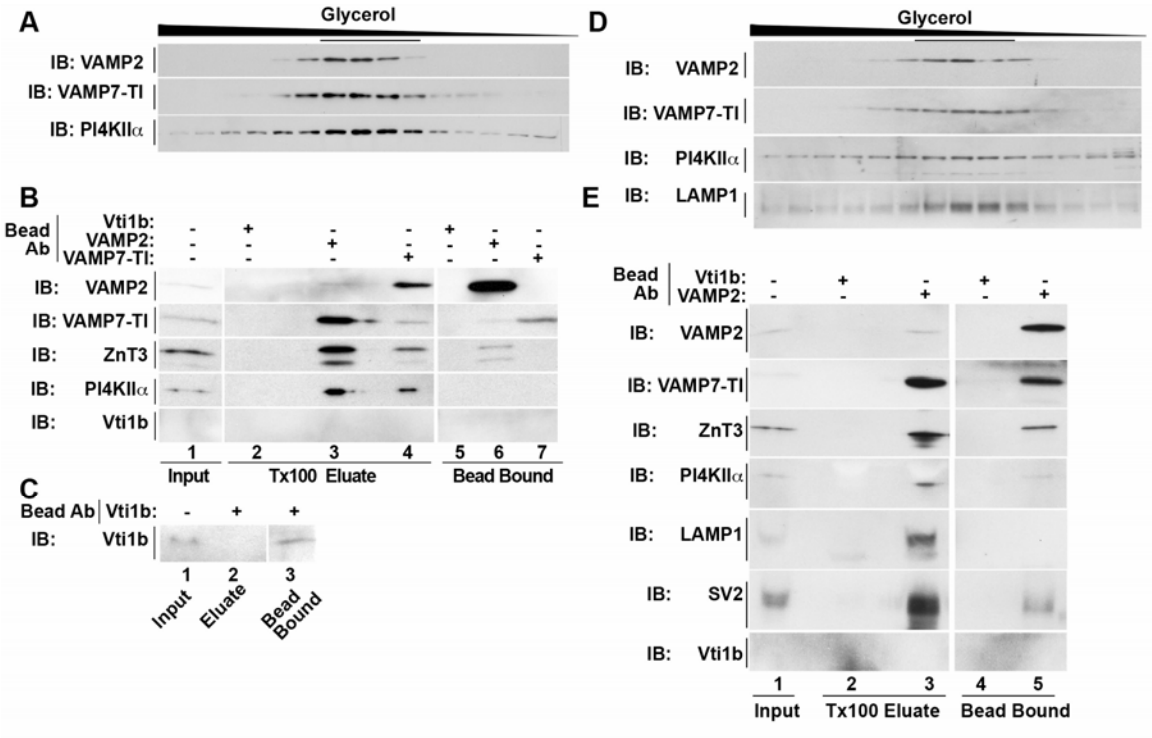

Figure 5: Synaptic vesicles and synaptic-like microvesicles contain AP-3 lysosomal cargoes. Glycerol gradient-sedimented synaptic-like microvesicles from PC12 cells (A) or mouse brain (C) were resolved by SDS-PAGE. Glycerol gradient fractions (A and C) were probed for VAMP2, VAMP7-TI, and PI4KIIα, as well as LAMP1 in mouse brain (C only). Synaptic-like microvesicles and synaptic vesicles peak in the middle of the gradient. (B and D) Immunomagnetic vesicular isolation from PC12 SLMVs and mouse brain SVs. Peak fractions (fractions 7–12, underlined) of above-mentioned glycerol gradients (A and C) were combined. Pooled vesicles were isolated with monoclonal antibodies to either the late endosome SNARE Vti1b, which serves as a negative control (B and D), the synaptic vesicle protein VAMP2 (B and D), or the AP-3 lysosomal cargo VAMP7-TI (B). Bound vesicles were eluted in Triton X-100 buffer, and both eluate and the remaining bead-bound material were

resolved by SDS-PAGE. Contents were analyzed by Western blotting for synaptic vesicle proteins (VAMP2, ZnT3, and SV2) or AP-3 lysosomal cargoes (LAMP1, PI4KIIα, and VAMP7-TI). Inputs represent 10%. Data are representative of three independent experiments.

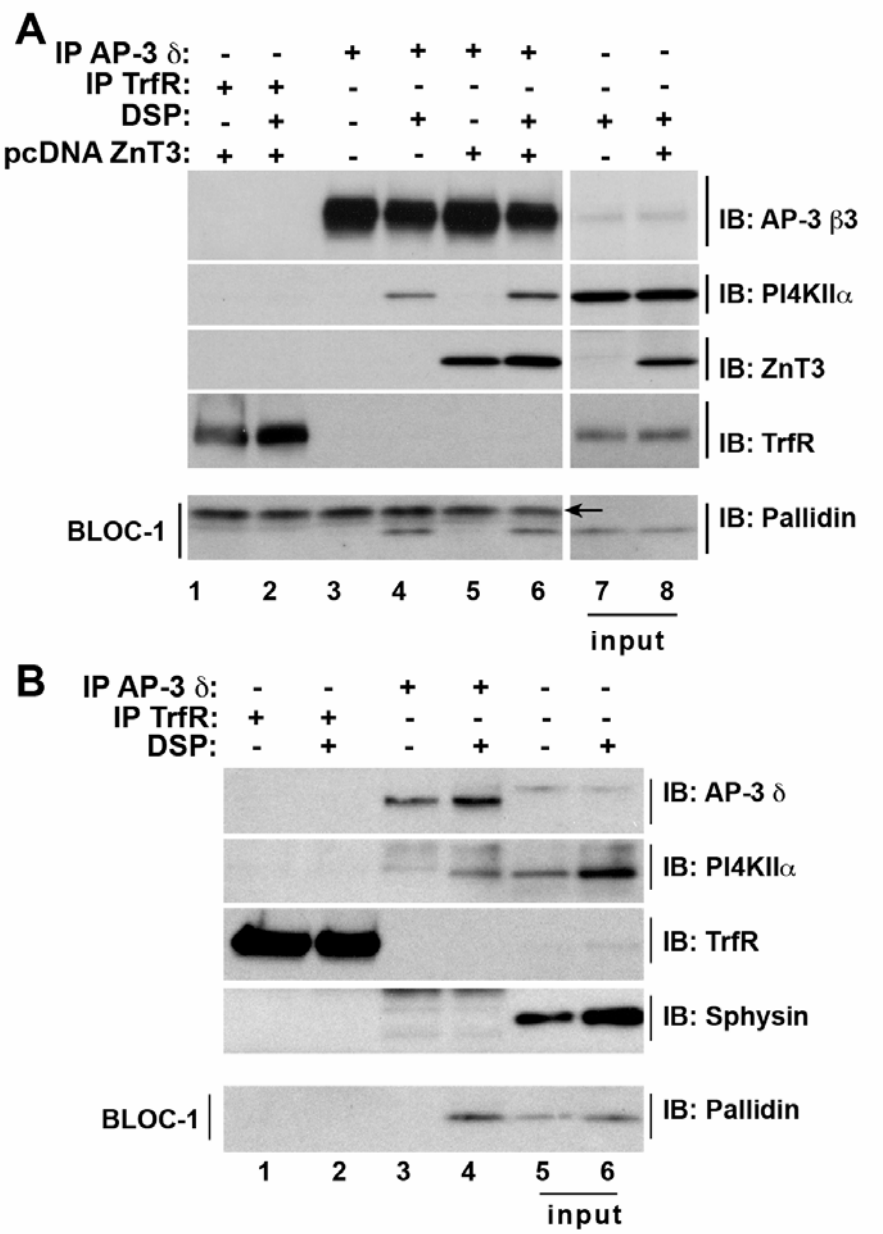

Figure 6: AP-3 and BLOC-1 form a complex in PC12 cells and mouse primary neurons. PC12 cells or PC12-ZnT3 cells (A) and E18.5 wild-type C57 mouse primary neurons (DIV 14) (B) were cross-linked with DSP. Cross-linked AP-3 complexes were immunoprecipitated with either AP-3 δ antibodies or transferrin receptor antibodies (TrfR). Immunocomplexes were resolved by SDS-PAGE and analyzed by immunoblot with antibodies against: the AP-3 subunits δ

and β3, transferrin receptor, synaptophysin (Sphysin), ZnT3, PI4KIIα, and pallidin, a BLOC-1 subunit. Input A, 1.4% and B, 3.33%. Arrow A indicates IgG light chains.

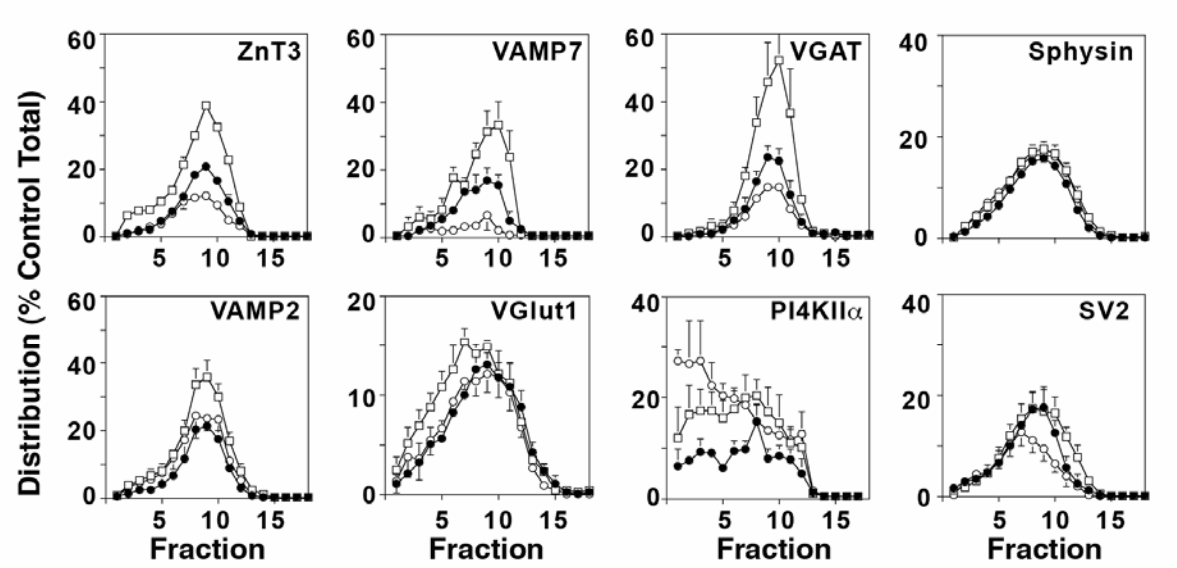

Figure 7: Ubiquitous and neuronal AP-3 isoforms regulate synaptic vesicle protein content. Glycerol gradient velocity sedimentation of S2 fractions from wild type C57B (closed circles), *Ap3b1*$^{-/-}$ (open squares), and *Ap3b2*$^{-/-}$ (open circles) mouse brains. Synaptic vesicle fractions were resolved by SDS-PAGE and analyzed by Western blot for the indicated protein. Protein levels were quantified using NIH Imager and were standardized to control C57B levels. In the absence of ubiquitous AP3 (*Ap3b1*$^{-/-}$), peak synaptic vesicle levels of ZnT3 ($p<0.003$), VAMP7-TI ($p<0.0008$), VGAT ($p<0.004$), and VAMP2 ($p<0.04$) increase, whereas VGLUT1 ($p<0.0005$) and PI4KIIα ($p<0.03$) show increases in larger vesicle fractions; synaptophysin and SV2 remain unaffected. In the absence of neuronal AP-3 (*Ap3b2*$^{-/-}$), peak synaptic vesicle levels of ZnT3 ($p<0.0001$), VAMP7 ($p<0.003$), VGAT ($p<0.02$), and SV2 decrease ($p<0.05$), whereas the levels of PI4KIIα increase in larger vesicle fractions ($p<0.0004$); synaptophysin (Sphysin), VAMP2, and VGlut1 remain unaffected. ZnT3, n = 7, 7;

VAMP7-TI, n = 4, 4; VGAT, n = 4, 5; Sphysin, n = 5, 10; PI4KIIα, n = 3, 3; SV2, n = 4, 4; VAMP2, n = 4, 4; VGlut1, n = 3, 3 (number of independent fractionations, number of independent Western blot analyses). One-way ANOVA Student–Newman–Keuls multiple comparison. Representative blots for these experiments can be found in Supplemental Figure 7.

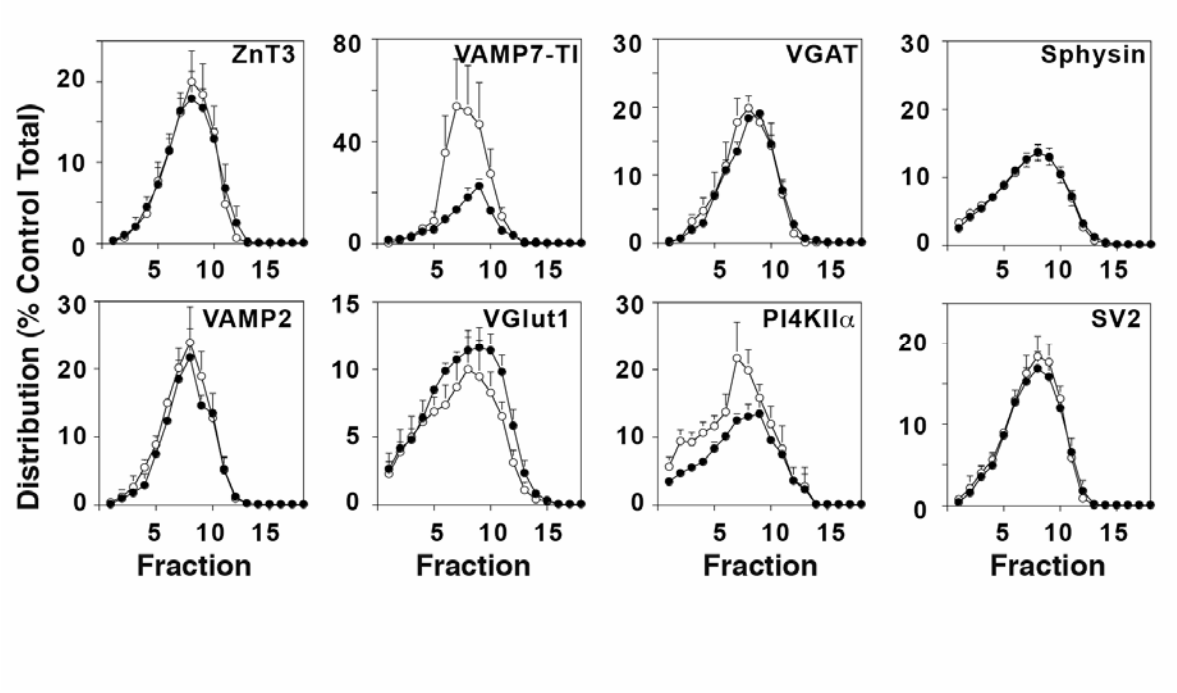

Figure 8: BLOC-1 selectively regulates synaptic vesicle levels of PI4KIIα and VAMP7-TI. Glycerol gradient velocity sedimentation of S2 fractions from BLOC-1-deficient $muted^{mu/mu}$ (open circles) and control $Muted^{+/mu}$ (closed circles) mouse brains. Synaptic vesicle fractions were resolved by SDS-PAGE and analyzed by Western blot for the indicated protein. Protein levels were quantified using NIH Imager and were standardized to control $muted^{+/mu}$ levels. Synaptic vesicle levels of ZnT3, VGAT, Sphysin, VAMP2, VGLUT1, and SV2 are unaffected by the loss of muted. However, the peak synaptic vesicle levels of both VAMP7-TI ($p<0.0005$) and PI4KIIα ($p<0.01$) increase in $Muted^{mu/mu}$. ZnT3, n = 3, 3; VAMP7-TI, n = 4, 4; VGAT, n = 4, 4; Sphysin, n = 4, 9; PI4KIIα, n = 4, 4; SV2, n = 3, 3; VAMP2, n = 3, 3; and VGlut1, n = 4, 4 (number of independent fractionations, number of independent Western blot analyses). Wilcoxon–Mann–Whitney test. Representative blots for these experiments can be found in Supplemental Figure 8.

Supplemental Figures:

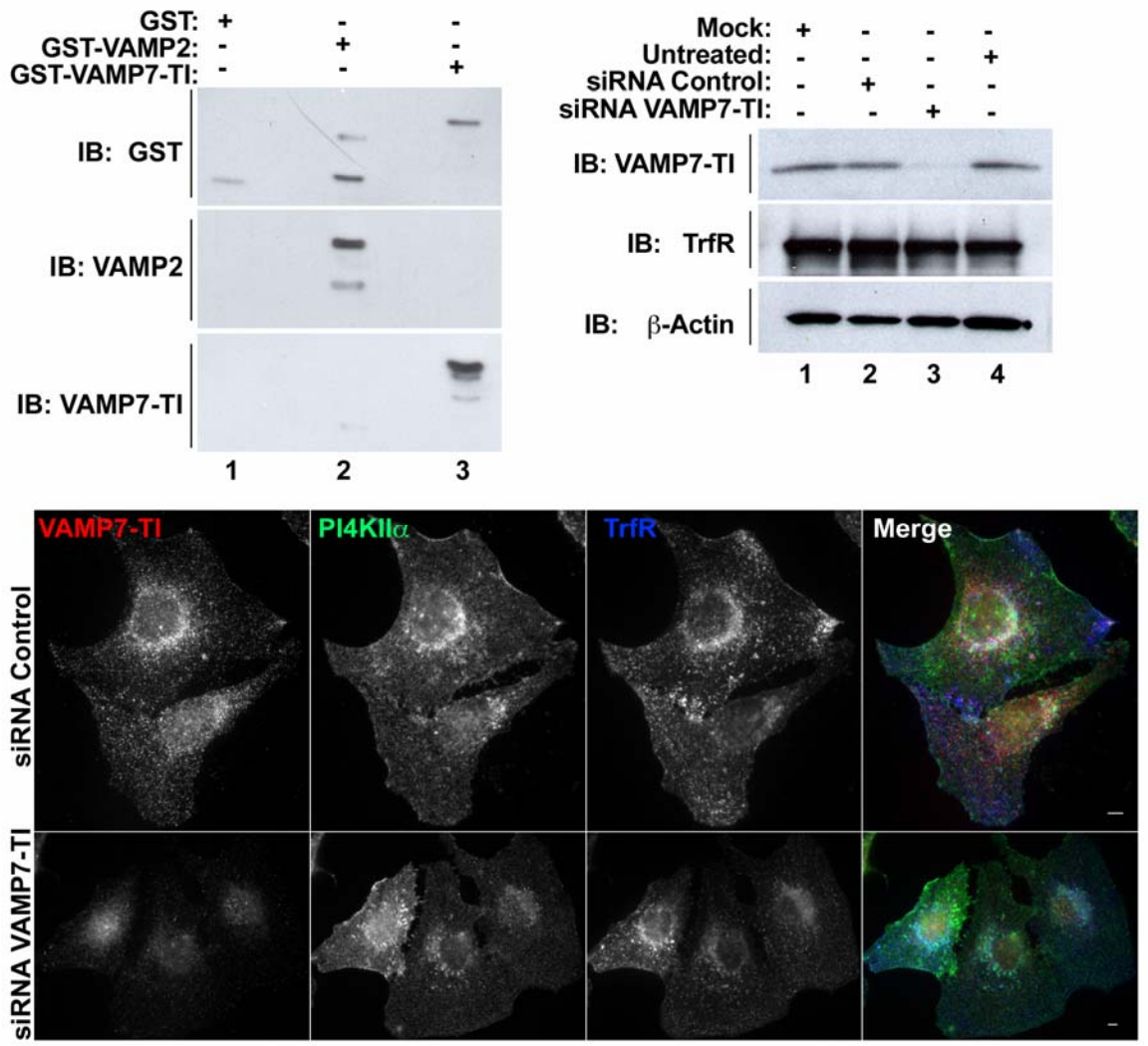

S. Figure 1: Characterization of VAMP7-TI Monoclonal Antibody.

A) Bacterially purified GST, VAMP2-GST, and VAMP7-TI-GST constructs are all recognized by a GST antibody. However, monoclonal antibodies against either VAMP2 or VAMP7-TI specifically recognize their substrates (lanes 2 and 3 respectively). B) VAMP7-TI siRNA-treatment of HELA specifically reduces VAMP7-TI protein levels, as detected by loss of VAMP7-TI immunoreactivity (lane3). Transferrin receptor (TrfR) and β-actin are unaffected by VAMP7-TI

siRNA treatment. C) VAMP7-TI siRNA reduces VAMP7-TI signal detection in fixed HELA cells. Scale Bar = 5μm.

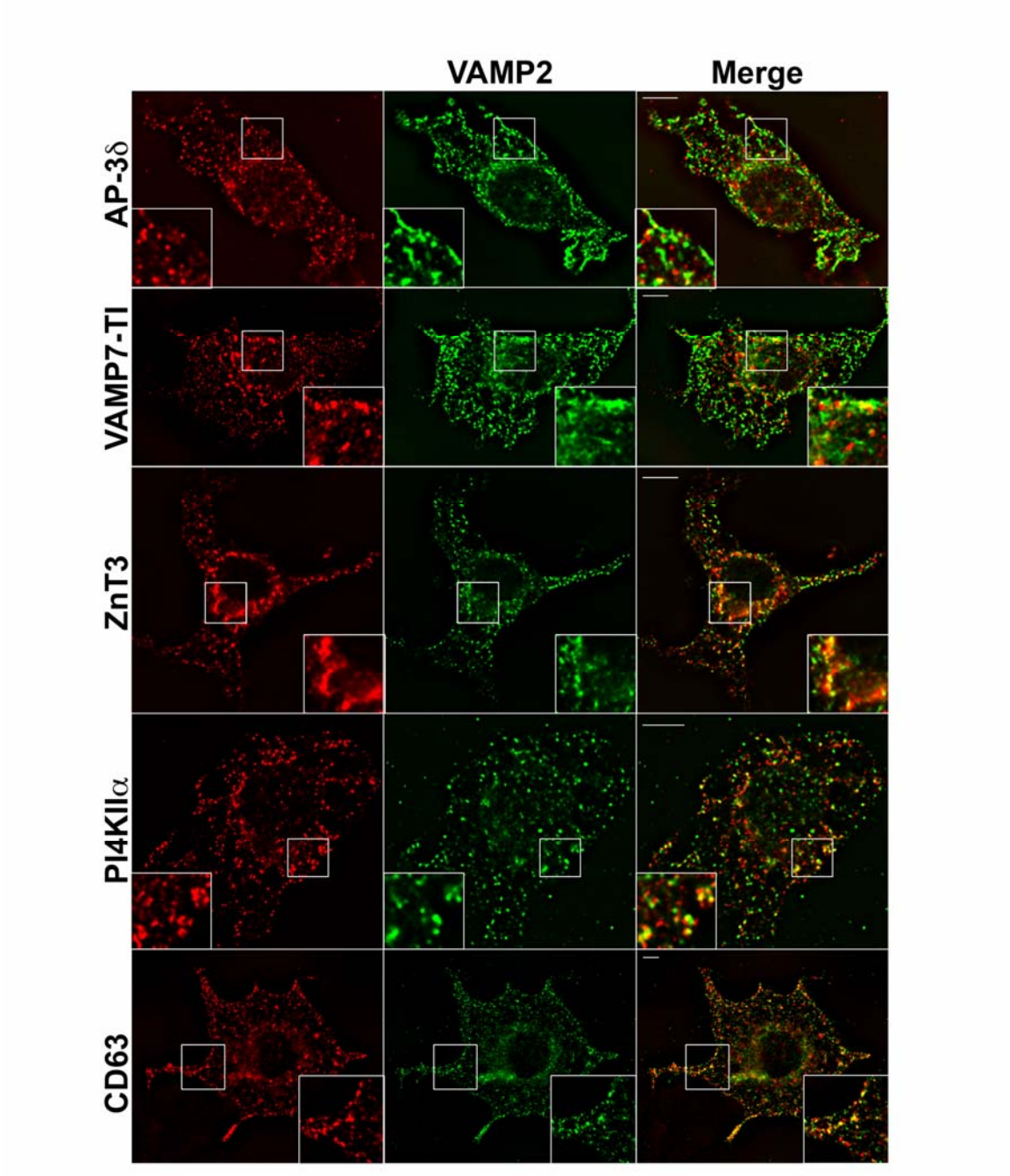

S. Figure 2: Synaptic Vesicle SNARE, VAMP2, Co-localizes with AP-3-Sorted Synaptic Vesicle and Lysosomal Proteins.

Fixed PC12 cells co-immunostained for synaptic vesicle SNARE, VAMP2 with one of the following: AP-3δ subunit, lysosomal proteins (VAMP7-TI, PI4KIIα, and CD63), and synaptic vesicle protein, ZnT3. Figure 1B reports quantification of

co-localization between VAMP2 and ZnT3, PI4KIIα, and CD63. Note that the cell stained with ZnT3 and VAMP2 was triple labeled with anti VAMP7-TI antibodies. The same cell with the ZnT3 and VAMP7-TI channels is shown in Figure 1. Scale Bar = 5μm.

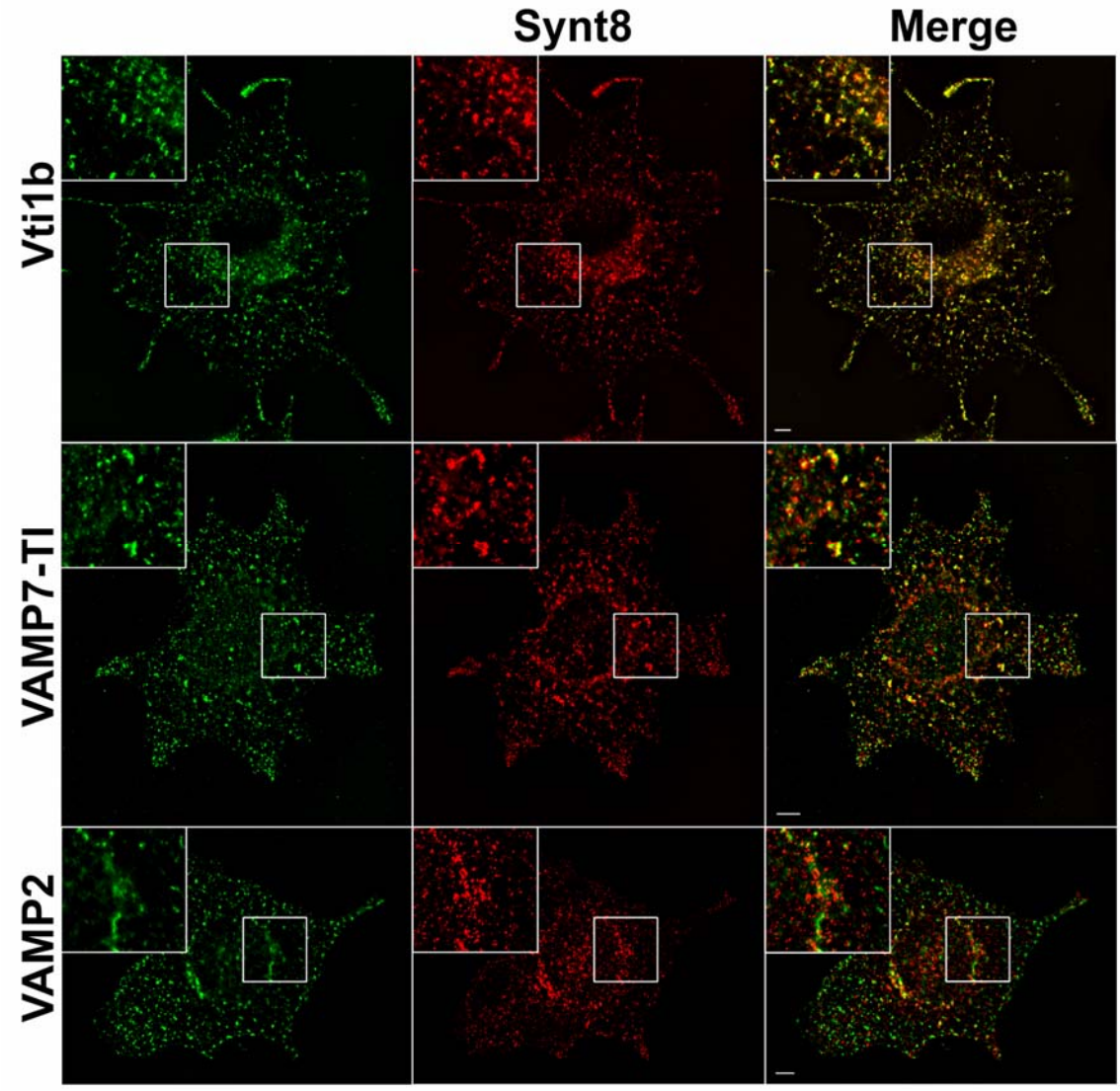

S. Figure 3: Syntaxin 8 Colocalization with Synaptic Vesicle and Lysosomal SNAREs.

Fixed PC12 cells co-immunostained for the lysosomal SNARE, syntaxin 8, and one of the following markers: the lysosomal SNARE vti1b; the cognate lysosomal SNARE, VAMP7-TI; and the synaptic vesicle SNARE, VAMP2. Figure 1B reports quantification of co-localization values. Scale Bar = 5μm.

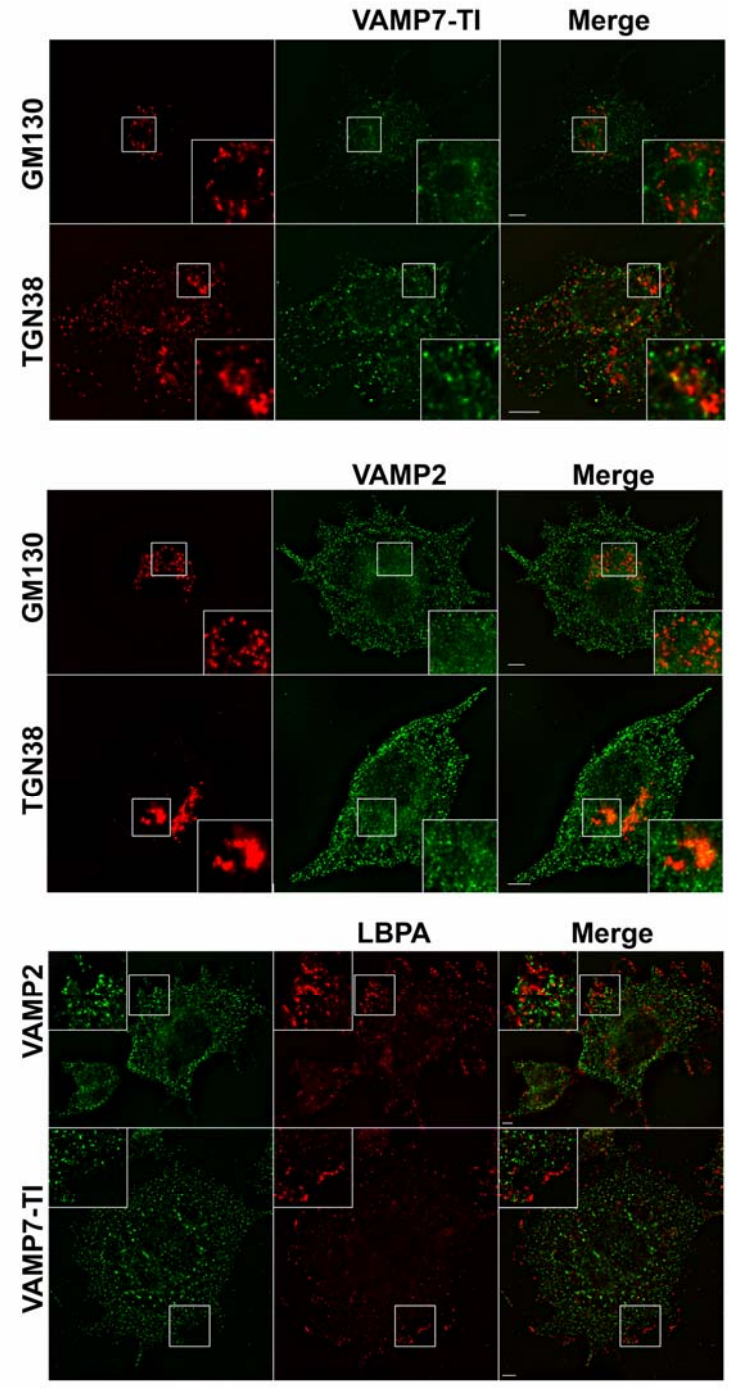

S. Figure 4: Negligible Co-Localization of VAMP7-TI and VAMP2 with Golgi and Late Endosomal Markers.

Fixed PC12 cells co-immunostained for A) VAMP7-TI and cis Golgi marker, GM130, or trans Golgi marker, TGN38; B) VAMP2 and GM130 or TGN38; C) late

endosomal marker, LBPA, and VAMP2 or VAMP7-TI. Quantification of these immunofluorescence pairs (Figure 1B) reveals minimal co-localization. Scale Bar = 5μm.

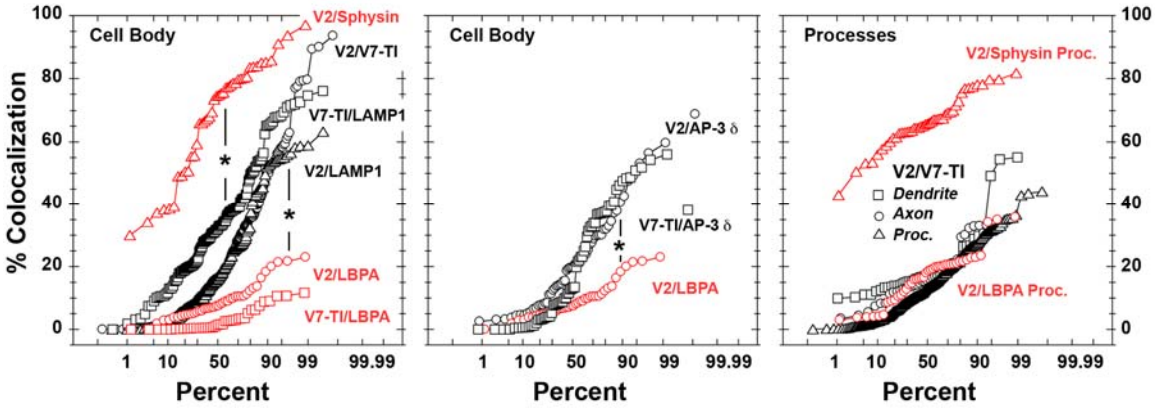

S. Figure 5: Quantification of Synaptic Vesicle and Lysosomal AP-3 Cargoes Co-Localization in Mouse Primary Neurons.

Data were obtained from images such as those presented in Figure 4. Data are depicted as probability plots in which the extent of colocalization between two markers is linearly represented in the y axis and the % of the population, arranged from the lowest to the highest colocalization values, are depicted logarithmically in the x axis. Fifty percent in the X axis establishes the median of the population (indicated by the gray arrow). For example, the median of colocalization between VAMP2 and synaptophysin is 74.5%. (Cell Body, left panel, red triangles, V2/Sphysin). Thus, half of all the VAMP2 and synaptophysin co-localization data fall below the median and they range between 30 to 74.5% colocalization. We defined the upper limits of colocalization by the signal overlap between two synaptic vesicle proteins, synaptophysin and VAMP2. Each data point represents the quantified co-localization of one z-plane. Three z planes represent each cell. Co-localization for neuronal cell bodies (left and middle panels): VAMP2/Synaptophysin (V2/Sphysin n=14), VAMP2/VAMP7-TI (V2/V7 n=76), VAMP2/LAMP1 (V2/LAMP1 n=45), VAMP2/LBPA (V2/LBPA n=10),

VAMP2/AP-3 delta (V2/AP-3 δ n=17), VAMP7-TI/LAMP1 (V7/LAMP1 n=44), VAMP7-TI/LBPA (V7/LBPA n=10), VAMP7-TI/AP-3 delta (V7/AP-3 δ n=20). Co-localization for all processes (right panel): V2/V7 (n=78), V2/Sphysin (n=15) and V2/LBPA (n=10). Dendrite and axons are analyzed from the following number of cells: V2/V7 n=5 and n=5, respectively. Dendrites were identified by MAP2 staining whereas axons were defined as MAP-2-negative processes. Asterisks represent $p<0.0001$ Kolmogorov-Smirnov test.

Within the neuronal cell body, lysosomal AP-3 cargo co-localization (VAMP7-TI/LAMP1) and synaptic vesicle/lysosomal co-localization (VAMP2/VAMP7-TI and VAMP2/LAMP1) exceeds the co-localization observed with late endosomal compartments, as indicated by LBPA. VAMP2/Synaptophysin co-localization indicates the upper limit of co-localization. Additionally, both VAMP2 and VAMP7 significantly co-localize with AP-3 in cell bodies.

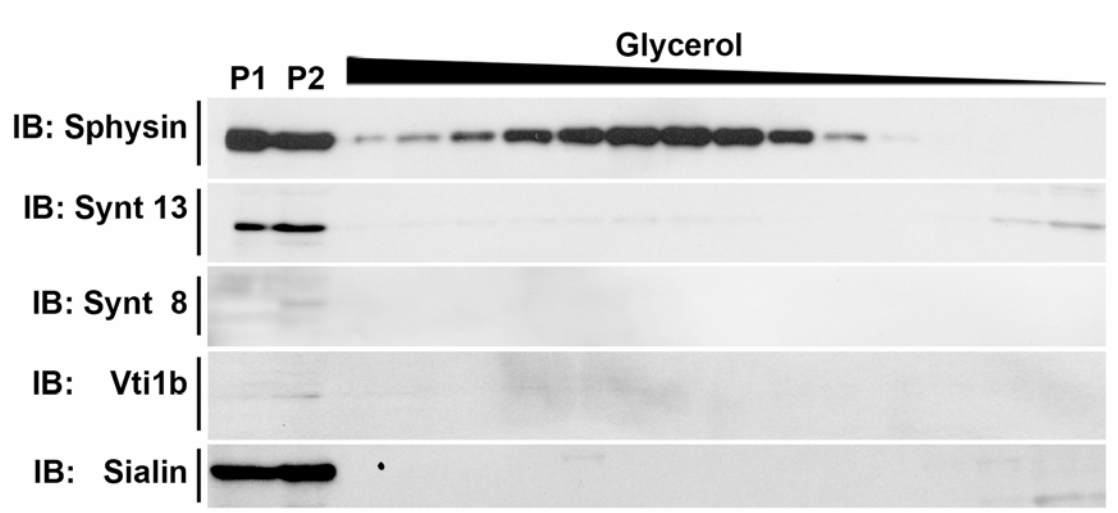

S. Figure 6: Synaptic Vesicle Fractions from Mouse Brains do not Contain Late and Recycling Endosome Markers.

S2 fractions from C57B or Muted+/mu were resolved in 5-25% glycerol gradients. Gradient fractions were resolved by SDS-PAGE and probed with antibodies against synaptophysin (Sphysin), syntaxin 13 (Synt13, recycling endosome), syntaxin 8 (Synt8, late endosome), Vti1b (late endosome). Sialin is a well characterized lysosomal protein (Sagne and Gasnier, 2008). Lanes 1 and 2 contain P1 and P2 fractions for a positive signal.

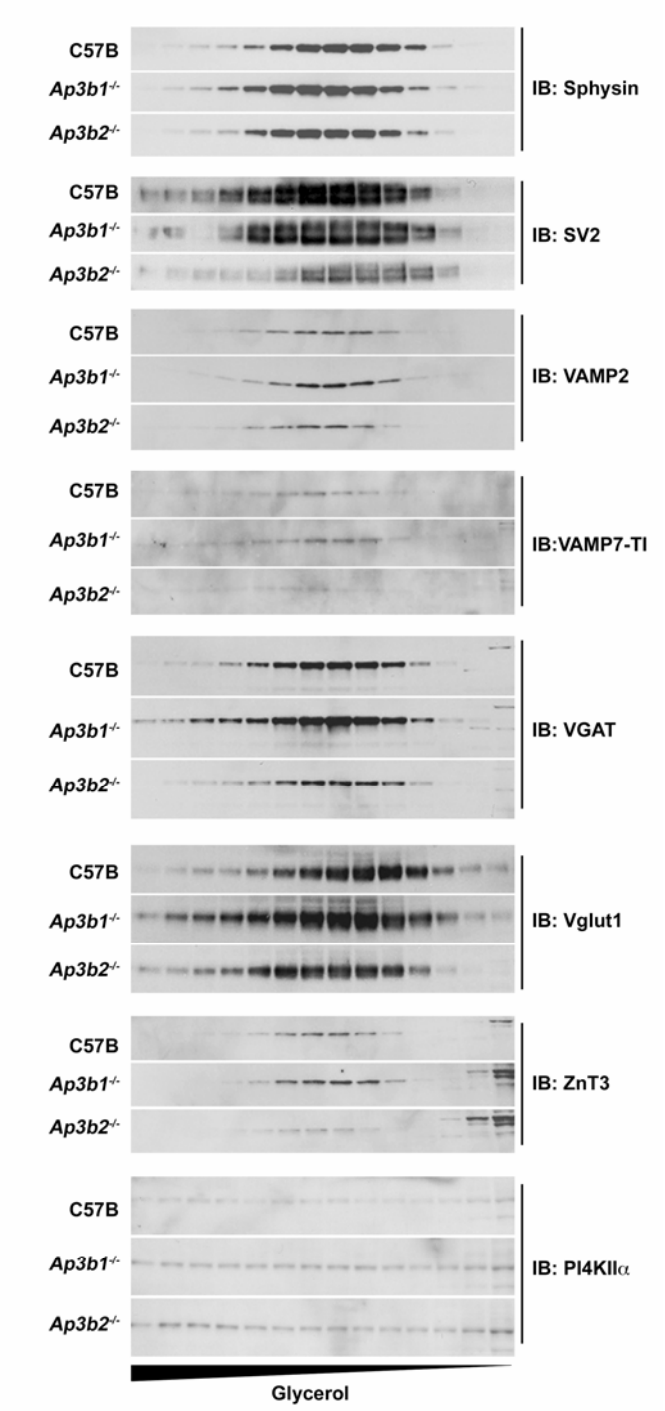

S. Figure 7: Glycerol Gradient Velocity Sedimentation of Synaptic Vesicle Fractions from AP-3-deficient Mouse Brains.

Representative western blots of 5-25% glycerol gradients of S2 fractions from wild type C57B, *Ap3b1*$^{-/-}$, and *Ap3b2*$^{-/-}$ mouse brain. Synaptophysin indicates

that synaptic vesicle fractions peak in the middle of the gradient, and also serves as a loading control for the different mice. Figure 7 reports quantification of the glycerol gradient fractions. Glycerol gradient density is indicated at the bottom of the figure, with larger vesicle fractions migrating toward 25% glycerol.

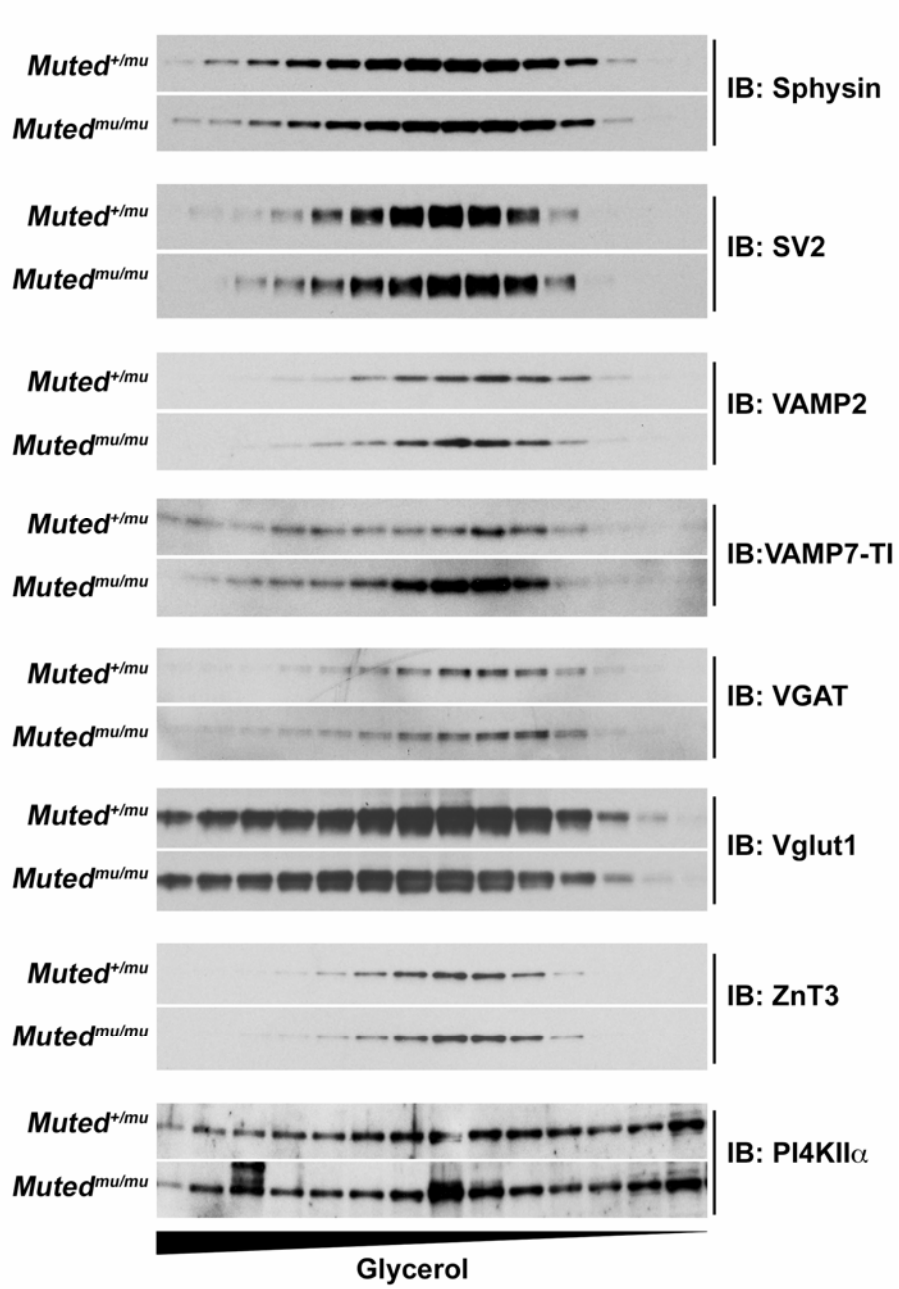

S. Figure 8: Glycerol Gradient Velocity Sedimentation of Synaptic Vesicle Fractions from BLOC-1-deficient (*muted*) Mouse Brains.

Representative western blots of 5-25% glycerol gradients of S2 fractions from heterozygous control, *Muted*$^{+/mu}$, and *muted* (*Muted*$^{mu/mu}$) mouse brains. Synaptophysin indicates that synaptic vesicle fractions peak in the middle of the gradient, and also serves as a loading control for the different mice. Figure 8

reports quantification of the glycerol gradient fractions. Glycerol gradient density is indicated at the bottom of the figure, with larger vesicle fractions migrating toward 25% glycerol and identified toward the left of the western blot, and cytoplasmic fractions migrating toward 5% and identified toward the right of the western blot.

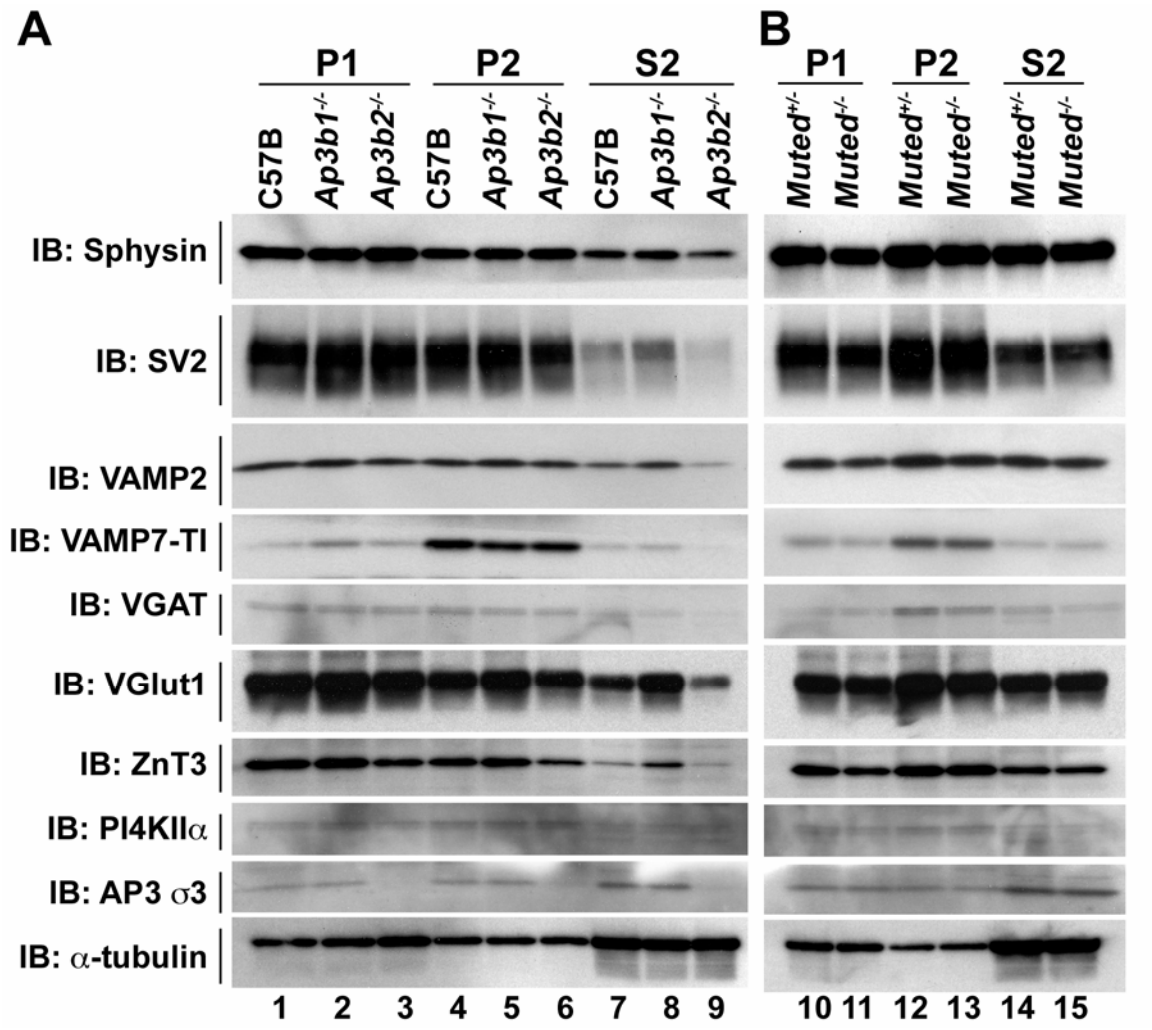

S. Figure 9: AP-3 and BLOC-1 Deficiency Do Not Globally Affect Synaptic Vesicle and AP-3 Sorted Lysosomal Proteins in Mouse Brain. Western blots of pellets (P1, P2) and final supernatant (S2) obtained from differential centrifugation of wild type C57B, *Ap3b1*$^{-/-}$, and *Ap3b2*$^{-/-}$ mouse brain as well as *Muted*$^{+/mu}$, and *Muted*$^{mu/mu}$ brains. Western blots were probed for the AP-3-sorted lysosomal and synaptic vesicle proteins. AP-3 σ3 indicates that AP-3 levels are most dramatically reduced in *Ap3b2*$^{-/-}$. α-tubulin serves as a loading control.

CHAPTER III

Hermansky-Pudlak Complexes, AP-3 and BLOC-1, Differentially Regulate Synaptic Composition in the Striatum and Hippocampus.

Karen Newell-Litwa[1,2], Sreenivasulu Chintala[5], LeeAnne McGaha[1,2], Yoland Smith[4], and Victor Faundez[2,3*]

[1]Graduate Program in Biochemistry, Cell, and Developmental Biology; [2]Department of Cell Biology; [3]Center for Neurodegenerative Diseases; and [4]Department of Neurology. Emory University, Atlanta, GA 30322. [5]Department of Molecular and Cellular Biology, Roswell Park Cancer Institute, Buffalo, NY 14263

Abstract

Endosomal sorting mechanisms mediated by AP-3 and BLOC-1 are perturbed in Hermansky-Pudlak Syndrome, a human genetic condition characterized by albinism and prolonged bleeding (OMIM #203300). Additionally, mouse models defective in either one of these complexes possess defective synaptic vesicle biogenesis (Newell-Litwa *et al.*, 2009). These synaptic vesicle phenotypes were presumed uniform throughout the brain. However, here we report that AP-3 and BLOC-1 differentially regulate the composition of pre-synaptic terminals in striatum and dentate gyrus of the hippocampus. Quantitative immunoelectron microscopy demonstrated that the majority of AP-3 in both wild type striatum and hippocampus localizes to pre-synaptic axonal compartments, where it regulates synaptic vesicle size. In the striatum, loss of AP-3 ($Ap3d^{mh/mh}$) results in decreased synaptic vesicle size. In contrast, loss of AP-3 in the dentate gyrus increases synaptic vesicle size, thus suggesting anatomically specific AP-3-regulatory mechanisms. Loss-of-function alleles of BLOC-1, $Pldn^{pa/pa}$ and $Muted^{mu/mu}$, reveal that this complex acts as a brain-region specific regulator of AP-3. In fact, BLOC-1 deficiencies selectively reduce AP-3 and AP-3 cargo immunoreactivity in pre-synaptic compartments within the dentate gyrus both at the light and/or electron microscopy level. However, neither striatum nor CA3 region of the hippocampus exhibited these BLOC-1-null phenotypes. Our results demonstrate that distinct brain regions differentially regulate AP-3-dependent synaptic vesicle biogenesis. We propose that anatomically restricted mechanisms within the brain diversify the biogenesis and composition of synaptic vesicles.

Introduction

Mechanisms of synaptic vesicle biogenesis are critical for proper neurotransmission. Defective biogenesis mechanisms affect synaptic vesicles with phenotypes that range from complete organelle depletion to changes in the composition and size of synaptic vesicles (Toshio Kosaka, 1983; González-Gaitán and Jäckle, 1997; Zhang *et al.*, 1998; Nonet *et al.*, 1999; Karunanithi *et al.*, 2002; Heerssen *et al.*, 2008; Kasprowicz *et al.*, 2008; Sato *et al.*, 2009). It is widely assumed that the biogenesis of synaptic vesicles is a homogenous process throughout the metazoan nervous system. However, recent genetic evidence challenges this conception (Karunanithi *et al.*, 2002; Hayashi *et al.*, 2008). Here we focus on the endosomal sorting mechanisms mediated by two complexes affected in Hermansky-Pudlak Syndrome, Adaptor Protein Complex-3 (AP-3) and Biogenesis of Lysosome-Related Organelle Complex-1 (BLOC-1). These complexes regulate the targeting of synaptic vesicle membrane proteins to these pre-synaptic organelles, thus affecting neurotransmission (Voglmaier *et al.*, 2006; Chen *et al.*, 2008; Newell-Litwa *et al.*, 2009). We report that contrary to the notion that synaptic vesicle biogenesis is anatomically and mechanistically homogenous, AP-3 and BLOC-1 distinctly regulate synaptic vesicle composition and morphology in different brain regions.

AP-3 and BLOC-1 belong to a family of five protein complexes, whose disruption results in Hermansky-Pudlak Syndrome (OMIM #203300) (Li *et al.*, 2004; Di Pietro and Dell'Angelica, 2005). AP-3 is encoded by four subunits (δ, β3, μ3, and σ3) and BLOC-1 is an octamer constituted by BLOS 1-3, cappuccino, dysbindin, muted, pallidin, and snapin. These protein complexes regulate

lysosome and lysosome-related organelle transport (Li *et al.*, 2004; Di Pietro and Dell'Angelica, 2005). Hermansky Pudlak Syndrome is characterized by systemic disorders, including albinism and prolonged bleeding, that result from disruption of lysosome/lysosome-related organelle transport (Li *et al.*, 2004; Di Pietro and Dell'Angelica, 2005). Mouse mutants in AP-3 delta (*Ap3d*$^{mh/mh}$), result in Hermansky Pudlak Syndrome and neurological phenotypes (Kantheti *et al.*, 1998; Di Pietro and Dell'Angelica, 2005; Newell-Litwa *et al.*, 2007). AP-3 is a Hermansky Pudlak complex that exists as two isoforms, a ubiquitous isoform and a neuronal-specific isoform. These two AP-3 isoforms are assembled by δ and σ3 subunits, which are common to both isoforms, while β3 and μ3 are expressed as ubiquitous and neuronal isoforms, A and B respectively (Newell-Litwa *et al.*, 2007). The ubiquitous AP-3 adaptor sorts cargo from early endosomes into vesicles delivered to lysosomes; genetic deficiencies of ubiquitous AP-3 (*Ap3b1*$^{-/-}$ *and Ap3b1*$^{pe/pe}$) result in the systemic phenotypes common to Hermansky Pudlak Syndrome (Feng *et al.*, 1999; Zhen *et al.*, 1999; Yang *et al.*, 2000; Peden *et al.*, 2004). In contrast, the neuronal AP-3 isoform mediates synaptic vesicle biogenesis from early endosomes; null alleles of the neuronal AP-3 subunits (*Ap3b2*$^{-/-}$ and *Ap3m2*$^{-/-}$) result in neurological phenotypes (Faundez *et al.*, 1998; Nakatsu *et al.*, 2004; Seong *et al.*, 2005; Newell-Litwa *et al.*, 2009). *Mocha*, a mouse deficient for the δ subunit of AP-3 and therefore lacking both AP-3 isoforms, exhibits systemic and neurological phenotypes (Kantheti *et al.*, 1998).

Importantly, both the ubiquitous and neuronal AP-3 isoforms sort cargo from early endosomes, and both isoforms are expressed in brain where they

regulate synaptic vesicle content by oppositely sorting similar cargo to either a synaptic vesicle or lysosomal fate (Newell-Litwa *et al.*, 2009).

Here, we analyzed the contributions of two endosomal sorting complexes, AP-3 and BLOC-1, to the composition of synaptic terminals in diverse brain regions. We found that while AP-3 is expressed throughout the brain, it exhibits prominent expression in both the striatum and hippocampus. Quantitative immunoelectron microscopy indicates that AP-3 is primarily localized to pre-synaptic axonal compartments. AP-3 selectively regulates the molecular composition of dentate gyrus nerve terminals, where AP-3-deficient *mocha* mouse ($Ap3d^{mh/mh}$) brain results in decreased levels of VAMP7-TI (Scheuber *et al.*, 2006). Loss of AP-3 does not affect VAMP7-TI expression in either the striatum or CA3 region of the hippocampus. These differential effects of AP-3 deficiency correlated with divergent changes in the morphology of synaptic vesicles. Loss of AP-3 in the dentate gyrus increased synaptic vesicle size, while in the striatum, loss of AP-3 resulted in decreased organelle size. These results are consistent with the hypothesis that AP-3-dependent vesicle trafficking mechanisms distinctly regulate the composition of synaptic terminals across diverse brain regions. Interestingly, BLOC-1 contributes to the region-specific effects of AP-3 by selectively regulating AP-3 expression and sub-synaptic distribution within the dentate gyrus but not in striatum and the CA3 region of the hippocampus. These results indicate a role for endosomal sorting mechanisms in generating diversity among pre-synaptic vesicles through both the regulation of molecular content and morphology of synaptic vesicles.

Materials and Methods

Animals and Tissue Preparation

Sprague Dawley Rats used in the synaptosome preparation were obtained from Harlan Laboratories (Indianapolis, IN). *Mocha* and *pallid* breeding pairs were obtained from Jackson Labs (Bar Harbor, Maine) and bred in house following IUCAC approved protocols. $Muted^{mu/mu}$ and $CHMU^{+/mu}$ (Zhang *et al.*, 2002) mice were obtained from Dr. Richard Swank (Roswell Park Cancer Institute, NY, USA) and bred in-house. All mice used in this study were between 2 to 10 months of age, with the exception of one $muted^{mu/mu}$ and its corresponding $CHMU^{+/mu}$ control, which were both 2 years old. Following anesthetization with either ketamine or nembutal, mice were transcardially perfused with Ringer's solution followed by a fixative mixture of 4% paraformaldehyde and 0.1% gluteraldehyde. Brains were also post-fixed overnight in the same fixative. Fixative was replaced by PBS on the following day. Brains were cut into 60μm thick sections with a vibrating microtome. Sections were stored in antifreeze at -20°C until immunohistochemical preparation.

Antibodies and Peptides

The following antibodies were used in this study: a monoclonal antibody against AP3-δ (SA4) from Developmental Studies Hybridoma Bank at the University of Iowa; a monoclonal antibody against Synaptophysin (SY38) from Chemicon International/Millipore (Billerica, MA, USA); a monoclonal antibody against Transferrin Receptor (H68.4) from Zymed Laboratories/Invitrogen (Carlsbad, California, USA). The monoclonal antibody against VAMP7-TI has been

described in (Advani *et al.*, 1999). The amino acid sequence for the AP-3δ peptide was reported in (Craige *et al.*, 2008).

Immunoperoxidase labeling for light and electron microscopy

Sections were first incubated in 1% Sodium Borohydride for 20 minutes at room temperature (RT), followed by extensive washing with PBS. Sections were then placed in cryoprotectant (PB 0.05 M, pH 7.4, 25% sucrose, 10% glycerol) for 20 minutes, frozen at -80°C for 20 minutes, and returned to decreasing amounts of cryoprotectant. Following cryoprotection, sections were rinsed in PBS. Sections were pre-incubated for 1 hour at RT in PBS + 1% Normal Horse Serum (NHS) + 1% Bovine Serum Albumin (BSA), followed by primary antibody incubation for 48 hours at 4°C in PBS + 1% NHS + 1% BSA and one of the following primary antibody dilutions: 1:5000 anti-AP-3δ (SA4), 1:5000 anti-VAMP7-TI, or 1:10000 anti-Synaptophysin (SY38). After PBS washes, the sections were incubated in a secondary antibody dilution of 1:200 biotinylated horse anti-mouse IgG (Vector Laboratories, Burlingame, CA, USA) for 90 minutes at RT. Sections were rinsed with PBS, and then incubated in a 1:100 dilution of the avidin-biotin peroxidase complex (ABC; Vector Laboratories). Sections were rinsed in PBS with a final rinse in Tris buffer (50 mM, pH 7.6) before a 10 minutes RT incubation in 0.025% 3,3'-diaminobenzidine (DAB; Sigma Aldrich, St. Louis, MO, USA), 1 mM imidazole (Fischer Scientific, Norcross, GA, USA), and 0.005% Hydrogen Peroxide in Tris buffer. For light microscopy analysis, sections were rinsed in PBS, mounted on gelatin-coated slides, dehydrated, and coverslipped with Permount. For electron microscopy analysis, sections were further processed as

follows. After rinsing in PB (0.1 M, pH 7.4), sections were incubated in 1% OsO_4 for 10 minutes, and then returned to PB before being dehydrated with concentrations of ethanol. At 70% ethanol, 1% uranyl acetate was added, and sections were incubated in the dark for 35 minutes in order to enhance the contrast of the tissue on the electron microscope. After dehydration, sections were treated with propylene oxide, and embedded in epoxy resin overnight (Durcupan ACM; Fluka, Buschs, Switzerland). On the next day, tissues were mounted onto slides and baked in a 60^{o}C oven for 48 hours. Sections of the striatum, CA3 and dentate gyrus were mounted on resin blocks, and cut into 60nm sections with an ultramicrotome (Leica Ultracut T2). Sections were collected on Pioloform-coated copper grids and stained with lead citrate for 5 minutes to enhance contrast on the electron microscope.

Immunofluorescence Labeling for Confocal Microscopy

Sections containing the hippocampus were first rinsed with PBS, and then incubated in 1% Sodium Borohydride in PBS for 20 minutes at RT, followed by extensive washing with PBS. Samples were pre-incubated in a solution of PBS + 5% NHS + 1% BSA + 0.3% Triton X-100 for 60 minutes at RT. Samples were incubated overnight at 4^{o}C in primary antibody solutions of PBS + 1% NHS + 1% BSA and either a mixture of anti-AP-3δ (SA4) and anti-VAMP7-TI (both at 1:5000), or anti-Synaptophysin (SY38) and anti-VAMP7-TI (at dilutions of 1:10000 and 1:5000, respectively). After rinsing in PBS, sections were incubated for 60 minutes in a secondary antibody solution of PBS + 1% NHS + 1% BSA and 1:500 dilutions of the following Alexa-conjugated isotype-specific secondary

antibodies: anti-IgG1 (for anti-AP-3δ and anti-Synaptophysin) and anti-IgG2B (for VAMP7-TI) (Invitrogen Molecular Probes, Carlsbad, CA, USA). Following PBS rinses, sections were incubated in a cupric sulfate solution (3.854 W/V Ammonium Acetate, 1.596 W/V Cupric Sulfate in distilled water, pH 5) for 30 minutes. Sections were washed with PBS and mounted on slides with Vectashield (Vector Laboratories).

Microscopy

Confocal Microscopy

Confocal microscopy of immunofluorescent samples was performed with an Anxiovert 100M (Carl Zeiss) coupled to an Argon laser. Images were acquired with LSM 510 sp1 software (Carl Zeiss) using Plan Apochromat 10x/0.5 dry and 40x/1.3, 63x/1.4, and 100x/1.4 oil DiC objectives. The emission filters used for fluorescence imaging were BP 505-530 and LP 560.

Deconvolution Microscopy

Immunofluorescence of mouse primary neurons has been previously described (Salazar *et al.*, 2004b; Craige *et al.*, 2008; Newell-Litwa *et al.*, 2009). Images were acquired with a scientific-grade cooled charge-coupled device (Cool-Snap HQ with ORCA-ERchip) on a multiwavelength, wide-field, three-dimensional microscopy system (Intelligent Imaging Innovations, Denver, CO), based on a 200M inverted microscope using a 63x numerical aperture 1.4 lens (Carl Zeiss, Thornwood, NY). Immunofluorescent samples were imaged at room temperature using a Sedat filter set (Chroma Technology, Rockingham, UT), in successive

0.20-µm focal planes. Out-of-focus light was removed with a constrained iterative deconvolution algorithm (Swedlow *et al.*, 1997).

Electron Microscopy

Electron microscopy was performed with a Zeiss EM-10C electron microscope with a CCD camera (DualView 300W; Gatan, Inc., Pleasanton, CA, USA). Images were acquired with Digital Micrograph Software (v. 3.10.1; Gatan, Inc.) Brightness and contrast were adjusted with Adobe Photoshop CS3 (v. 10.0.1).

Light Microscopy

Light microscopy was performed with a Leica DMRB microscope (Lieca Microsystems, Inc., Bannockburn, IL, USA) and images were captured with a CCD camera (Leica DC500). Images were acquired with Leica IM50 software. Images were converted to inverted grayscale images with Adobe Photoshop CS2 (v. 9.0.2) and image intensity was measured with Image J software.

Cell Culture and DSP Crosslinking of AP-3 immunocomplexes

PC12 cells were cultured in DMEM containing 10% Horse Serum, 5% Fetal Bovine Serum, and 100 U/ml penicillin and 100 ug/ml streptomycin at 10% CO_2 and 37^{o}C. Preparation of mouse neocortical neurons has been described in (Newell-Litwa *et al.*, 2009). DSP Crosslinking of AP-3 immunocomplexes and their isolation has been described in (Craige *et al.*, 2008).

Preparation of Synaptosomes

Synaptosomes were prepared from adult female rats (Harland Laboratories, Indianapolis, Indiana) following the procedure of Nagy and Delgado-Escueta except that Percoll sedimentation was omitted (Nagy and Delgado-Escueta, 1984). Briefly, rats were anesthetized by CO_2 narcosis and brains quickly removed, and washed in ice cold PBS. Tissue was homogenized in 0.32 M sucrose, 5 mM Hepes and 0.5 mM EDTA supplemented with Complete antiprotease mixture (Roche Diagnostics, Indianapolis, IN) by 16 strokes of a Potter-Elvehjem homogenizer at 800 rpm. Homogenates were spun at in a Sorvall SS-34 rotor at 1,000 xg for 10 min and S1 supernatants were recovered. S1 fractions were further sedimented at 12,000 xg for 20 min. This P2 pellet corresponds to a crude synaptosome fraction. These synaptosomes were resuspended in ice cold PBS and resedimented at 12,000 xg for 20 min before the addition of the DSP crosslinker. Cross-linking was performed in ice cold PBS as described.

Blinded Analysis of Synaptic Vesicle Size

Unstained sections of striatum or dentate gyrus from three *mocha* and three WT grizzled mice were dehydrated as previously described, and processed for electron microscopy. Grids of unstained 60nm sections were collected by person A. Person B then rearranged these grids and provided a code to mask the original identity of each grid. Person A then acquired electron micrographs as previously described, at zooms of both 25,000x and 50,000x. Asymmetric synapses were selected that contained a well-defined post-synaptic density. Synaptic vesicle area of each identifiable synaptic vesicle in an asymmetric pre-synaptic terminal of

high magnification images (50,000x) was determined with Image J software (freeware available at http://rsbweb.nih.gov/ij/index.html) by drawing a circle around the inner circumference of each vesicle. After data collection, person B revealed the original identity of each grid. Quantitative and statistical analysis of data was performed by Person C without knowledge of the genotype of the samples.

Behavioral Analysis

We performed rotarod analysis of mice, aged 7-12 weeks, according to (Krizkova and Vozeh, 2004). All genotypes were tested at 1 rpm, except for *Ap3b1*$^{-/-}$ and its corresponding control, *Ap3b1*$^{+/+}$, which were tested at 3 rpm.

Statistical Analysis

Experimental conditions were compared with the one-way ANOVA followed by Student-Newman-Keuls Multiple Comparison as a Post-Hoc test or Mann-Whitney U test using Synergy KaleidaGraph v4.03 (Reading, PA). Fisher exact test was performed using the engine: http://faculty.vassar.edu/lowry/VassarStats.html. Kolmogorov-Smirnoff test was performed with StatPlus Mac Built5.6.0pre/Universal (AnalystSoft, Vancouver, Canada).

Results

AP-3 is expressed throughout the brain with prominent expression in the hippocampus and striatum.

In order to assess brain region expression of both AP-3 isoforms, we used a monoclonal antibody against the δ subunit of AP-3, a subunit that assembles into neuronal and ubiquitous AP-3 isoforms (Peden *et al.*, 2004). Using this antibody, we performed an immunoperoxidase reaction on vibrotome brain sections from wild type (WT) and AP-3-deficient $Ap3d^{mh/mh}$ (*mocha*) mouse brains. We chose representative sections from the striatum, hippocampus, cortex and amygdala for imaging. Wild type and *mocha* brain sections were processed and imaged in parallel using identical parameters so that we could compare immunoperoxidase reaction intensity. We determined immunoperoxidase reaction specificity of this antibody in brain sections from $Ap3d^{mh/mh}$ (*mocha*) brains, which are null for δ adaptin. The AP-3 δ monoclonal antibody (SA4) generates immunoperoxidase positive reaction products in wild type, but not $Ap3d^{mh/mh}$, brain tissue (Figure 1A). Furthermore, the immunoperoxidase signal observed in wild type can be outcompeted by incubation with an antigenic δ peptide corresponding to the amino acids 680-710 of human delta adaptin (AAD03777; GI:1923266) and common with the murine ortholog (Craige *et al.*, 2008) (Figure 1A).

By light microscopy, AP-3-positive reactions localize throughout the brain, including the amygdala, cortex, hippocampus and striatum (Figure 1B and data not shown). However, AP-3 expression is most prominent within the hippocampus and striatum (Figure 1B). Because of the strong expression of AP-3

in striatum and hippocampus, the following light and electron microscopy analyses will focus on these two brain regions.

AP-3 localizes to pre-synaptic axons and terminals.

To discern the neuronal subcellular compartments where AP-3 is present, we performed immunofluorescence colocalization of AP-3 in primary cultured neurons from wild type brain and vibrotome sections of mouse hippocampal dentate gyrus. Synaptic elements were identified with antibodies against the synaptic vesicle proteins VAMP2 and synaptophysin in cultured neurons and brain sections respectively. As a representative membrane protein sorted to synaptic vesicles by AP-3-dependent mechanisms, we focused on VAMP7-TI. VAMP7-TI is a v-(R)-SNARE whose targeting to synaptic vesicles is altered in all AP-3 deficiencies (Salazar *et al.*, 2006; Scheuber *et al.*, 2006; Newell-Litwa *et al.*, 2009). Deconvolution immunofluorescence microscopy of mouse primary neurons (E18.5; DIV 14) demonstrates that AP-3, the AP-3 cargo VAMP7-TI, and the synaptic vesicle protein, synaptobrevin/VAMP2, co-localize in discrete punctae along neuronal processes (Figure 2A). Confocal microscopy of mouse hippocampal sections shows that AP-3 and VAMP7-TI significantly co-localize in synaptic terminals of the dentate gyrus (Figure 2C). Unlike VAMP7-TI, AP-3 also exhibits strong expression in cell bodies of the dentate gyrus (Figure 2C, see inset). Because VAMP7-TI and AP-3 possess overlapping expression in synaptic terminals of the dentate gyrus, we used VAMP7-TI to indicate AP-3-expressing synaptic terminals. Both VAMP7-TI staining and Synaptophysin (Sphysin), colocalized is discrete elements of the dentate gyrus neuropil (Figure 2B). These

results suggest that AP-3 exist alongside its membrane protein cargo VAMP7-TI in nerve terminals *in vitro* as well as *in vivo*.

We further defined the ultrastructural and sub-synaptic localization of AP-3 by quantitative immunoelectron microscopy. We used the monoclonal antibody against the δ subunit of AP-3 due to the signal specificity using immunoperoxidase detection of antigen-antibody complexes (Figure 1). AP-3 immunoreactive material was detected at the ultrastructural level with biotinylated anti-mouse antibodies and avidin-biotin peroxidase complex. We documented AP-3 expression in the following elements according to their characteristic brain morphology as schematically represented in Supplemental Figure 1: dendrites, spines, small unmyelinated axons, pre-terminal axons, axon terminals, myelinated axons, glia, and 'other' for elements that lack a clear ultrastructure. As suggested by the immunofluorescence microscopy, AP-3 preferentially localizes to axons and nerve terminals in the striatum and hippocampus (CA3 and dentate gyrus) of mouse brain. In contrast, AP-3 was minimally detected in either dendritic or glial structures in both the striatum and hippocampus (Figure 4A, $p<0.0001$ axons v. dendrites for all brain regions). Immunoreactive axonal structures include small unmyelinated axons (Figure 3C, G and H), pre-terminal axons (Figure 3C), axon terminals (Figure 3A-F), and on rare occasions, myelinated axons (Figure 3H). In both the striatum and hippocampus, the majority of axonal AP-3 localizes to axonal segments prior to the synapse, either small unmyelinated axons or pre-terminal axons (Figure 4B). Thus, while AP-3 labels both axons and dendrites of cultured mouse primary neurons (Seong *et al.*, 2005), this is the first *in vivo* demonstration that AP-3

possesses a polarized distribution in neurons where it is primarily restricted to axonal structures.

Interestingly, AP-3 immunoreactivity in pre-terminal axons and nerve terminals frequently only partially labeled these structures, rather than entirely filling the axon. This is especially unusual for avidin-biotin-complex (ABC) immunoperoxidase reactions, which generally result in intense signals that fill the entire structure (Hsu *et al.*, 1981). Quantification of AP-3 coverage in axons reveals that AP-3 shows partial labeling in ~3-5 axons per 11.14 μm^2, while the number of axons with total AP-3 coverage is on average less than half of this amount (~1.5 axons per 11.14 μm^2) (Figure 4C; Figure 3A-H show axons with partial labeling, while Figure 3A, G and H show small unmyelinated axons with complete coverage). AP-3 in axon terminals closely associates with synaptic vesicle profiles (Figure 3A-F). Thus, this partial AP-3 coverage of axons most likely results from AP-3's association with a specific subset of vesicles present at the synapse. These AP-3 positive vesicles could represent synaptic vesicles and/or synaptic vesicle precursors derived from upstream neuronal compartments.

Ap3d$^{mh/mh}$* alters *synaptic vesicle size in asymmetric synapses of perfusion-fixed adult mouse brain.

The presence of AP-3 in axons and nerve terminals suggests that deficiencies in AP-3 could alter the ultrastructural organization of the synapse. Although, we have determined that AP-3 regulates the sorting of selected synaptic vesicle membrane proteins (Salazar *et al.*, 2004a; Salazar *et al.*, 2004b; Salazar *et al.*, 2005a; Seong *et al.*, 2005; Newell-Litwa *et al.*, 2009), we have yet

to determine whether changes in synaptic vesicle composition lead to modifications in pre-synaptic architecture. We performed double-blinded quantitative ultrastructural morphometric analysis of pre-synaptic elements. We focused on determining the area of synaptic vesicles in asymmetric 'glutamatergic' synapses from the striatum and dentate gyrus of wild type and *Ap3d*$^{mh/mh}$ *mocha* brains. We selected these brain regions because AP-3 immunoreactive levels were the highest in these anatomical locations (Fig. 1). We scored asymmetric synapses because these terminals are mostly glutamatergic and are readily identified by their characteristic electron-dense post-synaptic density (Conti *et al.*, 1989; Baude *et al.*, 1995; Garner and Kindler, 1996). Moreover, the presence of post-synaptic density offers an ultrastructural landmark to unequivocally identify organelles in close apposition to synaptic contacts. Importantly, AP-3 interacts with a marker of glutamatergic synapses, Vesicular Glutamate Transporter-1 (VGlut1), both in neuronal cell lines as well as fractions enriched in nerve terminals (Figure 7) (Newell-Litwa *et al.*, 2009). Synaptic vesicle luminal cross-sectional areas scored in striatum distributed into two populations. One of these populations (500-550 nm^2) predicts an inner vesicle diameter of ~25 nm similar to that reported in CA1 excitatory synapses in the rodent hippocampus (Schikorski and Stevens, 1997). Notably, the bimodal distribution of synaptic vesicle area was not observed in wild type dentate gyrus. In fact, dentate gyrus vesicles exhibited a significantly reduced area in comparison with synaptic vesicles from wild type striatum (Figure 6A $p<0.0001$ Kolmogorov-Smirnoff test). These differences in synaptic vesicle area were

observed irrespective of whether either brain was analyzed independently or whether data from all three wild type brains were pooled and analyzed together.

When we compared *mocha* and wild type synaptic vesicles from the striatum, we observed a shift to smaller-sized vesicles in *mocha* as reflected in both area histograms as well as probability plots. (Figure 5A-G, 6B $p<0.0001$ Kolmogorov-Smirnoff test). In contrast to these changes in striatum synaptic vesicle size, loss of AP-3 oppositely impacts synaptic vesicle area in the dentate gyrus, with *mocha* exhibiting larger vesicles (Figure 5H-K, 6C $p<0.0001$ Kolmogorov-Smirnoff test). These results show AP-3 deficiencies, in addition to determining synaptic vesicle composition (Seong *et al.*, 2005; Newell-Litwa *et al.*, 2009), also affect the ultrastructure of the synapse in perfusion-fixed adult mouse brain. Moreover, they unveil region specific differences in wild type and AP-3 null synaptic vesicles that were also previously unrecognized.

BLOC-1 deficiencies selectively affect synapses in the dentate gyrus.

Region specific differences in the morphometry of wild type and AP-3-null synaptic vesicles suggest two non-exclusive hypotheses. First, region specific differences in synaptic vesicle composition, in both wild type and AP-3 null brains, may determine differences in synaptic vesicle morphometry. Second, AP-3 interacting factors that modulate AP-3 sorting function may possess region specific effects, which could be reflected either as changes in nerve terminal architecture or composition. We genetically tested this last hypothesis using mouse models deficient in subunits of the BLOC-1 complex. BLOC-1 is an octameric complex that interacts with AP-3 (Di Pietro *et al.*, 2006; Salazar *et al.*,

2006; Newell-Litwa *et al.*, 2009). We analyzed mice carrying null alleles in two BLOC-1 subunits, either pallidin ($Pldn^{pa/pa}$) or muted ($Muted^{mu/mu}$). We selected these particular BLOC-1 deficiencies because of their documented role in AP-3 mediated membrane protein sorting (Di Pietro *et al.*, 2006; Salazar *et al.*, 2006; Newell-Litwa *et al.*, 2009; Salazar *et al.*, 2009). Both deficiencies lead to a destabilization of the other BLOC-1 subunits (Falcon-Perez *et al.*, 2002; Li *et al.*, 2003). Furthermore, these BLOC-1 null-alleles are in different genetic backgrounds (Huang *et al.*, 1999; Zhang *et al.*, 2002). Thus, phenotypes observed in $Pldn^{pa/pa}$ and $Muted^{mu/mu}$ exclude background-specific effects. Finally, $Pldn^{pa/pa}$ and $Muted^{mu/mu}$ possess neurological phenotypes shared with AP-3 deficient mice (see Supplemental Figure 2).

We first confirmed biochemically that BLOC-1 and AP-3 form a complex in fractions enriched in brain nerve terminals (synaptosomes). We used as a control neuroendocrine PC12 cells expressing Vglut1 (Salazar *et al.*, 2005a). We previously performed crosslinking with the cell-permeable crosslinker DSP followed by complex immunoprecipitation in naïve PC12 cells (Craige *et al.*, 2008; Newell-Litwa *et al.*, 2009; Salazar *et al.*, 2009). DSP crosslinking stabilizes adaptor-protein interactions allowing us to selectively isolate AP-3 immunocomplexes under stringent biochemical conditions (Salazar *et al.*, 2009). We isolated AP-3-immunocomplexes using the AP-3 δ monoclonal antibody (SA4), and resolved bead bound material by SDS-PAGE. The composition of the cross-linked AP-3 complexes was assessed by immunoblot. Both in synaptosomes as well as PC12 cells expressing Vglut1, the interaction of AP-3 with BLOC-1 was revealed by the presence of the following BLOC-1 subunits:

pallidin, dysbindin and/or muted (Figure 7A, Lanes 5 and 6; Figure 7B, Lane 4). We used as positive controls two membrane proteins targeted to synaptic vesicles by AP-3 dependent mechanism, the excitatory neurotransmitter transporter, VGlut1, and/or phosphatidylinositol-4-kinase type II alpha (PI4KIIα) (Salazar *et al.*, 2005a; Salazar *et al.*, 2005b; Craige *et al.*, 2008) (Figure 7A, Lanes 5 and 6; Figure 7B, Lane 4). In contrast, AP-3 complexes isolated from either synaptosomes or PC12 cells expressing Vglut1 were free of membrane proteins not sorted by AP-3, such as transferrin receptor (TrfR) and/or synaptophysin (Figure 7A, Lanes 5 and 6; Figure 7B, Lane 4). Neither BLOC-1 subunits nor synaptic vesicle proteins sorted by AP-3 (Vglut1 and PI4KIIα) were detected in control beads either lacking antibodies or decorated with transferrin receptor antibodies (Figure 7A, Lanes 1-4; Figure 2B, Lanes 1 and 2). These results indicate AP-3 and BLOC-1 complexes interact in brain fractions enriched in nerve terminals.

We determined whether $Pldn^{pa/pa}$ and $Muted^{mu/mu}$ affect synaptic terminals in a region-selective fashion by assessing the immunoreactivity levels and distribution of membrane proteins targeted to the synapse. We used monoclonal antibodies to detect either the AP-3 cargo, VAMP7-TI, or the AP-3-independent synaptic vesicle protein, Synaptophysin. We performed similar analyses in AP-3 deficient *mocha* brains as controls since this mouse mutant has more pronounced neurological phenotypes than BLOC-1 deficiencies (Kantheti *et al.*, 1998; Kantheti *et al.*, 2003; Salazar *et al.*, 2004b; Newell-Litwa *et al.*, 2007). To assess the reliability of phenotypes across multiple experiments and animals as well as data dispersion, we measured immunoreactivity by developing a gross

semi-quantitative method that measures the intensity of antigen-positive immunoreactivity by Image J. Using immunoperoxidase light microscopy, we detected a significant and selective reduction in VAMP7-TI immunoreactivity within AP-3-deficient *mocha* dentate gyrus (Figure 8, compare C2 and D2 with C3 and D3; quantification of VAMP7-TI expression, Figure 8G, $p<0.0001$) (Scheuber *et al.*, 2006). Similarly, BLOC-1 deficiencies also significantly and selectively reduced VAMP7-TI immunoreactivity within the dentate gyrus (Figure 8, compare E2 and F2 with E3 and F3; quantification of VAMP7-TI expression, Figure 8G, $p<0.015$, $Muted^{mu/mu}$ and $p<0.004$, $Pldn^{pa/pa}$). VAMP7-TI immunoreactivity remained unaffected in either the striatum or CA3 region of the hippocampus in both BLOC-1 deficiencies (Figure 8G) as well as $Ap3d^{mh/mh}$ *mocha* brains ($p<0.0001$). Notably, despite the fact that AP-3 is absent from all *mocha* brain regions, loss of AP-3 mirrors BLOC-1 deficiencies by selectively reducing VAMP7-TI within the dentate gyrus (Figure 8, compare A2-D2 with A3-D3, quantification of VAMP7-TI expression, Figure 8G). Neither AP-3 nor BLOC-1 deficiencies altered the immunoreactivity levels of synaptophysin in any of the analyzed brain regions (Figure 8, compare A-F with A1-F1, quantification of Sphysin, Figure 8G). This result therefore excludes the possibility that reductions in VAMP7-TI immunoreactivity may result from a selective loss of synaptic terminals in the dentate gyrus.

BLOC-1 deficiency reduces AP-3 expression in the dentate gyrus.

Based on the association of BLOC-1 with AP-3, the similarity between the VAMP-7-TI region specific phenotypes in BLOC-1 and AP-3 null dentate gyrus,

we examined whether the absence of BLOC-1 could alter AP-3 content in a region-selective manner. We used immunoperoxidase light and immunoelectron microscopy to detect the δ subunit of AP-3. We examined AP-3 expression in the striatum and hippocampus of two BLOC-1 deficiencies, *Pallidin*$^{pa/pa}$ (*Pldn*$^{pa/pa}$) and *Muted*$^{mu/mu}$. In both of these BLOC-1 deficiencies, AP-3 was significantly reduced in the hilus of the dentate gyrus (DGh) (Figure 9, compare B, D, and E with B', D', and E'). When measured, AP-3 immunoreactivity levels were reduced by ~30% in the dentate gyrus of either *Pldn*$^{pa/pa}$ or *Muted*$^{mu/mu}$ when compared to control brain sections (Figure 9F, $p<0.0007$). In contrast, AP-3 was not significantly reduced in either the striatum or CA3 region of the hippocampus (Figure 9, compare A-C with A'-C'; quantification of AP-3 expression, Figure 9F). We used quantitative immunoelectron microscopy to determine the subcellular neuronal compartments where this AP-3 reduction occurred. Similar to light microscopy, electron microscopy of both striatum and the CA3 region of the hippocampus revealed similar amounts of AP-3-labeled elements per field area between control *Muted*$^{+/mu}$ and BLOC-1-deficient *Muted*$^{mu/mu}$ mouse brain (Figure 10A). However, immunoelectron microscopy of AP-3 within the dentate gyrus of BLOC-1-null mouse brain (*Muted*$^{mu/mu}$) shows that AP-3 positive elements are reduced by a third (Figure 10A, $p<0.0003$). The absence of BLOC-1 most dramatically affects the labeling of axonal structures, decreasing AP-3 axonal expression to ~60% of control levels (Figure 10B, $p<0.0001$). This reduction significantly affects small unmyelinated axons and pre-terminal axons (Figure 10C, $p<0.003$, SUA, and $p<0.006$, PT). Neither does loss of BLOC-1 affect AP-3 targeting to post-synaptic dendrites or glia (Figure 10C and 10B

'Other'). These data indicate that BLOC-1 selectively regulates AP-3 subcellular distribution and content in the dentate gyrus of the hippocampus. Collectively, our findings support the hypothesis that factors that interact with the AP-3 complex, such as BLOC-1, modulate AP-3–dependent synaptic vesicle biogenesis in a region-specific manner.

Discussion

Synaptic vesicle biogenesis mechanisms determine quantal neurotransmission. Defects of synaptic vesicle biogenesis pathways result in phenotypes ranging from altered synaptic vesicle composition and morphology to the complete absence of synaptic vesicles from nerve terminals (Toshio Kosaka, 1983; González-Gaitán and Jäckle, 1997; Zhang *et al.*, 1998; Nonet *et al.*, 1999; Karunanithi *et al.*, 2002; Heerssen *et al.*, 2008; Kasprowicz *et al.*, 2008; Sato *et al.*, 2009). The Hermansky Pudlak complex, AP-3, participates in synaptic vesicle biogenesis from endosomes, with AP-3 deficiencies altering the synaptic vesicle content of perfusion-fixed mouse brain (Faundez and Kelly, 2000; Nakatsu *et al.*, 2004; Salazar *et al.*, 2004a; Salazar *et al.*, 2005a; Salazar *et al.*, 2005b; Seong *et al.*, 2005; Newell-Litwa *et al.*, 2009). Here we demonstrated that AP-3-dependent synaptic vesicle biogenesis mechanisms differentially regulate the composition of synaptic terminals in a brain region-specific fashion. In addition to regulating the molecular composition of the synapse, AP-3 likewise uniquely controls synaptic vesicle size between the striatum and the dentate gyrus of the hippocampus. How do different brain regions modify AP-3-dependent synaptic vesicle biogenesis mechanisms to produce diverse synaptic

vesicle phenotypes? Anatomically restricted AP-3 deficient phenotypes are not related to a restricted pattern of AP-3 expression in wild type brain. In fact, AP-3 is present throughout the brain, although more prominently expressed in both the striatum and hippocampus (Figure 1). Furthermore, quantitative immunoelectron microscopy indicates that the sub-synaptic distribution of AP-3 is similar between striatum and hippocampus (Figure 3). Therefore, we proposed two alternative mechanisms that could account for anatomically restricted AP-3-dependent phenotypes. One possibility is that the repertoire of synaptic vesicle membrane proteins present in these vesicles differs across brain regions both in their type and in their stoichiometry. We did not further evaluate this hypothesis in our current research. However, in order to limit variability in synaptic vesicles due to the type of neurotransmitter stored in them, we focused our analysis of synaptic vesicles on asymmetric excitatory synapses, which tend to be glutamatergic in nature. At a minimum, the striatum and dentate gyrus share in common the AP-3 cargo, VAMP7-TI as well as the AP-3-independent synaptic vesicle protein, synaptophysin (Figure 8). Alternatively, a non-exclusive mechanism is that AP-3 interacting proteins or protein complexes are either selectively expressed or they specifically modulate AP-3-dependent vesicle biogenesis in a brain region-selective manner. We tested this hypothesis by examining AP-3 and AP-3 cargo expression in BLOC-1 complex deficiencies. We chose to examine how BLOC-1 might distinctively regulate AP-3-dependent synaptic composition for the following reasons. First, AP-3 and BLOC-1 form a complex in multiple cell types, including non-neuronal and neuronal cells (Figure 7) (Di Pietro *et al.*, 2006; Salazar *et al.*, 2006; Newell-Litwa *et al.*, 2009; Salazar

et al., 2009). Importantly, this AP-3/BLOC-1 supramolecular complex localizes to brain fractions enriched for nerve terminals (synaptosomes) (Figure 7). Secondly, BLOC-1 deficiencies alter the sorting of AP-3-dependent cargo, including the targeting of particular AP-3 cargo to synaptic vesicle fractions (Di Pietro *et al.*, 2006; Salazar *et al.*, 2006; Newell-Litwa *et al.*, 2009; Salazar *et al.*, 2009). Moreover, BLOC-1 subunits are expressed throughout the brain (Talbot *et al.*, 2006; Feng *et al.*, 2008). Intriguingly, we observed that two BLOC-1-null alleles selectively reduce the AP-3 cargo, VAMP7-TI in the dentate gyrus. This observation is similar to the VAMP7-TI phenotype reported here (Figure 8) and by (Scheuber *et al.*, 2006) in AP-3-null brain. Furthermore, this BLOC-1-dependent regulation of VAMP-TI specifically within the dentate gyrus correlates with the finding that BLOC-1 deficiencies also specifically reduce AP-3 expression within pre-synaptic axons of the dentate gyrus (Figures 9 and 10). Thus, BLOC-1 serves as a dentate gyrus-specific regulator of AP-3-dependent sorting to pre-synaptic axonal compartments.

Ultimately these findings challenge the belief that uniform synaptic vesicle biogenesis mechanisms across brain regions result in synaptic vesicles of uniform size (Zhang *et al.*, 1999). Importantly, differences in synaptic vesicle size have been observed as early as 1977 when electric stimulation of the *Torpedo* electric organ induced the formation of a smaller-sized synaptic vesicle pool (Zimmermann and Denston, 1977). Furthermore, more recent research demonstrates different sized synaptic vesicles at two distinct glutamatergic terminals in *Drosophila* (Karunanithi *et al.*, 2002). Here, we demonstrate that synaptic vesicle size is on average smaller in asymmetric excitatory synapses of

the dentate gyrus than the striatum (Figures 5 and 6). Furthermore, rather than a uniform synaptic vesicle population in the striatum, we observe a bimodal distribution of synaptic vesicle size in the striatum of wild-type mouse brains (Figures 5 and 6). These inherent differences in synaptic vesicle size suggest the presence of unique synaptic vesicle biogenesis pathways. Importantly, AP-3-dependent endosomal sorting to synaptic vesicles contributes to brain regions-specific differences in synaptic vesicle size (Figures 5 and 6). As we have stated, BLOC-1 uniquely regulates AP-3-dependent synaptic composition specifically within the dentate gyrus.

Thus, contrary to the current view that synaptic vesicle biogenesis mechanisms are uniform throughout the brain, our research indicates that diverse brain regions exhibit unique synaptic composition and morphology as a consequence of brain region-specific endosomal sorting mechanisms that regulate synaptic vesicle biogenesis. Global loss of AP-3, while expressed throughout the brain, differentially regulates synaptic composition and morphology in the striatum versus the dentate gyrus. Specifically, AP-3 reduced select synaptic vesicle cargo expression in the dentate gyrus, without affecting the striatum. These cargo differences correlate with either increased synaptic vesicle size in the dentate gyrus or decreased synaptic vesicle size in the striatum. These results suggested that different brain regions distinctively influence AP-3-dependent sorting to synaptic vesicles to result in the observed synaptic alterations.

Acknowledgements

Karen Newell-Litwa is particularly indebted to the members of Dr. Yoland Smith's laboratory for their shared expertise. Jim Bogenpohl, Susan Jenkins, Darlene Mitrano, Jean-Francois Pare, and Rosa Villalba deserve special thanks for their time spent training K.N-L.

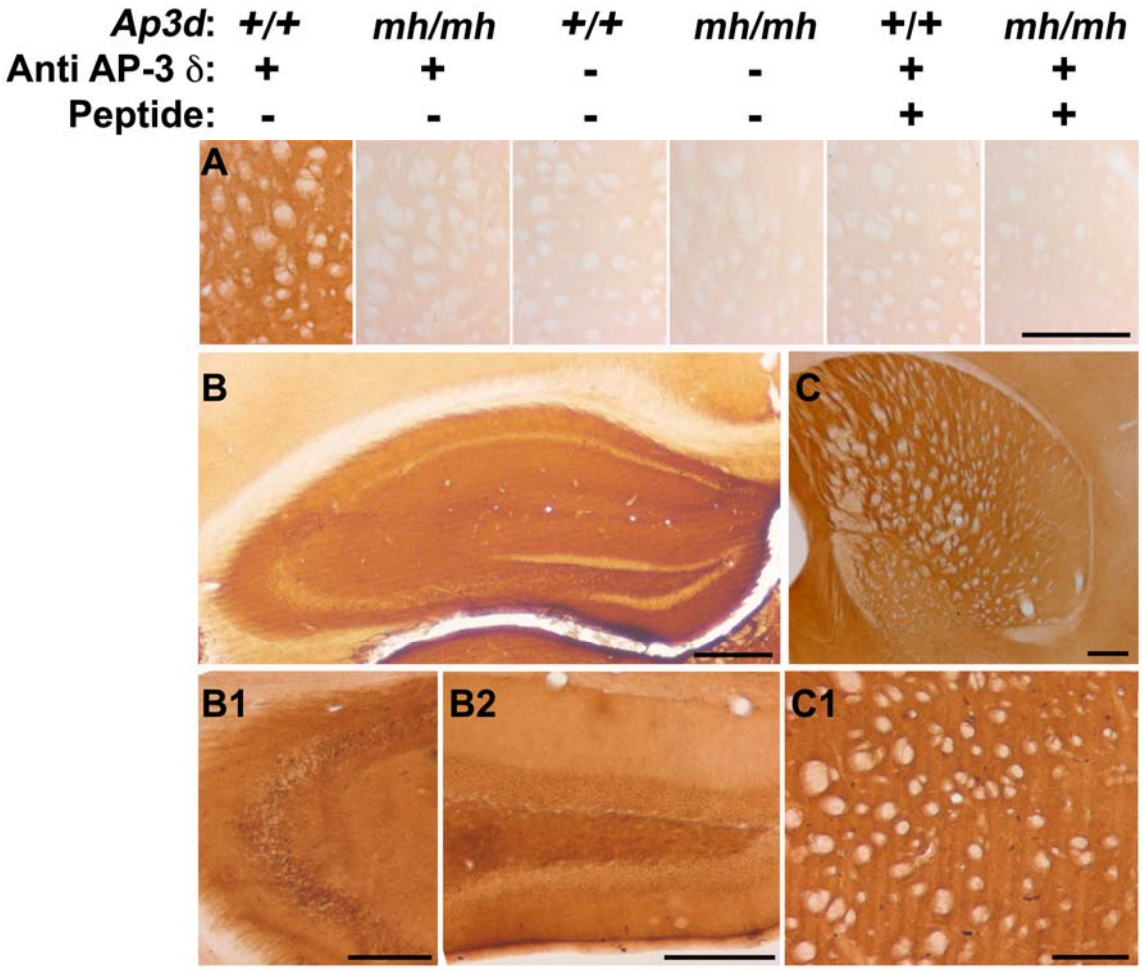

Figure 1: AP-3 is expressed throughout the brain with prominent expression in the hippocampus and striatum. **A)** Immunoperoxidase labeling of wild type (+/+) and AP-3-deficient *mocha* (mh/mh) striatum in the presence or absence of the monoclonal primary antibody against the δ subunit of AP-3 (Anti AP-3 δ). Binding of the anti-AP-3 δ antibody to the endogenous antigen is outcompeted by incubation with the antigenic δ peptide corresponding to the amino acids 680-710 of human delta adaptin (AAD03777; GI:1923266). **B-C2)** Immunoperoxidase labeling of AP-3 in the **(B)** hippocampus, (**B1)** the CA3

region of the hippocampus, (**B2)** the dentate gyrus of the hippocampus, and **(C-C1)** the striatum of control mouse brain. Scale bar = 1mm.

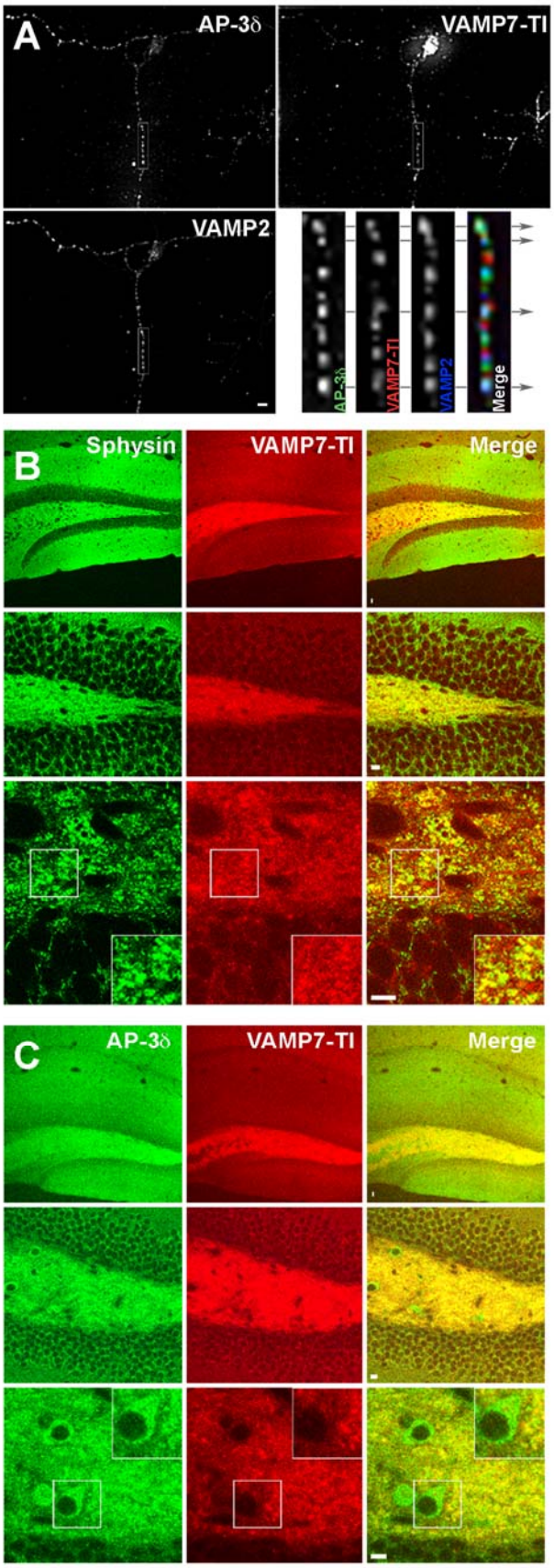
A
AP-3δ
VAMP7-TI
VAMP2
AP-3δ
VAMP7-TI
VAMP2
Merge
B
Sphysin
VAMP7-TI
Merge
C
AP-3δ
VAMP7-TI
Merge

Figure 2: AP-3 localizes to synaptic terminals of the dentate gyrus. A) Fixed E18.5 wild type C57 mouse primary neuron (DIV 14) immunostained for AP-3, the AP-3 cargo VAMP7-TI, and the synaptic vesicle protein VAMP2/synaptobrevin. Arrows indicate discrete punctae within the neuronal process where all three proteins co-localize. **B)** Confocal images of wild type *grizzled* dentate gyrus immunostained for AP-3 cargo, VAMP7-TI, and the synaptic vesicle protein, synaptophysin. **C)** Confocal images of wild type *grizzled* dentate gyrus immunostained for AP-3 and the AP-3 cargo, VAMP7-TI. Scale bar = 5μm.

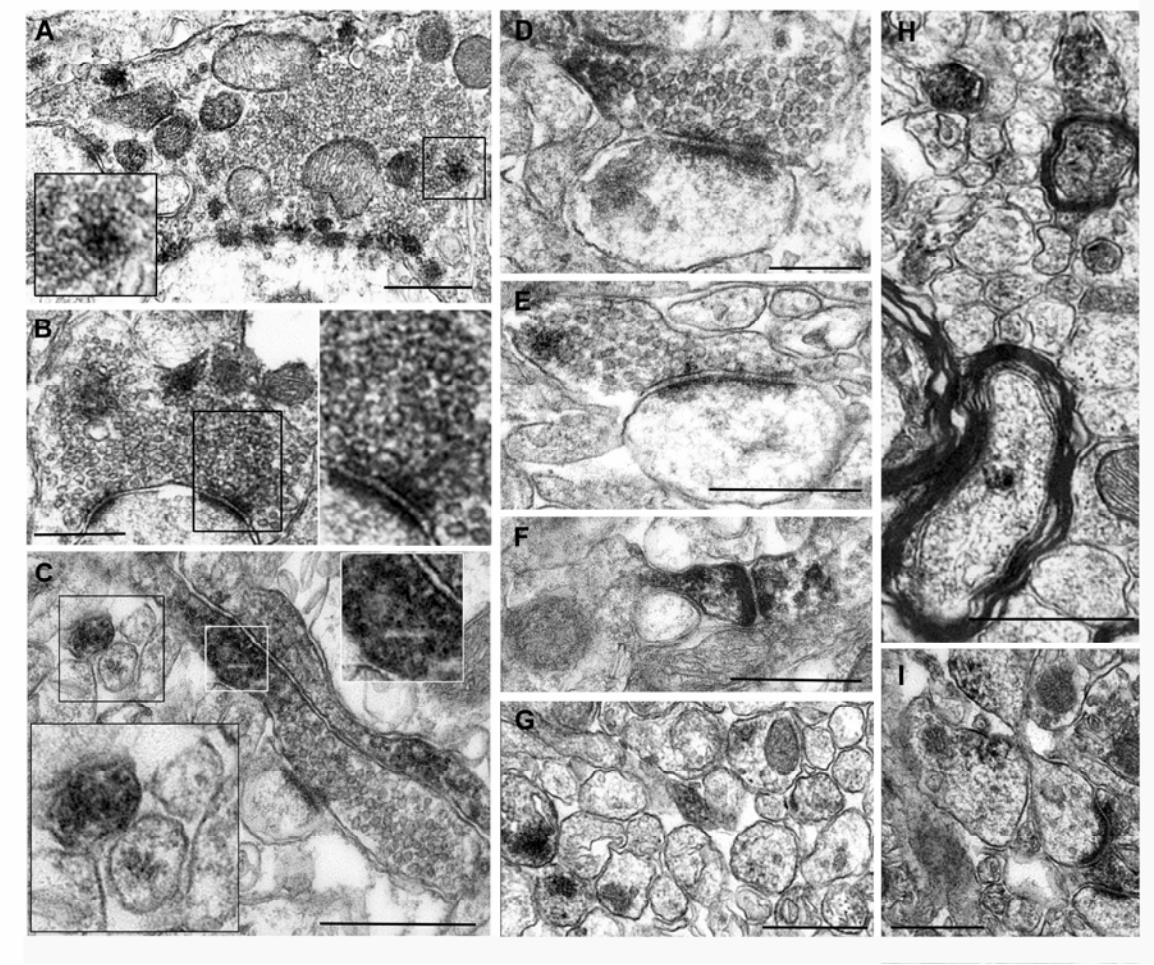

Figure 3: Sub-synaptic localization of AP-3 by immunoelectron microscopy. AP-3 was detected with the monoclonal antibody against the AP-3 δ subunit and revealed by biotinylated anti-mouse antibodies and the avidin-biotin peroxidase complex. AP-3 partially labels axon terminals of the striatum **(C, E, and F)**, the CA3 region of the hippocampus **(A)**, and the dentate gyrus **(B, D)**. AP-3 partially labels a pre-terminal axon in the striatum **(C).** AP-3 either partially or wholly labels small unmyelinated axons of the striatum **(C, H)** and the dentate gyrus **(G)**. In **(H)**, AP-3 partially labels two myelinated axons of the striatum. AP-3 also labels a dendritic spine in the striatum **(F)**, and two

dendrites in the CA3 region of the hippocampus **(I)**. The frequency of a particular labeled element is quantified in Figure 4. Scale bar = 0.5µm.

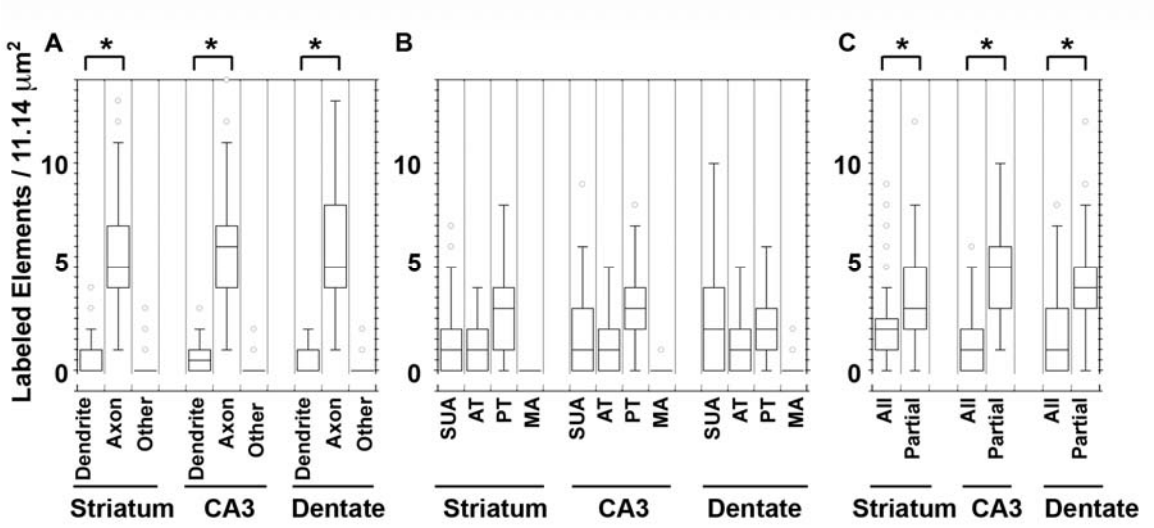

Figure 4: The majority of AP-3 partially labels axons in the striatum and hippocampus. Quantification of the number and type of elements immunoreactive for AP-3 per 11.14 μm² in electron micrographs of control mouse brain (wild type *grizzled* and heterozygous $Muted^{+/mu}$). We classified the following elements: dendrites (spines and proximal dendrites), axons (axon terminals (AT), myelinated axons (MA), pre-terminal axons (PT), and small unmyelinated axons (SUA)), and 'other' (glia and unidentifiable structures) (see Supplemental Figure 1). **A)** In both the striatum and hippocampus (CA3 and dentate gyrus), AP-3 labels significantly more axons (~5-6 AP-3-positive axons/11.14 μm²) than either dendrites (~0.5-1 AP-3-positive dendrite/11.14 μm²; *p<0.0001 for all brain regions) or other elements (~0.1-0.15 AP-3-positive other/11.14 μm²). **B)** AP-3 localizes to both pre-terminal axon structures (~1.3-2.4 SUA/11.14 μm²; ~2-3 PT/11.14 μm²; negligible AP-3 immunoreactivity in MA) and axon terminals (~1 AT/11.14 μm²). **C)** The majority of AP-3-positive axons exhibit partial labeling (~3-5 partially-labeled axons/11.14 μm²) rather than immunoperoxidase labeling throughout the terminal ('all') (~1.4-1.9 'all'/11.14

μm^2; *$p<0.0001$). (n = 4; 147 for striatum; n = 4; 76 for CA3; n = 4; 102 for dentate gyrus; n = number of animals; number of analyzed 11.14 μm^2 electron micrographs)

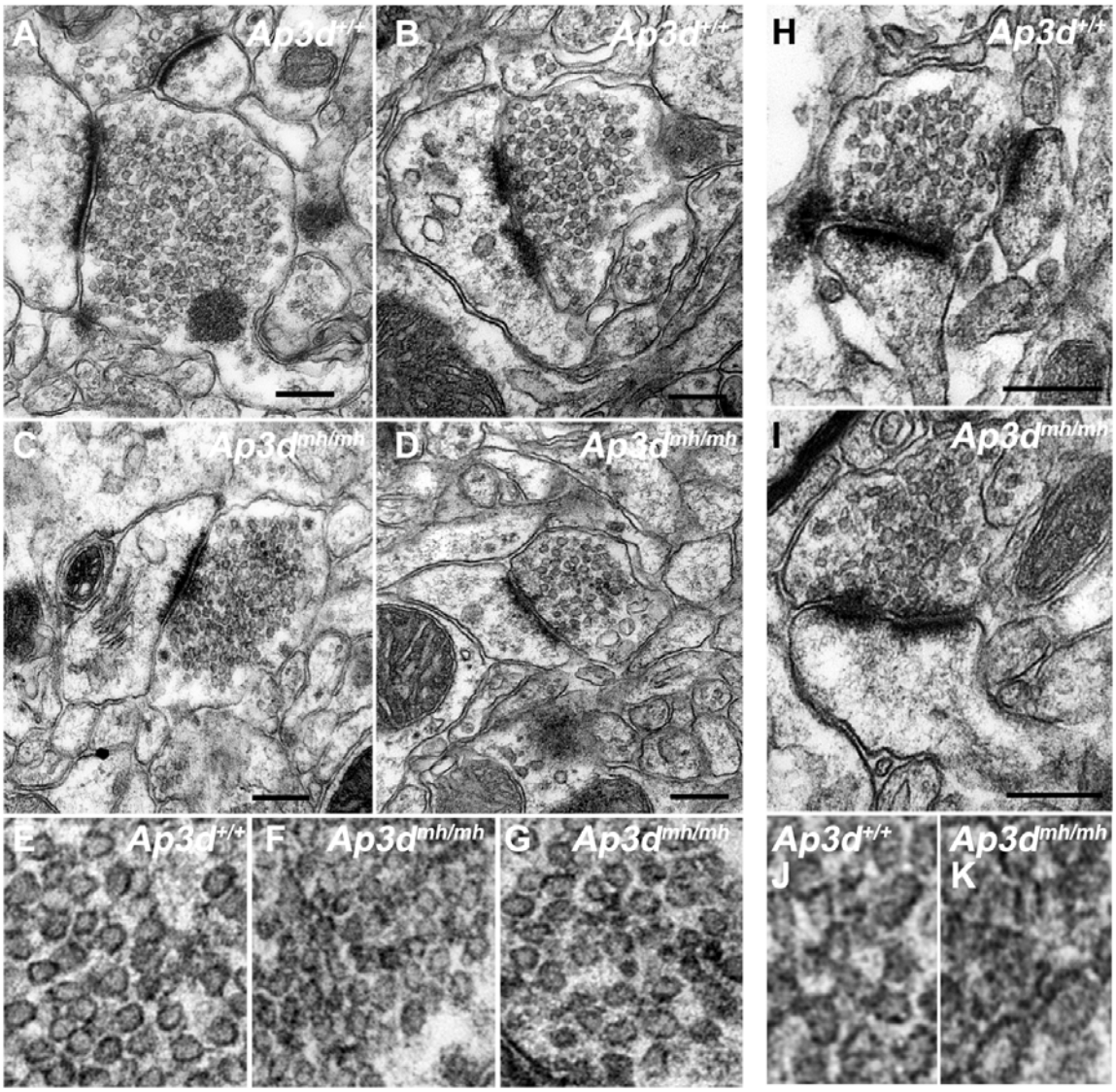

Figure 5: AP-3 differentially regulates synaptic vesicle size in asymmetric excitatory synapses of the striatum and dentate gyrus. Representative electron micrographs of asymmetric excitatory synapses from **(A-B)** wild type ($Ap3d^{+/+}$) and **(C-D)** AP-deficient ($Ap3d^{mh/mh}$) striatum. Synaptic vesicles from asymmetric synapses of the striatum in $Ap3d^{mh/mh}$ **(F-G)** exhibit smaller-sized synaptic vesicles than $Ap3d^{+/+}$ **(E).** Representative electron micrographs of asymmetric excitatory synapses from **(H)** wild type ($Ap3d^{+/+}$) and **(I)** AP-deficient ($Ap3d^{mh/mh}$) dentate gyrus. Synaptic vesicles from

asymmetric synapses of the dentate gyrus in *Ap3d*$^{mh/mh}$ **(K)** exhibit larger-sized synaptic vesicles than *Ap3d*$^{+/+}$ **(J).** Synaptic vesicle size is quantified in Figure 5. Scale bar =0.2 μm.

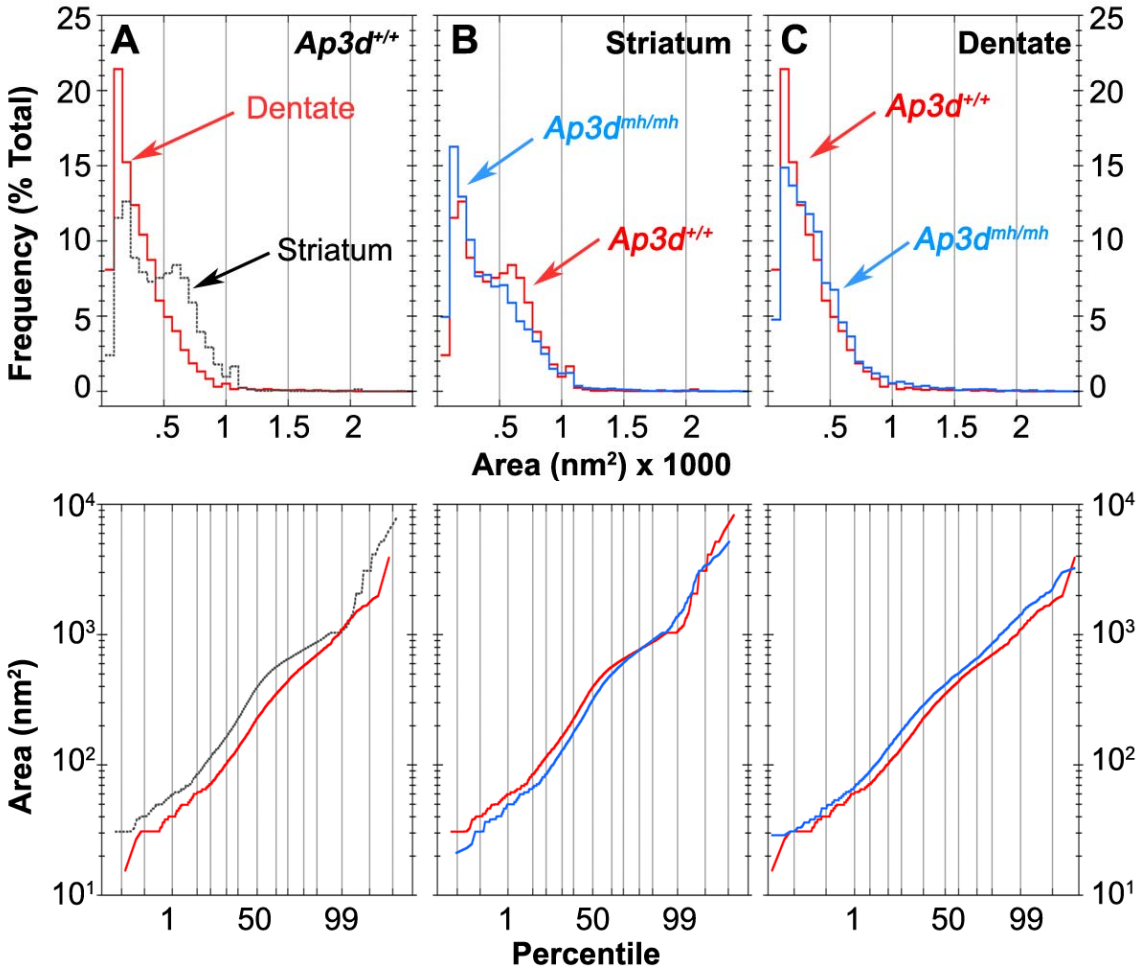

Figure 6: Quantification of synaptic vesicle size in asymmetric excitatory synapses from the striatum and dentate gyrus of *Ap3d*$^{+/+}$ and *Ap3d*$^{mh/mh}$ mouse brain. The distribution in the area of individual synaptic vesicles is represented as both a frequency histogram (top panel) and probability plot (bottom panel). **A)** Synaptic vesicles from asymmetric synapses of wild type dentate gyrus are statistically smaller than those of wild type striatum ($p<0.0001$ Kolmogorov-Smirnoff test). **B)** Loss of AP-3 (*Ap3d*$^{mh/mh}$) significantly reduces synaptic vesicle size in asymmetric synapses of the striatum ($p<0.0001$ Kolmogorov-Smirnoff test). **C)** Loss of AP-3 (*Ap3d*$^{mh/mh}$) significantly

increases synaptic vesicle size in asymmetric synapses of the dentate gyrus ($p<0.0001$ Kolmogorov-Smirnoff test). n = 3; 75; 9456 for *Ap3d*$^{+/+}$ striatum; n = 3; 32; 5472 for *Ap3d*$^{mh/mh}$ striatum; n = 3; 19; 3402 for *Ap3d*$^{+/+}$ dentate gyrus; n = 3; 18; 3376 for *Ap3d*$^{mh/mh}$ dentate gyrus; n = number of animals; number of analyzed synaptic terminals; total number of analyzed synaptic vesicles.

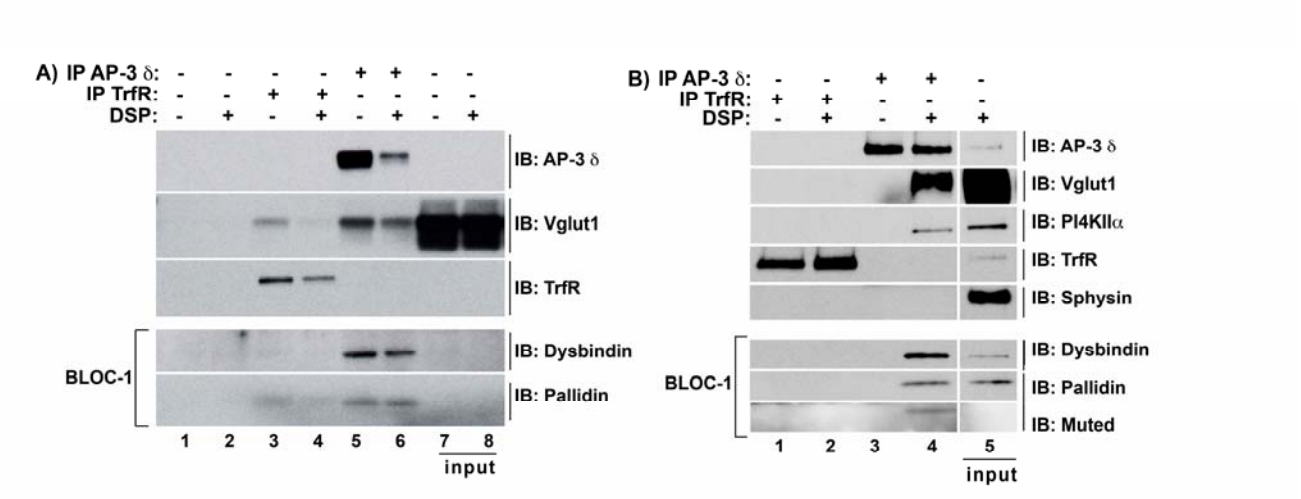

Figure 7: AP-3 and BLOC-1 form a complex in PC12 cells and synaptosome-enriched rat brain fractions. A) Immunoprecipitation of AP-3 complexes from PC12 cells. Immunoprecipitation with the monoclonal antibody against AP-3 δ (Lanes 5 and 6) isolates AP-3 and the following interacting proteins: VGlut1 and the BLOC-1 subunits, dysbindin and pallidin, with (Lane 6) or without DSP (Lane 5). AP-3 does not interact with Transferrin Receptor (TrfR) (Lanes 5 and 6). Immunoprecipitation with antibodies against TrfR, while capable of isolating TrfR, do not bring down AP-3, VGlut1, or BLOC-1 subunits, dysbindin and pallidin (Lanes 3 and 4). Lanes 1 and 2 are an empty bead control to detect non-specific binding to beads. Lanes 7 and 8 = 5% Input. **B)** Immunoprecipitation of AP-3 complexes from synaptosome-enriched rat brain fractions. Immunoprecipitation with the monoclonal antibody against AP-3 δ (Lanes 3 and 4) isolates AP-3 and the following interacting proteins: VGlut1 and the BLOC-1 subunits, dysbindin and pallidin in the presence of DSP selective crosslinking (Lane 4). AP-3 does not interact with Transferrin Receptor (TrfR) (Lanes 3 and 4). Immunoprecipitation with antibodies against TrfR, while

capable of isolating TrfR, do not bring down AP-3, VGlut1, or BLOC-1 subunits, dysbindin and pallidin (Lanes 1 and 2). Lane 5 = 5% Input.

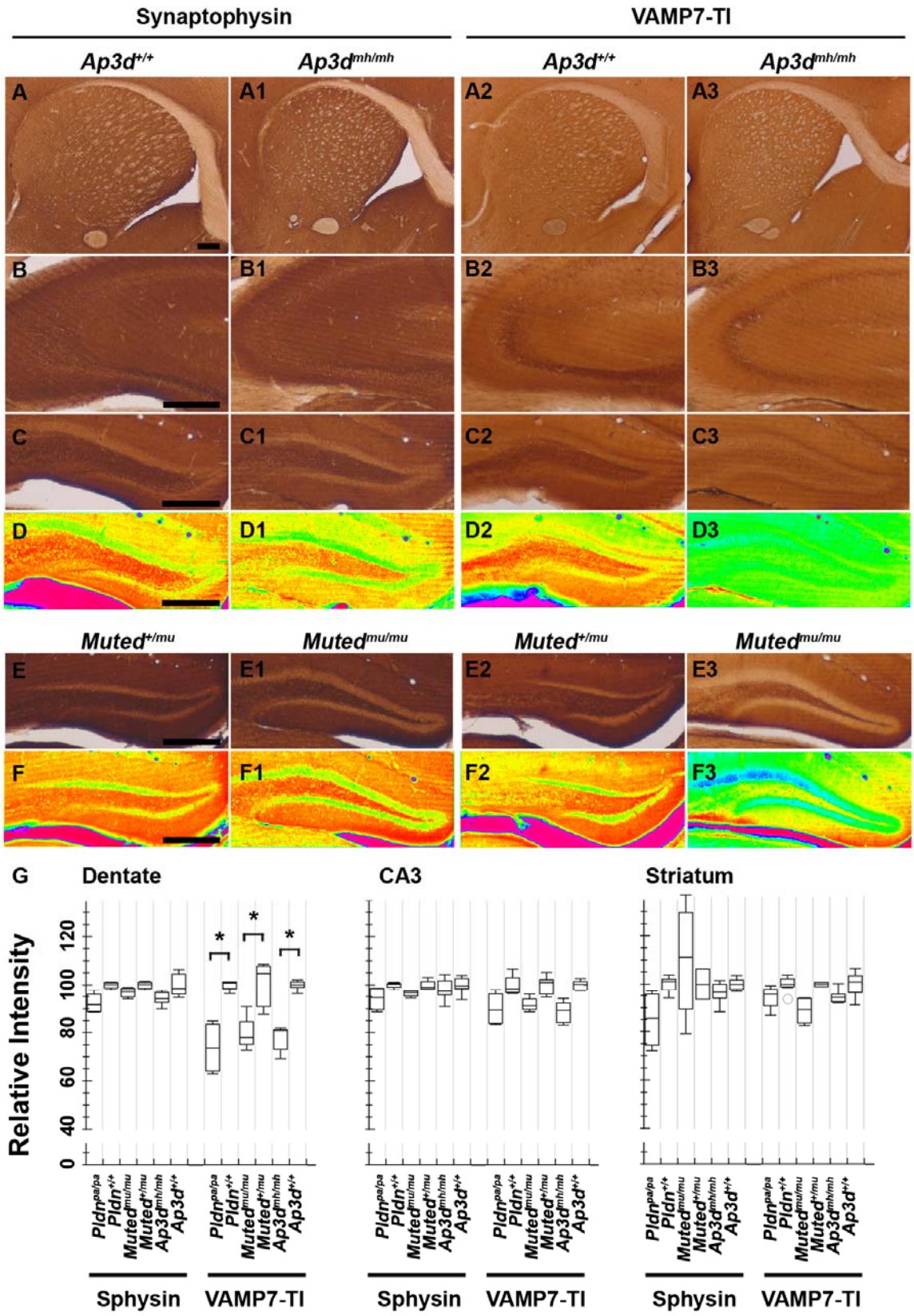
Synaptophysin
VAMP7-TI
Ap3d+/+
Ap3dmh/mh
Ap3d+/+
Ap3dmh/mh
A
A1
A2
A3
B
B1
B2
B3
C
C1
C2
C3
D
D1
D2
D3
Muted+/mu
Mutedmu/mu
Muted+/mu
Mutedmu/mu
E
E1
E2
E3
F
F1
F2
F3
G
Dentate
CA3
Striatum
Relative Intensity
0
40
60
80
100
120
*
*
*
Pldnpa/pa
Pldn+/+
Mutedmu/mu
Muted+/mu
Ap3dmh/mh
Ap3d+/+
Sphysin
VAMP7-TI
Sphysin
VAMP7-TI
Sphysin
VAMP7-TI

Figure 8: Deficiencies of AP-3 and BLOC-1 selectively reduce VAMP7-TI, but not synaptophysin, expression in the dentate gyrus. A-F1) Immunoperoxidase labeling with a monoclonal antibody against synaptophysin in **(A-F)** control (*Ap3d*$^{+/+}$ and *Muted*$^{+/mu}$) and **(A1-F1)** AP-3 and BLOC-1 deficient mouse brain (*Ap3d*$^{mh/mh}$ and *Muted*$^{mu/mu}$) in the **(A-A1)** striatum, **(B-B1)** CA3 region of the hippocampus, and **(C-F1)** the dentate gyrus of the hippocampus. Heat maps of the dentate gyrus are represented in **D-D1** and **F-F1. A2-F3)** Immunoperoxidase labeling with a monoclonal antibody against VAMP7-TI in **(A2-F2)** control (*Ap3d*$^{+/+}$ and *Muted*$^{+/mu}$) and **(A3-F3)** AP-3 and BLOC-1 deficient mouse brain (*Ap3d*$^{mh/mh}$ and *Muted*$^{mu/mu}$) in the **(A2-A3)** striatum, **(B2-B3)** CA3 region of the hippocampus, and **(C2-F3)** the dentate gyrus of the hippocampus. Heat maps of the dentate gyrus are represented in **D2-D3** and **F2-F3. G)** Quantification of Synaptophysin (Sphysin) and VAMP7-TI expression in the dentate gyrus, CA3 pyramidal cell layer of the hippocampus, and the striatum in control (*Pldn*$^{+/+}$, *Muted*$^{+/mu}$, and *Ap3d*$^{+/+}$) and BLOC-1-deficient (*Pldn*$^{pa/pa}$, *Muted*$^{mu/mu}$) and AP-deficient (*Ap3d*$^{mh/mh}$) mouse brain. Synaptophysin is unaffected by either AP-3 or BLOC-1 deficiencies in all brain regions. VAMP7-TI is specifically reduced in the dentate gyrus of the hippocampus in all AP-3 and BLOC-1 deficiencies (*p=0.05, *Muted*$^{mu/mu}$; *p<0.03, *Pldn*$^{pa/pa}$; *p< 0.0007, *Ap3d*$^{mh/mh}$). n = (number of animals/number of vibrotome brain sections), and are listed in the following order *Pldn*$^{pa/pa}$; *Pldn*$^{+/+}$; *Muted*$^{mu/mu}$; *Muted*$^{+/mu}$; *Ap3d*$^{mh/mh}$; *Ap3d*$^{+/+}$. For Sphysin in the dentate gyrus and CA3 region of the hippocampus, n = (2,4); (2,4); (2,4); (2,4); (3,6); (3,8). For VAMP7-TI in the dentate gyrus and CA3 region of the hippocampus, n = (2,4);

(2,4); (2,4); (2,5); (3,6); (3,8). For Sphysin and VAMP7-TI in the striatum, n = (2,4); (2,8); (2,4); (1,2); (3,6); (3,8). All intensity readings were normalized to background intensity of AP-3 immunoreactivity in AP-deficient ($Ap3d^{mh/mh}$) or unstained mouse brain sections. Asterisks mark anatomical location used for quantifications.

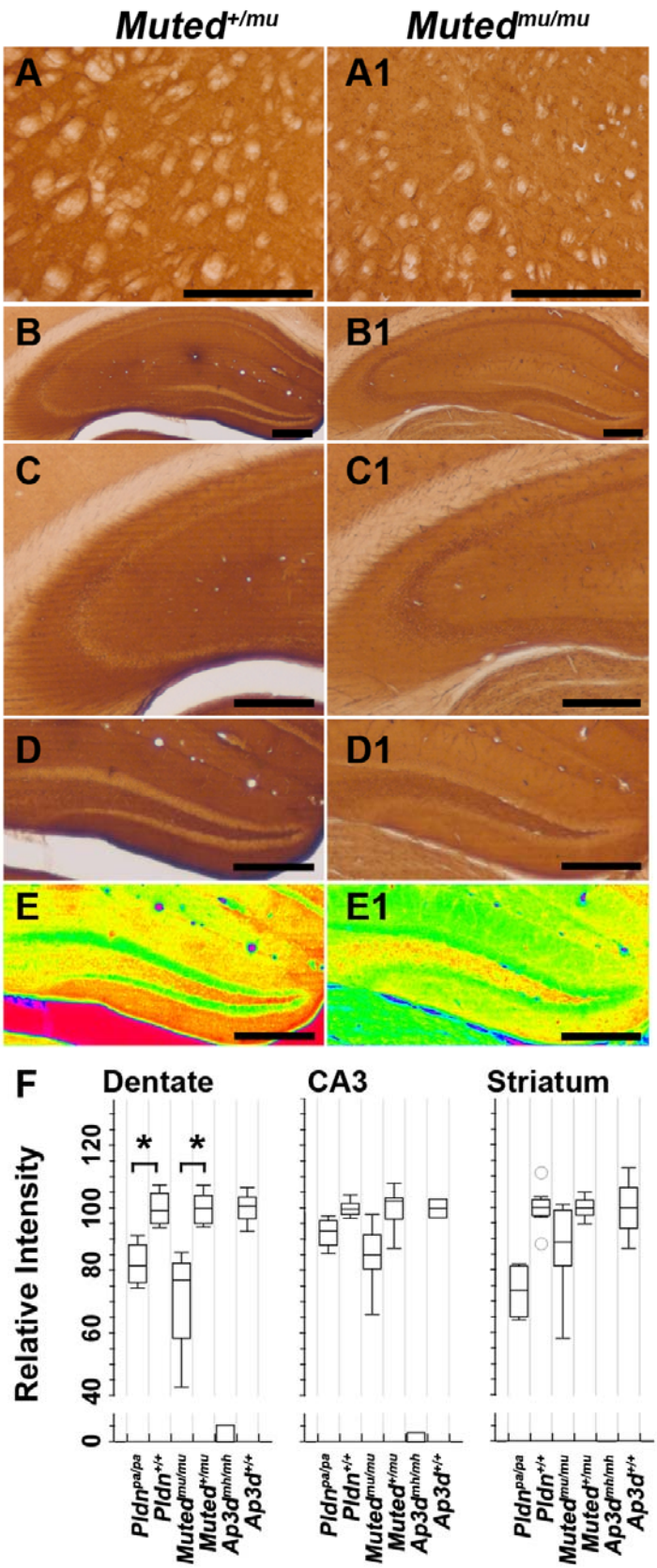
Muted+/mu
Mutedmu/mu
A
A1
B
B1
C
C1
D
D1
E
E1
F
Dentate
CA3
Striatum
Relative Intensity
0
40
60
80
100
120
*
*
Pldnpa/pa
Pldn+/+
Mutedmu/mu
Muted+/mu
Ap3dmh/mh
Ap3d+/+

Figure 9: BLOC-1 deficiencies reduce AP-3 expression in the dentate gyrus. A-E1) Immunoperoxidase labeling of control ($Muted^{+/mu}$) and BLOC-1-deficient ($Muted^{mu/mu}$) mouse brain with the monoclonal antibody against the δ subunit of AP-3 in **(A-A1)** striatum, **(B-B1)** hippocampus, **(C-C1)** CA3 region of the hippocampus, and **(D-D1)** the dentate gyrus of the hippocampus. Heat maps of the dentate gyrus are represented in **E-E1**. **F)** Quantification of AP-3 expression in the dentate gyrus, CA3 pyramidal cell layer of the hippocampus, and the striatum in control ($Pldn^{+/+}$, $Muted^{+/mu}$, and $Ap3d^{+/+}$) and BLOC-1-deficient ($Pldn^{pa/pa}$, $Muted^{mu/mu}$) and AP-deficient ($Ap3d^{mh/mh}$) mouse brain. The relative intensity of AP-3 is significantly decreased in the dentate gyrus (*p<0.004 for $Muted^{mu/mu}$ and p<0.0002 for $Pldn^{pa/pa}$). n = (number of animals/number of vibrotome brain sections), and are listed in the following order $Pldn^{pa/pa}$; $Pldn^{+/+}$; $Muted^{mu/mu}$; $Muted^{+/mu}$; $Ap3d^{mh/mh}$; $Ap3d^{+/+}$. For AP-3 in the dentate gyrus, n = (2,4); (2,8); (4,8); (2,8); (1,2); (1,3). For AP-3 in the CA3 region of the hippocampus, n = (2,4); (2,8); (4,8); (2,8); (1,2); (1,2). For AP-3 in the striatum, n = (2,4); (2,8); (4,8); (2,6); (1,4); (1,4). All intensity readings were normalized to background intensity of AP-3 immunoreactivity in AP-deficient ($Ap3d^{mh/mh}$) or unstained mouse brain sections.

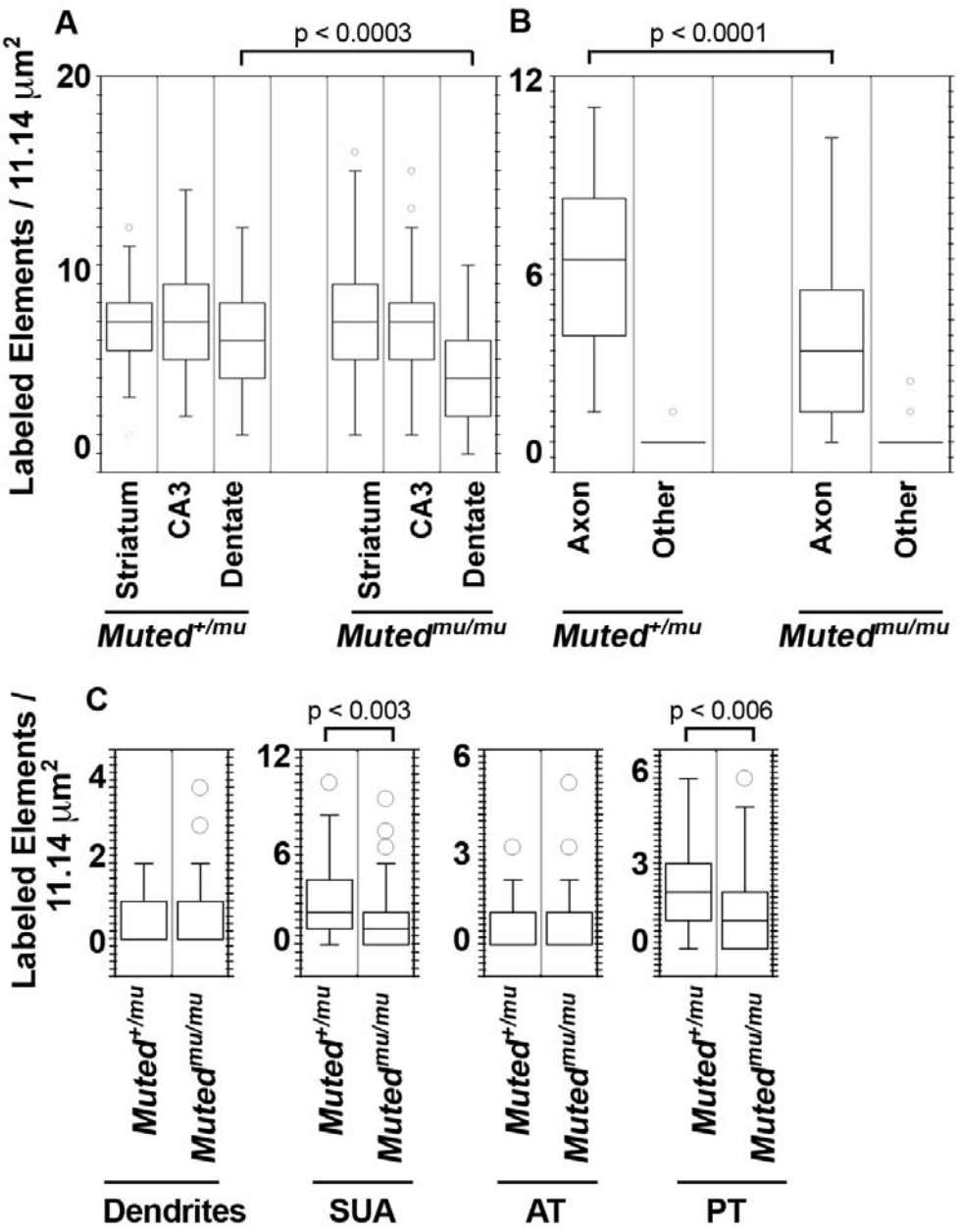

Figure 10: BLOC-1 deficiency reduces axonal AP-3 in the dentate gyrus. Quantification of the number and type of elements immunoreactive for AP-3 per 11.14μm² in electron micrographs of control (*Muted*$^{+/mu}$) and BLOC-1-deficient (*Muted*$^{mu/mu}$) mouse brain. **A)** Total number of AP-3-labeled elements in the striatum, CA3 region of the hippocampus, and the dentate gyrus in

Muted$^{+/mu}$ and *Muted*$^{mu/mu}$ electron micrographs. AP-3 labeling is significantly reduced in the dentate gyrus ($p<0.0003$). **B)** Comparison of axonal AP-3 labeling with labeling in 'other' (glia and unidentifiable) elements in the dentate gyrus of *Muted*$^{+/mu}$ and *Muted*$^{mu/mu}$. BLOC-1 deficiency significantly reduces AP-3 labeling in axons ($p<0.0001$). **C)** AP-3 labeling of dendrites, small unmyelinated axons (SUA), axon terminals (AT), and pre-terminal axons (PT) in the dentate gyrus of *Muted*$^{+/mu}$ and *Muted*$^{mu/mu}$. BLOC-1 deficiency significantly reduces the number of AP-3-labeled SUAs ($p<0.003$) and PTs ($p<0.006$). (n = 2; 52 for *Muted*$^{+/mu}$ striatum; n = 3; 82 for *Muted*$^{mu/mu}$ striatum; n = 2; 37 for *Muted*$^{+/mu}$ CA3; n = 3; 80 for *Muted*$^{mu/mu}$ CA3; n = 2; 47 for *Muted*$^{+/mu}$ dentate gyrus; n = 3, 97 for *Muted*$^{mu/mu}$ dentate gyrus; n = number of animals; number of analyzed 11.14μm^2 electron micrographs)

Supplemental Figures

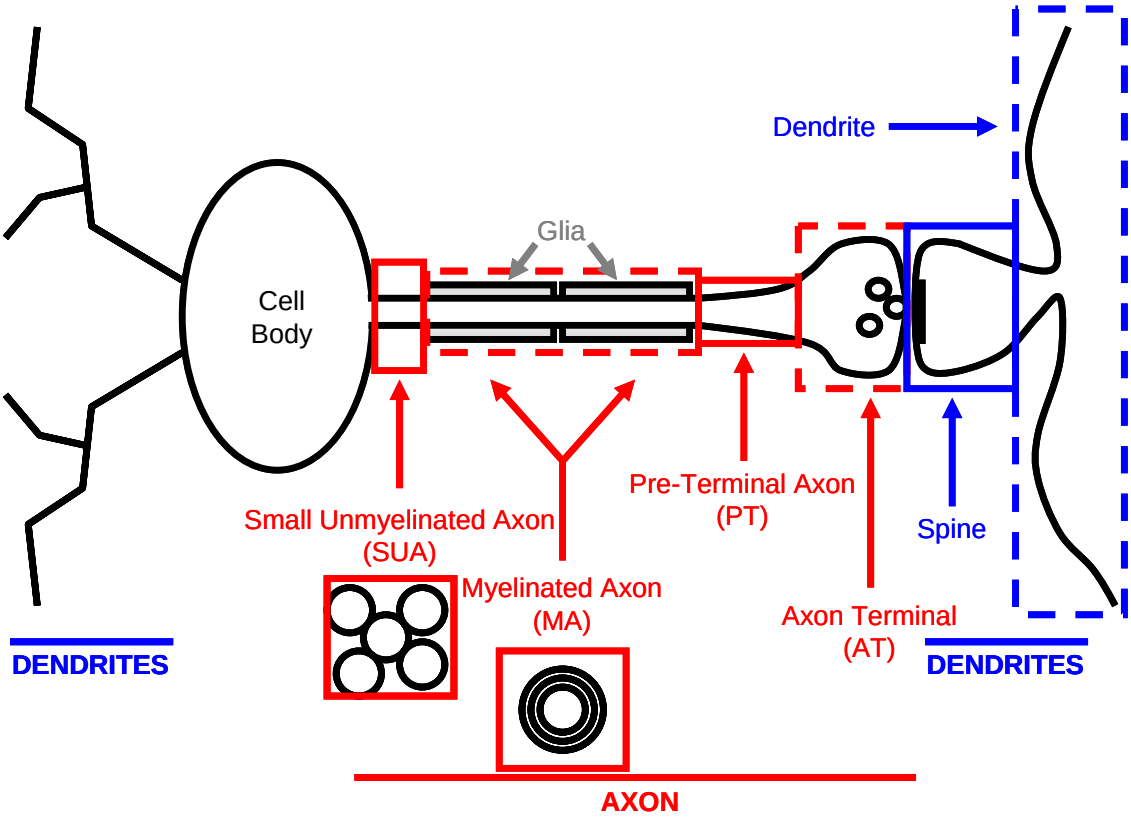

Supplemental Figure 1: Schematic Representation of Identified Elements. In our electron microscopy analyses, we identified the following elements of the central nervous system. The three broad categories are post-synaptic dendrites (blue), pre-synaptic axons (red) and other (grey). Dendrites are classified as either proximal dendrites (dendrite) or spines. Mature spines are characteristically 'mushroom-shaped', and in asymmetric synapses, they display an electron-dense post-synaptic density. Axons are subdivided into pre-terminal axons and axon terminals. Pre-terminal axons include small unmyelinated axons (SUA), myelinated axons (MA), and pre-terminal axons (PT) immediately prior to the axon terminal. As drawn in the insets, small unmyelinated axons are generally cluster into groups with other small

unmyelinated axons. Myelinated axons are wrapped in concentric circles of myelin as depicted in the inset. Axon Terminals (AT) are identified by the presence of synaptic vesicles and the formation of a synapse with a dendrite or dendritic spine. Other elements include glia and unidentifiable structures. Glia include astrocytes and oligodendrocytes (myelin).

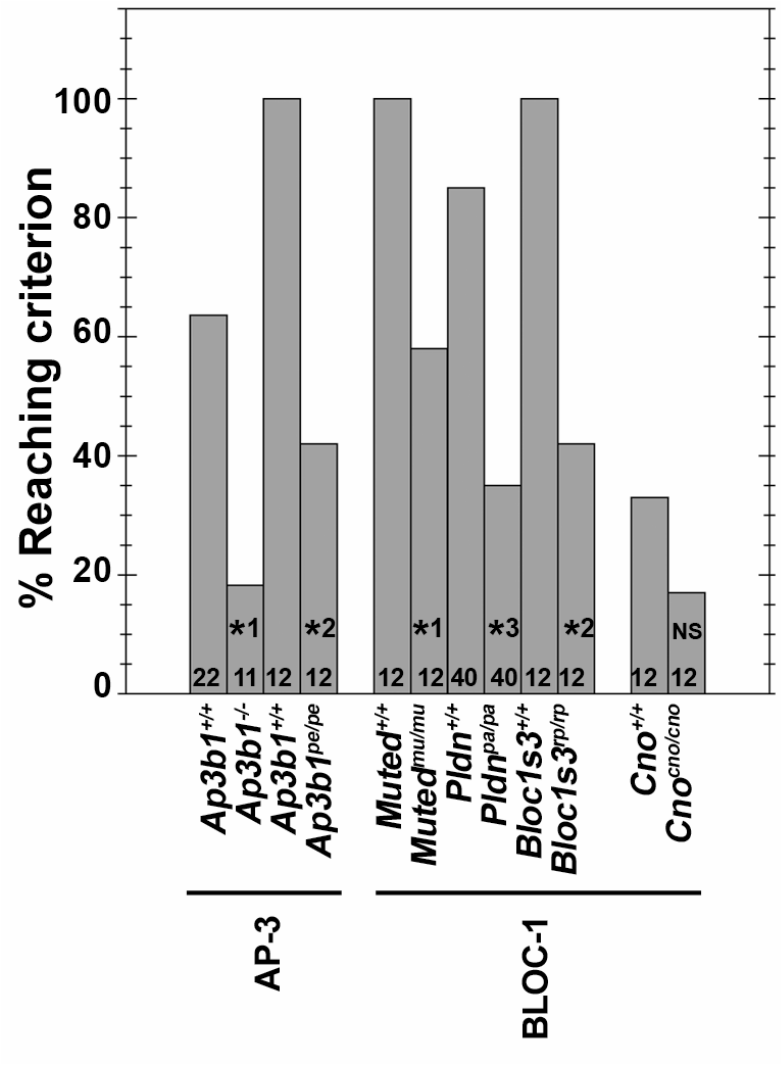

Supplemental Figure 2: Mice deficient for ubiquitous AP-3 or BLOC-1 exhibit motor coordination defects. Ubiquitous AP-3-deficient mice, *Ap3b1*$^{-/-}$ or *pearl* (*Ap3b1*$^{pe/pe}$), significantly fail the rotarod analysis of motor coordination in comparison to their wild type counterparts (*Ap3b1*$^{+/+}$). BLOC-1-deficient mice, *muted* (*Muted*$^{mu/mu}$), *pallid* (*Pldn*$^{pa/pa}$), *reduced pigmentation* (*Bloc1s3*$^{rp/rp}$), and *cappuccino* (*Cno*$^{cno/cno}$), exhibit a similar failure rate in comparison to wild type and controls (*Muted*$^{+/mu}$, *Pldn*$^{+/+}$ and *Pldn*$^{+/pa}$, *Bloc1s3*$^{+/+}$, and *Cno*$^{+/+}$). However, the failure rate of *cappuccino* is not significant. All mice were tested at 1 rpm, except for AP3b1$^{-/-}$ and their

counterpart control mice, which were tested at 3 rpm. Mice are 7-12 weeks of age. Figures at the bottom of the bars represent the number of mice tested. P values *1 $p < 0.05$, *2 $p < 0.005$, *3 $p < 0.0005$, Fisher Exact Test.

CHAPTER IV

DISCUSSION

Karen Newell-Litwa

Synopsis of Findings and Their Significance

The goal of my dissertation was to identify mechanisms that regulate synaptic vesicle composition and size. These two attributes of synaptic vesicles, molecular composition and size, determine the luminal content of neurotransmitter (Edwards, 2007). Despite the profound impact that such mechanisms have for neurotransmission, they currently remain largely unknown (Edwards, 2007). My dissertation research demonstrated that AP-3 and BLOC-1 endosomal sorting mechanisms regulate the molecular architecture of the synapse by influencing both synaptic vesicle content and size.

The Hermansky Pudlak complexes, AP-3 and BLOC-1, regulate sorting from endosomes to lysosomes in non-neuronal cells (Di Pietro and Dell'Angelica, 2005; Newell-Litwa *et al.*, 2007). In addition to a ubiquitous AP-3 isoform that mediates lysosomal biogenesis mechanisms, neurons also contain a neuronal-specific AP-3 isoform that mediates synaptic vesicle biogenesis from endosomes (Danglot and Galli, 2007; Newell-Litwa *et al.*, 2007). In my dissertation, I tested the hypothesis that the machinery involved in the biogenesis of lysosomes, ubiquitous AP-3 and BLOC-1, would also regulate synaptic vesicle composition by competing with neuronal AP-3 for similar cargoes on shared donor early endosomes. The following sections review:

1) the traditional model for endosomal sorting in neurons;
2) the hypothesis of my dissertation, which challenges the traditional model;
3) experimental evidence that supports my hypothesis;
4) the significance of these findings for our understanding of endosomal vesicle traffic in neurons; and finally,

5) untested hypotheses raised by my findings concerning the endosomal mechanisms that underlie synaptic architecture.

Traditional Conception of Endosomal Sorting in Neurons

As discussed in the Introduction (Chapter 1), the current model for endosomal sorting in neurons separates endosomal sorting at the synapse from endosomal sorting at the level of the cell body. This model derives from findings in non-neuronal cells, where endosomal sorting to lysosomes and endosomal sorting to the cell surface through a recycling pathway are both molecularly and spatially distinct. This distinction, when superimposed on neurons, restricts endosomal sorting at the synapse to synaptic vesicle recycling and endosomal sorting in the cell body to lysosomal delivery (Figure 1). These distinct routes are also believed to deliver specific, non-overlapping, cargo populations: lysosomal cargoes to lysosomes, and synaptic vesicle cargoes to synaptic vesicles. As such, only endosomal sorting mechanisms at the synapse should regulate synaptic composition. In summary, the traditional model predicts that:

1) Synaptic vesicle and lysosomal cargoes are sorted from distinct donor early endosomes or distinct sites on donor early endosomes.
2) Synaptic vesicle and lysosomal cargoes are restricted in their interactions with AP-3, such that synaptic vesicle cargoes interact solely with neuronal AP-3 and are sorted to synaptic vesicles, while lysosomal cargoes are sorted by ubiquitous AP-3 to lysosomes.
3) Based on predictions 1 and 2, synaptic vesicle and AP-3-sorted lysosomal cargoes should not significantly co-localize in neuronal cells.

4) Only neuronal AP-3 should significantly regulate synaptic vesicle composition and the molecular composition of the synapse.

Challenges to the Traditional Model

Yet recent proteomes of both AP-3-derived synaptic-like microvesicles and rat brain synaptic vesicles identified lysosomal proteins that either genetically and/or biochemically interact with AP-3 (Salazar *et al.*, 2005b; Takamori *et al.*, 2006). Although at the time, these findings were perplexing (see comment in (Südhof, 2006)), in my dissertation I provided a mechanism that accounts for the presence of lysosomal proteins in synaptic vesicles. These proteomic findings suggested that neuronal AP-3 may be capable of sorting both synaptic vesicle proteins and AP-3-sorted lysosomal cargoes into synaptic vesicles. From these findings, I hypothesized that ubiquitous and neuronal AP-3 sort similar synaptic vesicle and lysosomal cargo from shared donor early endosomes (Figure 2). In contrast with the traditional model, my hypothesis leads to the following predictions:

1) Synaptic vesicle and AP-3-sorted lysosomal cargoes co-reside in shared early endosomes, where they co-localize in 'sorting patches' of the limiting membrane.
2) Ubiquitous and neuronal AP-3 are capable of sorting shared cargoes, both synaptic vesicle and lysosomal. I can biochemically isolate a synaptic vesicle population that contains both synaptic vesicle proteins and AP-3-sorted lysosomal proteins.

3) Synaptic vesicle and AP-3-sorted lysosomal cargoes significantly co-localize in neuronal cells.
4) Both ubiquitous AP-3 and BLOC-1 regulate synaptic vesicle composition.
5) Deficiencies of AP-3, as well as BLOC-1, impact the molecular composition of the synapse.

Experimental Evidence Demonstrates a Competitive Endosomal Sorting Mechanism for Synaptic Vesicle Regulation.

In my dissertation, I have extensively analyzed each of these predictions. Through the following results, I propose a new mechanism for synaptic vesicle biogenesis, whereby both lysosomal sorting pathways and neuronal AP-3-mediated synaptic vesicle biogenesis converge in the regulation of synaptic composition.

Co-localization of cargoes destined for similar vesicles originates in a donor compartment (Chapter 1, Figures 1 and 2). Both AP-3 isoforms sort cargo from donor early endosomes (Chapter 1, Figure 1). Therefore, if these AP-3 isoforms coordinately sort both synaptic vesicle and lysosomal cargo, then I should be able to identify a donor early endosome, where both AP-3-sorted synaptic vesicle and lysosomal cargoes co-localize in 'sorting patches' along the limiting membrane. In Chapter 2, I demonstrate by both kinetic labeling of the endocytic pathway and quantitative immunofluorescence of Rab5Q79L-enlarged early endosomes the existence of a donor early endosome shared by both AP-3-sorted synaptic vesicle and lysosomal cargo (Chapter 2, Figures 2 and 3) (Newell-Litwa *et al.*, 2009). Importantly, these cargoes along with AP-3 co-localize in

'sorting patches' around the limiting membrane of Rab5Q79L-enlarged early endosomes (Chapter 2, Figure 2) (Craige *et al.*, 2008; Newell-Litwa *et al.*, 2009).

If synaptic vesicle and lysosomal cargo are co-sorted to a similar vesicle population, then I should be able to biochemically isolate a synaptic vesicle population that contains both synaptic vesicle proteins and AP-3-sorted lysosomal cargoes. I should note that while AP-3-sorted lysosomal proteins were identified in AP-3-derive synaptic-like microvesicles and synaptic vesicles, these studies did not differentiate between whether these proteins were contained within the same vesicle or where separated to two distinct vesicle populations with similar fractionation profiles (Salazar *et al.*, 2005b; Takamori *et al.*, 2006). Therefore, I used immunomagnetic vesicular isolation to specifically isolate synaptic vesicles by the presence of the synaptic vesicle v-(R)-SNARE VAMP2/synaptobrevin 2. Synaptobrevin 2 is a universally accepted constituent of synaptic vesicles (Schiavo *et al.*, 1992; Hunt *et al.*, 1994). By immunoblot, these VAMP2-containing synaptic vesicles also contain the AP-3-sorted lysosomal proteins, VAMP7-TI, PI4KIIα, and LAMP1 (Chapter 2, Figure 5), demonstrating that both AP-3-sorted lysosomal and synaptic vesicle cargoes are similarly sorted to a synaptic vesicle population (Newell-Litwa *et al.*, 2009).

These biochemical results are further supported by deconvolution immunofluorescent microscopy in diverse neuronal cells, either in primary culture or immortalized cell lines. In fact, deconvolution microscopy of neuroendocrine PC12 cells, mouse neuronal N2a cells, and mouse primary neurons demonstrates co-localization of AP-3-sorted synaptic vesicle and lysosomal cargoes in discrete punctae of the cell body and neuronal processes

(Chapter 2, Figures 1 and 4, data not shown for N2a cells) (Newell-Litwa *et al.*, 2009).

These findings suggested that synaptic vesicle and lysosomal cargoes could be sorted by either AP-3-mediated lysosomal or synaptic vesicle sorting pathways. I tested two critical aspects of this prediction:

1. If ubiquitous AP-3-mediated lysosomal sorting normally sorts synaptic vesicle cargo to a lysosomal fate, then in the absence of ubiquitous AP-3, these cargoes should be increased in synaptic vesicle fractions.
2. Likewise, the absence of neuronal AP-3 should oppositely favor targeting of these same cargoes to a lysosomal route, decreasing their expression in isolated synaptic vesicle fractions.

I tested these predictions using genetic deficiencies that selectively abrogate ubiquitous and neuronal AP-3 isoforms, *Ap3b1*$^{-/-}$ and *Ap3b2*$^{-/-}$. My results from synaptic vesicles isolated from *Ap3b1*$^{-/-}$ and *Ap3b2*$^{-/-}$ mouse brains show that these two AP-3-dependent sorting pathways regulate the synaptic vesicle targeting of overlapping, as well as distinct, cargo populations in a manner predicted by the hypothesis (Chapter 2, Figure 7) (Newell-Litwa *et al.*, 2009). I further challenged my hypothesis that lysosomal sorting machinery regulates synaptic vesicle composition by isolating synaptic vesicles from BLOC-1-deficient *Muted*$^{mu/mu}$ mouse brain. BLOC-1 interacts with AP-3 in mouse primary neurons and shares sorting phenotypes with AP-3 in non-neuronal cells (Chapter 2, Figure 6) (Di Pietro *et al.*, 2006; Salazar *et al.*, 2006; Newell-Litwa *et al.*, 2009; Salazar *et al.*, 2009). Similar to ubiquitous AP-3, BLOC-1 affects the synaptic

vesicle targeting of at least two AP-3-sorted lysosomal cargo, VAMP7-TI and PI4KIIα (Chapter 2, Figure 8) (Newell-Litwa *et al.*, 2009). These results demonstrate that in addition to the clearance of unwanted molecules, lysosomal sorting pathways also regulate the composition of synaptic vesicles through a competitive endosomal sorting mechanism.

Do AP-3 and BLOC-1 synaptic vesicle biogenesis mechanisms affect the molecular architecture of the synapse in brain tissue? Chapter 3 addresses this question through light and electron immuno-microscopy approaches in mouse brain of both AP-3-deficient *mocha*, which lacks both AP-3 isoforms, and two null alleles of BLOC-1 ($Muted^{mu/mu}$ and $Pallidin^{pa/pa}$). These results illustrate that while AP-3 is expressed throughout the brain, it differentially regulates both the molecular composition and morphology of synapses from distinct brain regions. Specifically, AP-3 localizes throughout the brain with prominent expression in both the striatum and hippocampus (Chapter 3, Figure 1). Both AP-3 and the AP-3 lysosomal cargo, VAMP7-TI, co-localize with synaptic vesicle markers, VAMP2/Synaptobrevin or Synaptophysin, in either cultured mouse primary neurons or nerve terminals of the dentate gyrus (Chapter 3, Figure 2; see also, Chapter 2, Figure 4 for further examples of AP-3 and AP-3 cargo co-localizations in mouse primary neurons). By mapping the sub-synaptic distribution of AP-3 by immuno-electron microscopy, I observed that AP-3 primarily localizes to pre-synaptic axons and terminals of both the striatum and hippocampus (CA3 and dentate gyrus) (Chapter 3, Figures 3 and 4). While mouse primary neuron cultures show AP-3 equally distributed to either dendrites or axons (Seong *et al.*, 2005), these results demonstrate that *in vivo* AP-3 displays a more restricted

localization, preferring axonal over dendritic compartments. Additionally, in the majority of AP-3-positive axons, AP-3 only partially labels the axon, suggesting association of AP-3 with a specific subset of synaptic vesicles or precursors of these organelles (Chapter 3, Figures 3 and 4).

Since AP-3 both regulates synaptic vesicle composition (Chapter 2) and primarily localizes to pre-synaptic axons and terminals (Chapter 3), it is uniquely positioned to regulate the molecular composition, and perhaps the morphology, of the pre-synaptic compartment. I experimentally tested the consequences of AP-deficiency to the molecular composition of the synapse, by examining the expression of an AP-3 lysosomal cargo that is also found in synaptic vesicles, VAMP7-TI, in the striatum and hippocampus of wild type and AP-3-deficient *mocha* mouse brains. Immunoreactivity for VAMP7-TI was selectively reduced in the dentate gyrus of *mocha* mouse brain, without affecting the levels of VAMP7-TI in either the CA3 region of the hippocampus or the striatum (Chapter 3, Figure 8). Thus, AP-3 differentially regulates the synaptic composition of distinct brain regions.

The notion that AP-3-dependent mechanisms modulate the composition of synapses in an anatomically restricted manner is further reinforced by my analysis of synapse ultrastructure in different brain regions. I examined whether loss of AP-3 translates into morphological changes in synaptic ultrastructure. Specifically, I performed a double-blind analysis of synaptic vesicle size in asymmetric excitatory synapses of both the striatum and dentate gyrus of wild type and AP-3-deficient *mocha* mouse brain. Similar to brain region-specific effects on synaptic composition, AP-3 deficiency also differentially regulates

synaptic vesicle size across diverse brain regions. Specifically, AP-3-deficient *mocha* mouse brain reduces synaptic vesicle size in the striatum, while it increases synaptic vesicle size in the dentate gyrus (Chapter 3, Figures 5 and 6). I conclude that AP-3-dependent pre-synaptic vesicle biogenesis mechanisms contribute to brain region-specific diversity by altering both the molecular composition and ultrastructure of the synapse.

Despite the fact that AP-3 is expressed throughout the brain, loss of AP-3 uniquely alters synaptic composition of different brain regions. I hypothesized that AP-3-interacting proteins (or protein complexes) could uniquely modify AP-3-dependent function in a brain region-specific manner. As a candidate AP-3 modifier, I chose BLOC-1, a complex that interacts with AP-3 to similarly regulate targeting of AP-3 cargo in both non-neuronal and neuronal cells as demonstrated in Chapter 2 (Di Pietro *et al.*, 2006; Salazar *et al.*, 2006; Newell-Litwa *et al.*, 2009; Salazar *et al.*, 2009). Interestingly, BLOC-1-deficient $Muted^{mu/mu}$ and $Pallidin^{pa/pa}$ mirror AP-3- deficient mouse brain by selectively reducing VAMP7-TI expression within the dentate gyrus (Chapter 3, Figure 8). Could BLOC-1 copy AP-3-deficient vesicle traffic phenotypes (Chapters 2 and 3) by directly regulating AP-3? In fact, loss of BLOC-1 reduces AP-3 expression selectively within the dentate gyrus, similar to its effects on VAMP7-TI (Chapter 3, Figure 9). Furthermore, BLOC-1 alters the sub-synaptic distribution of AP-3 by acutely reducing AP-3 expression in axons of the dentate gyrus, without affecting the distribution of AP-3 in either the striatum or CA3 region of the hippocampus (Chapter 3, Figure 10). Thus, BLOC-1 functions as a brain region-specific

modifier of AP-3 and AP-3-dependent synaptic composition specifically within the dentate gyrus.

Contributions to a New Model of Endosomal Sorting in Neurons

How do these results illuminate the role of endosomal sorting for brain synaptic architecture? First of all, the traditional model of endosomal sorting dissociates ubiquitous AP-3-mediated lysosomal sorting in the cell body from neuronal AP-3-mediated synaptic vesicle biogenesis at nerve terminals (Chapter 4, Figure 1). However, my dissertation demonstrates that the coordinated sorting of these two AP-3-dependent vesicle traffic mechanisms serves to balance the content of synaptic vesicles, and specifically to introduce AP-3-sorted lysosomal proteins into synaptic vesicle fractions (Chapter 2) (Salazar *et al.*, 2005b; Scheuber *et al.*, 2006; Takamori *et al.*, 2006; Newell-Litwa *et al.*, 2009). Thus, the discussion in Chapter 2 introduces a 'see-saw' model, where the two AP-3-dependent sorting pathways act as arms of the see-saw while the shared donor early endosome containing both AP-3-sorted synaptic vesicle and lysosomal cargoes serves as the pivotal fulcrum (Figure 2). When these two AP-3-dependent pathways are in tension with one another for the sorting of similar cargo, then the molecular content of synaptic vesicles is balanced. However, loss of either of these competing pathways upsets this balance by either reducing the synaptic vesicle content, as with loss of neuronal AP-3, or increasing synaptic vesicle content, as with loss of ubiquitous AP-3 or BLOC-1 (Chapter 2, Figures 7 and 8).

By examining multiple AP-3-sorted synaptic vesicle and lysosomal proteins, I was able to identify proteins that preferentially interact with a specific AP-3-dependent sorting pathway versus proteins that are shared by the ubiquitous and neuronal AP-3 adaptor isoforms. Proteins affected by AP-3-dependent sorting include both neurotransmitter and ionic transporters, VGlut1, VGAT, and ZnT3, all of which determine the luminal content of neurotransmitter (Chapter 2, Figures 7 and 8) (Nakatsu *et al.*, 2004; Salazar *et al.*, 2005a; Newell-Litwa *et al.*, 2009). Proteins affected by AP-3 deficiencies also include v-(R)-SNAREs, VAMP2/Synaptobrevin and VAMP7-TI, that regulate synaptic vesicle exocytosis (Chapter 2, Figures 7 and 8) (Scheuber *et al.*, 2006; Newell-Litwa *et al.*, 2009). Interestingly, the synaptic vesicle proteins, VGlut1 and VAMP2/Synaptobrevin, are selectively affected by loss of ubiquitous AP-3-mediated lysosomal sorting, but remain unaltered by neuronal AP-3 deficiency (Chapter 2, Figure 7) (Newell-Litwa *et al.*, 2009). In the final section of my dissertation discussion, I will present a hypothetical model in which BLOC-1 mediates the retrograde delivery of synaptic vesicle proteins to cell body endosomes for lysosomal delivery by ubiquitous AP-3. This model accounts for ubiquitous AP-3-specific effects on synaptic vesicle content as well as the shared synaptic vesicle content of ubiquitous AP-3 and BLOC-1-deficient mice (Chapter 2, compare Figures 7 and 8) (Newell-Litwa *et al.*, 2009).

In addition to the regulation of synaptic vesicle content, my dissertation also revealed the consequences of AP-3 and BLOC-1-mediated pre-synaptic vesicle biogenesis for synaptic composition. Specifically, AP-3 and BLOC-1-mediated pre-synaptic vesicle biogenesis contributes to brain region-specific

diversity through both the molecular composition and morphology of the synapse. In particular, AP-3 differentially regulates VAMP7-TI content at synapses of the striatum and dentate gyrus of the hippocampus (Chapter 3, Figure 8). These differences in pre-synaptic cargo content correspond with morphological differences in the size of synaptic vesicles from the striatum and the dentate gyrus (Chapter 3, Figures 5 and 6). In the final section of my dissertation discussion, I will present the hypothesis that AP-3-mediated differential targeting of cargo to the nerve terminal causes distinct morphological changes in synaptic vesicle size. Intriguingly, BLOC-1 acts as a brain-region specific modulator of the AP-3 sorting function in the dentate gyrus, where it selectively reduces AP-3 expression in axons. This final section will also discuss potential mechanisms by which BLOC-1 may restrict the sub-synaptic localization of AP-3.

Future Questions

The following questions stem from novel findings of my dissertation. Future research aimed at answering these questions would further elucidate how endosomal sorting mechanisms in neurons underlie brain synaptic architecture.

Question #1: Does BLOC-1 at the synapse affect AP-3-dependent sorting to lysosomes?

Hypothesis #1: BLOC-1 mediates the retrograde delivery of synaptic vesicle proteins to the cell body for ubiquitous AP-3-dependent lysosomal delivery.

In Chapter 2, I documented two synaptic vesicle cargo, VGlut1 and VAMP2, whose synaptic vesicle content was specifically altered by ubiquitous AP-3, not neuronal AP-3, deficiency (Chapter 2, Figure 7) (Newell-Litwa *et al.*, 2009). This result demonstrates that certain synaptic vesicle cargoes are regulated by ubiquitous AP-3 through a different mechanism than competitive endosomal sorting with neuronal AP-3. BLOC-1 could account for AP-3-isoform-specific synaptic vesicle effects by favoring the targeting of certain synaptic vesicle cargo to a ubiquitous AP-3-dependent sorting route. Indeed, synaptic vesicle fractions from either ubiquitous AP-3-deficient, *Ap3b1*$^{-/-}$, or BLOC-1-deficient, *Muted*$^{mu/mu}$, mouse brain exhibited similar increased levels of VAMP7-TI in peak synaptic vesicle fractions (Chapter 2, Figures 7 and 8) (Newell-Litwa *et al.*, 2009). However, unlike ubiquitous AP-3, which is restricted to the neuronal cell body (Seong *et al.*, 2005), BLOC-1 is found in pre-synaptic terminals (Talbot *et al.*, 2004; Talbot *et al.*, 2006).

Could this synaptic pool of BLOC-1 contribute to ubiquitous AP-3-dependent sorting? I hypothesize that BLOC-1 functions in both the cell body and synapse to sort synaptic vesicle cargo toward a ubiquitous AP-3-mediated lysosomal sorting route. In the cell body, BLOC-1 would contribute to the competitive sorting of synaptic vesicle proteins, such as VAMP7-TI and PI4KIIα (Chapter 2 Figure 8), so that these proteins reach the lysosome. Alternatively, in the synapse, BLOC-1 would sort specific synaptic vesicle proteins to a retrograde transport vesicle for delivery to the neuronal cell body for ubiquitous AP-3-mediated lysosomal sorting. These hypothetical BLOC-1 retrograde transport vesicles would include synaptic vesicle proteins, such as VGlut1 and VAMP2,

which are sorted into synaptic vesicles by a neuronal AP-3-independent route, and would therefore bypass the competitive endosomal sorting mechanism in the cell body.

In order to best consider this hypothesis, let us examine how BLOC-1 deficiencies would affect synaptic vesicle cargo sorting in the cell body versus synaptic vesicle cargo sorting at the synapse. VAMP7-TI is a lysosomal SNARE that is also found in synaptic vesicles. This SNARE is competitively sorted by ubiquitous AP-3/BLOC-1 and neuronal AP-3 (Chapter 2, Figure 7). In the absence of BLOC-1, VAMP7-TI would be targeted to a neuronal AP-3-dependent pathway and therefore increase in synaptic vesicles. However, despite the fact that VAMP7-TI increases as expected in synaptic vesicles from BLOC-1-deficient mouse brain (Chapter 2, Figure 8), these vesicles fail to reach the synapse since BLOC-1 deficiency prevents entry of AP-3 into axons (Chapter 3, Figure 10). Therefore, VAMP7-TI is decreased in synaptic terminals of BLOC-1-deficient dentate gyrus, but increases in the cell body (Scheuber *et al.*, 2006; Newell-Litwa *et al.*, 2009). However, in the case of VGlut1, a protein that is sorted to synaptic vesicles independent of AP-3, BLOC-1 would function solely in the retrograde delivery of VGlut1 to the cell body. Therefore, BLOC-1 deficiency should increase VGlut1 levels at the synapse. Indeed, brains from schizophrenia patients with reduced levels of the BLOC-1 subunit, dysbindin, exhibit increased levels of VGlut1 in synaptic terminals of the inner molecular layer of the dentate gyrus (Talbot *et al.*, 2004). While I did not observe increased levels of VGlut1 in synaptic vesicle fractions isolated from the whole brain of BLOC-1-deficient mice, this could be because BLOC-1-dependent regulation of VGlut1 expression is

restricted to the dentate gyrus, similar to its effects on VAMP7-TI and AP-3 expression (Chapter 2, Figure 8 and Chapter 3, Figures 8 and 9). However, I did observe BLOC-1 in a complex with VGlut1 in rat brain fractions enriched for nerve terminals (synaptosomes) (Chapter 3, Figure 7).

While tentative, there are several experimental approaches that would be useful in the initial investigation of this hypothesis. First of all, one could determine whether VAMP2, like VGlut1, is similarly increased in synaptic terminals of the dentate gyrus. Furthermore, more detailed mapping of the interactions between BLOC-1 and these proposed retrograde cargoes could facilitate the formation of BLOC-1 point mutations that selectively disrupt retrograde transport activity. Live cell imaging of fluorescent-tagged constructs of VGlut1 in wild type and BLOC-1-deficient mouse primary neurons would show whether VGlut1 experiences retrograde transport and whether this transport is disrupted in the absence of BLOC-1. Likewise overexpression of BLOC-1 should increase VGlut1 retrograde transport, eventually depleting it from nerve terminals. These experiments would ultimately help to determine whether the synaptic pool of BLOC-1 contributes to ubiquitous AP-3-mediated lysosomal sorting.

Question #2: How does AP-3 regulate synaptic vesicle size?

Hypothesis: AP-3-sorted cargoes regulate synaptic vesicle size through membrane composition and luminal content.

In Chapter 3, I demonstrated that AP-3 differentially regulates the size of synaptic vesicles in asymmetric excitatory synapses of the dentate gyrus versus

the striatum. AP-3 deficiency increased the size of synaptic vesicles in the dentate gyrus, while decreasing the size of synaptic vesicles in the striatum (Chapter 3, Figures 5 and 6). One hypothesis that accounts for the brain region-specific differences in AP-3-mediated synaptic vesicle size is that genetic deficiencies in AP-3 expose a previously unrecognized AP-3-dependent sorting of cargoes in a brain-region specific manner. For example, loss of AP-3 differentially affected the expression of the AP-3 cargo, VAMP7-TI, in the dentate gyrus versus the striatum by reducing VAMP7-TI levels in the dentate gyrus without affecting the striatum (Chapter 3, Figure 8). I hypothesize that the differential expression of AP-3 synaptic vesicle cargoes in these two brain regions accounts for changes in synaptic vesicle size. The idea that adaptor protein complexes may influence synaptic vesicle morphology through particular synaptic vesicle cargo is supported by studies where either loss of AP180 or the synaptic vesicle cargo, synaptotagmin, similarly affect synaptic vesicle size (Reist *et al.*, 1998; Zhang *et al.*, 1998; Nonet *et al.*, 1999; Zhang *et al.*, 1999). VAMP7-TI and other AP-3-affected cargo could alter synaptic vesicle size through either membrane composition and curvature or the luminal content of neurotransmitter (Edwards, 2007). AP-3-dependent effects on synaptic vesicle composition most likely result from changes in both membrane and luminal composition, and I will propose AP-3-dependent cargo that may fulfill each of these roles.

An example of an AP-3 cargo that may alter synaptic vesicle size through membrane composition is PI4KIIα. PI4KIIα is a lipid kinase that regulates AP-3 recruitment to membranes and AP-3-mediated vesicle formation from early endosomes (Salazar *et al.*, 2005b; Craige *et al.*, 2008). siRNA-mediated

knockdown of PI4KIIα results in enlarged endosomes (Craige *et al.*, 2008). Importantly, PI4KIIα is reduced in the dentate gyrus of AP-3-deficient *mocha* mouse brain (Salazar *et al.*, 2005b; Salazar *et al.*, 2006), where I observe increased synaptic vesicle size (Chapter 3, Figures 5 and 6). PI4KIIα is capable of regulating membrane composition through both the phosphinositide and protein content, as diverse AP-3 cargoes associate with enlarged endosomes that result from the loss of PI4KIIα (Craige *et al.*, 2008).

In combination with PI4KIIα, AP-3-sorted neurotransmitter and ionic transporters could affect synaptic vesicle size by altering the luminal content of synaptic vesicles. Increased glutamate content in *Drosophila* mutants has been shown to increase synaptic vesicle size rather than the concentration of neurotransmitter (Karunanithi *et al.*, 2002). VGlut1 is an AP-3-sorted glutamate transporter that is increased in larger vesicle fractions of AP-3-deficient *mocha* mouse brain (Salazar *et al.*, 2005a). This altered VGlut1 content could increase glutamate in synaptic vesicles of AP-3-deficient *mocha* mouse brain, resulting in the observed increase of synaptic vesicle size in asymmetric excitatory synapses of the dentate gyrus.

In order to test whether brain region-specific differences in either PI4KIIα, VGlut1 or other AP-3-sorted cargo account for changes in synaptic vesicle size, it would be necessary to compare brain region expression of these proteins in the striatum and dentate gyrus of wild type and AP-3-deficient *mocha* mouse brain as I have demonstrated for VAMP7-TI (Chapter 3, Figure 8). Changes in expression could be measured by the semi-quantitative method that we developed in Chapter 3 to document changes in VAMP7-TI immunoreactivity

levels. Proteins, like VAMP7-TI, that exhibit brain region-specific changes in *mocha* mouse brain could be further evaluated for their contribution to synaptic vesicle size by overexpression or siRNA-mediated knockdown in the neuroendocrine PC12 cell line, which produce synaptic-like microvesicles. Importantly, PC12 cells faithfully reproduce AP-3-dependent phenotypes in mouse brain, are easily transfected, and can be grown in sufficient quantities for biochemical assays (Salazar *et al.*, 2005a; Salazar *et al.*, 2005b; Newell-Litwa *et al.*, 2009). Changes in synaptic vesicle size could be measured by either synaptic vesicle fractionation or immunoelectron microscopy.

Question #3: How does loss of BLOC-1 specifically reduce the levels of AP-3 in axons?

Hypothesis: BLOC-1 modulates microtubule motors, either in their binding or their motor activity, in AP-3-coated vesicles for delivery into axons.

My dissertation research demonstrated that BLOC-1 deficiency specifically reduces AP-3 content in axons of the dentate gyrus (Chapter 3, Figure 10). This is despite the fact that loss of BLOC-1 does not reduce overall levels of AP-3 in the brain (Chapter 2, Supplemental Figure 9) (Newell-Litwa *et al.*, 2009). Nor does BLOC-1 influence the recruitment of AP-3 to membranes (Salazar *et al.*, 2006). Therefore, this specific reduction of AP-3 in axons most likely reflects a redistribution of AP-3 from axons to the cell body. There are two distinct mechanisms by which BLOC-1 could affect the targeting of AP-3 to axons. BLOC-1 could modulate the association of AP-3 with either an axonal kinesin for

anterograde delivery to pre-synaptic axonal compartments or an axonal dynein for retrograde delivery to the cell body. In the first mechanism, BLOC-1 would positively regulate either the interaction of AP-3 with an axonal kinesin or kinesin motor activity in AP-3-coated vesicles. In the second mechanism, BLOC-1 would negatively regulate the association or motor activity of an axonal dynein with AP-3-coated vesicles, leading to their accumulation in pre-synaptic axonal compartments. Importantly, proteomes of AP-3-derived synaptic-like microvesicles or AP-3-interacting proteins reveal several candidate dyneins and kinesins (Salazar *et al.*, 2005b; Salazar *et al.*, 2009). This hypothesis is further supported by ultrastructural evidence for an association between the BLOC-1 subunit, dysbindin, and microtubules in the dentate gyrus (Talbot *et al.*, 2006).

I will illustrate how BLOC-1 may modulate the association of an axonal motor with AP-3 by focusing on kif1Bbeta, an axonal kinesin identified in the AP-3 vesicle proteome (Salazar *et al.*, 2005b). kif1Bbeta regulates the trafficking of synaptic vesicle precursors in neurons (Zhao *et al.*, 2001). I propose that BLOC-1 brings together AP-3 and kif1Bbeta to facilitate the delivery of AP-3-derived pre-synaptic vesicles from the cell body into the axon (Figure 3).

There are multiple experimental approaches that would allow me to address the hypothesis that BLOC-1 brings together AP-3 and the axonal kinesin, kif1Bbeta. Initially, I would want to confirm an interaction between AP-3, BLOC-1 and kif1Bbeta. If BLOC-1 regulates the association of kif1Bbeta, then BLOC-1 deficiencies should either abolish or reduce the levels of AP-3-associated kif1Bbeta. My dissertation has already demonstrated that the use of selective DSP-crosslinking is particularly suited for detecting low affinity adaptor

interactions (Chapter 2, Figure 6 and Chapter 3, Figure 7) (Craige *et al.*, 2008; Newell-Litwa *et al.*, 2009; Salazar *et al.*, 2009). Furthermore, I could disrupt kif1Bbeta microtubule-based transport by using either siRNA-mediated knockdown or expression of dominant negative kif1Bbeta constructs, such as the mutant kif1Bbeta found in Charcot Marie Tooth Disease or kif1Bbeta mutants specific for motor activity (Zhao *et al.*, 2001; Masafumi Matsushita, 2004; Chu *et al.*, 2006). Using either siRNA-mediated knockdown of kif1Bbeta and/or expression of mutant kif1Bbeta in either neuronal cell lines or mouse primary neurons, I could then determine whether loss of kif1Bbeta microtubule-based transport reduces AP-3 expression in axons by immunofluorescence microscopy. This combined biochemical and immunomicroscopy approach should enable me to determine whether BLOC-1 mediates the association of AP-3 and the axonal kinesin, kif1Bbeta, to allow the entry of AP-3 into axons of the dentate gyrus.

An alternative hypothesis for BLOC-1-mediated sub-synaptic distribution of AP-3 is that BLOC-1 serves as a cargo-specific adaptor for AP-3-derived vesicles, and that this BLOC-1-sorted cargo regulates AP-3 entry into axons. In my analysis, BLOC-1 deficiency specifically increases the synaptic vesicle content of VAMP7-TI and PI4KIIα (Chapter 2, Figure 8) (Newell-Litwa *et al.*, 2009). Apart from these cargoes favoring interactions with factors isolated to the neuronal cell body, it is difficult to understand how increases in synaptic vesicle cargo could negatively regulate axonal AP-3. However, BLOC-1 could reduce synaptic vesicle levels of a yet undetermined cargo. It would be interesting to perform a comparative proteomic analysis of AP-3-derived synaptic-like microvesicles in wild-type and BLOC-1-deficient PC12 cells. While potentially

illuminating, this alternative hypothesis lacks a directed rationale that would account for the sub-synaptic distribution of AP-3.

Summary

My dissertation revealed that AP-3 and BLOC-1-mediated endosomal sorting regulates synaptic vesicle composition and size and ultimately result in the unique pre-synaptic composition of diverse brain regions. I initially discovered a competitive endosomal sorting mechanism between ubiquitous AP-3/BLOC-1-mediated lysosomal sorting and neuronal AP-3 synaptic vesicle biogenesis that regulates synaptic vesicle content. This finding demonstrated a previously unknown regulatory function for AP-3-dependent lysosomal sorting in synaptic vesicle composition, in spite of the fact that lysosomal and synaptic vesicle biogenesis pathways have traditionally been viewed as both spatially and functionally segregated. Ultimately, AP-3 and BLOC-1-mediated regulation of synaptic vesicle content results in brain region-specific alterations in synaptic composition and morphology. Specifically, AP-3 deficiency differentially regulated cargo content and synaptic vesicle size between pre-synaptic terminals of the striatum and dentate gyrus of the hippocampus. BLOC-1 specifically regulated AP-3-dependent sorting to pre-synaptic terminals of the dentate gyrus. Thus, while synaptic vesicle biogenesis mechanisms were previously thought to be uniform throughout the brain, I demonstrate that AP-3 and BLOC-1 contribute to diversity in synaptic vesicle biogenesis mechanisms and synaptic composition of diverse brain regions. Importantly, the novel findings of my dissertation contributed to the development of several hypotheses for future

investigation. These hypotheses pertain to the role of BLOC-1 at synapses, molecular mechanisms for AP-3-dependent regulation of synaptic vesicle size, and a potential mechanism for how BLOC-1 determines the sub-synaptic distribution of AP-3.

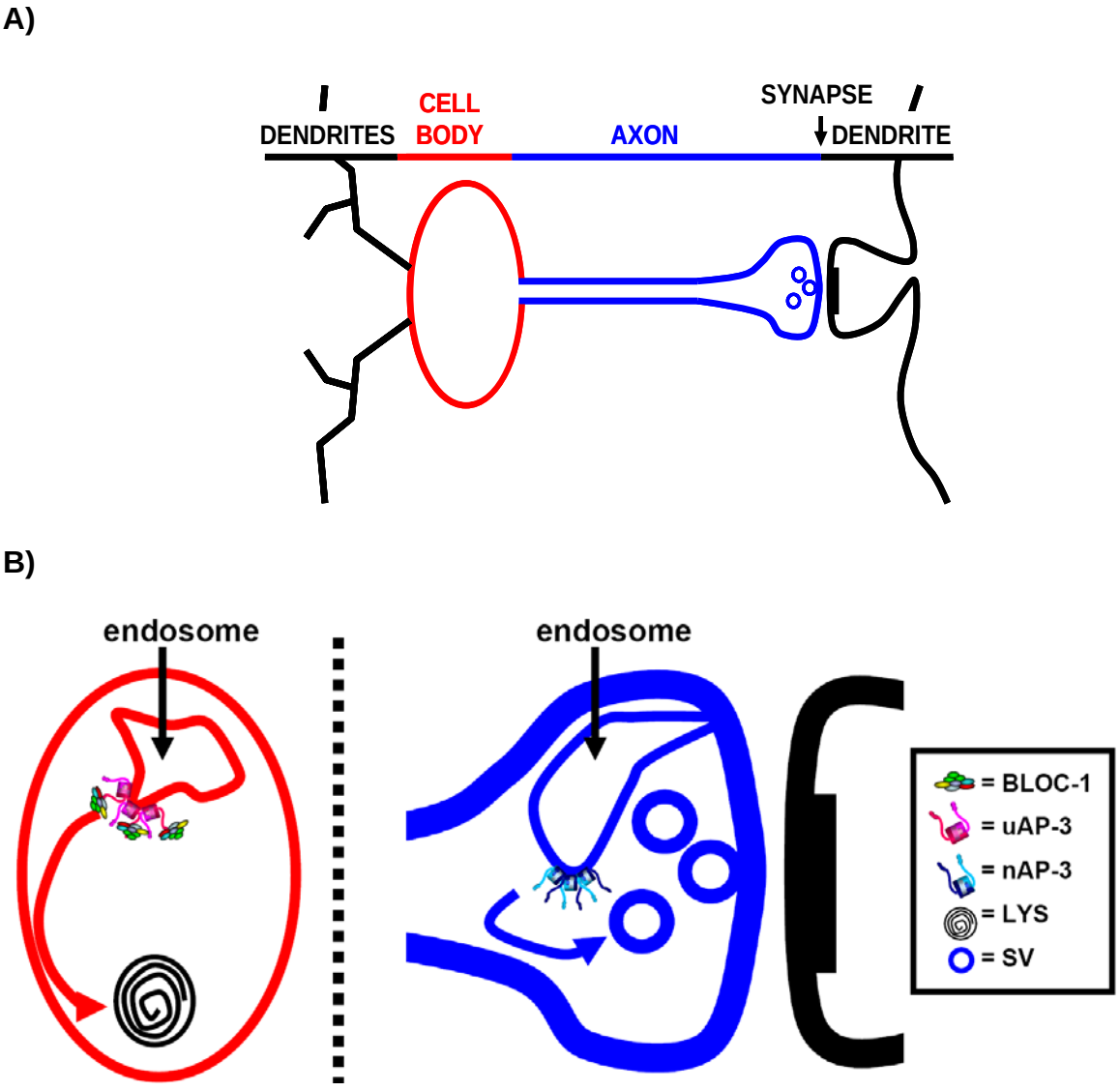

Figure 1: Traditional Model of Endosomal Sorting in Neurons. A) Schematic Representation of Polarized Compartmentalization in neurons into post-synaptic dendrites (black) and pre-synaptic axon (blue) that stem from the neuronal cell body. **B)** A traditional model of endosomal sorting in neurons separates endosomal sorting to lysosomes in the cell body with endosomal sorting to synaptic vesicles in the axon terminal. On the left (red), ubiquitous AP-3 (uAP-3) and BLOC-1 sort cargo from endosomes for delivery to lysosomes (LYS). Both ubiquitous AP-3 and lysosomes are restricted to the cell body (Seong

et al., 2005). In the synapse on the right (blue), neuronal AP-3 (nAP-3) mediates synaptic vesicle (SV) biogenesis from endosomes alongside of AP-2-mediated synaptic vesicle biogenesis from the plasma membrane.

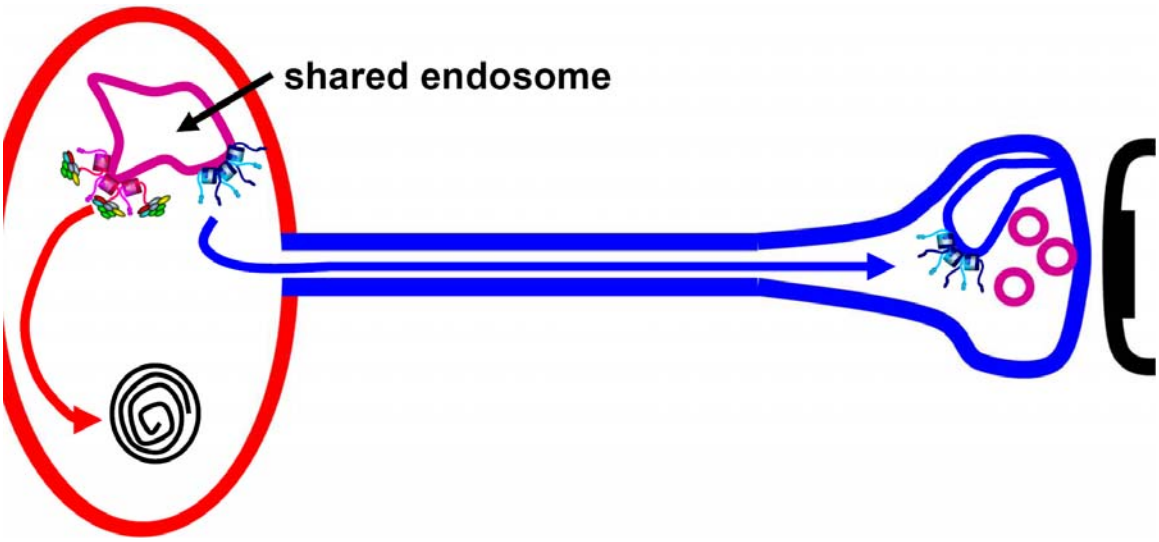

Figure 2: Novel Endosomal Mechanism for Synaptic Regulation in Neurons: The 'See-Saw' Model. Ubiquitous AP-3 and BLOC-1-mediated transport to lysosomes and neuronal AP-3-mediated synaptic vesicle biogenesis converge at the level of shared early endosomes (cell body, purple), where they sort similar synaptic vesicle and lysosomal cargoes. This model allows for the entry of AP-3-sorted lysosomal cargoes into synaptic vesicles (synapse, purple). Furthermore, this model accounts for the regulation of synaptic vesicle content by lysosomal transport factors. AP-3 and BLOC-1-mediated regulation of synaptic vesicle content ultimately underlies the molecular composition and ultrastructure of the synapse. Refer to key in Chapter 4, Figure 1.

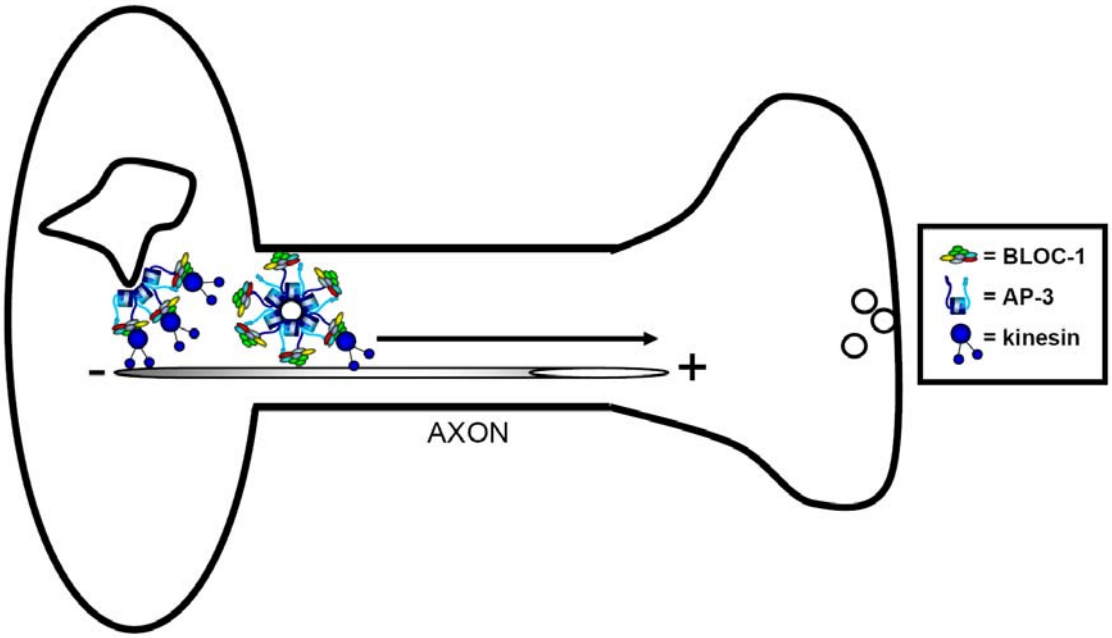

Figure 3: Hypothetical BLOC-1-mediated Association of AP-3 and an Axonal Kinesin. One way that loss of BLOC-1 could diminish the presence of AP-3 in axons is by mediating the interaction of AP-3 and an axonal kinesin. I propose kif1Bbeta as a candidate kinesin for AP-3 axonal transport.

CHAPTER V

REFERENCES

Karen Newell-Litwa

Advani, R.J., Yang, B., Prekeris, R., Lee, K.C., Klumperman, J., and Scheller, R.H. (1999). VAMP-7 mediates vesicular transport from endosomes to lysosomes. J Cell Biol *146*, 765-776.

Alberts, P., Rudge, R., Hinners, I., Muzerelle, A., Martinez-Arca, S., Irinopoulou, T., Marthiens, V., Tooze, S., Rathjen, F., Gaspar, P., and Galli, T. (2003). Cross talk between tetanus neurotoxin-insensitive vesicle-associated membrane protein-mediated transport and L1-mediated adhesion. Mol Biol Cell *14*, 4207-4220.

Antonin, W., Holroyd, C., Fasshauer, D., Pabst, S., Von Mollard, G.F., and Jahn, R. (2000). A SNARE complex mediating fusion of late endosomes defines conserved properties of SNARE structure and function. EMBO J *19*, 6453-6464.

Arantes, R.M., and Andrews, N.W. (2006). A role for synaptotagmin VII-regulated exocytosis of lysosomes in neurite outgrowth from primary sympathetic neurons. J Neurosci *26*, 4630-4637.

Bahr, B.A., and Bendiske, J. (2002). The neuropathogenic contributions of lysosomal dysfunction. J Neurochem *83*, 481-489.

Balla, A., and Balla, T. (2006). Phosphatidylinositol 4-kinases: old enzymes with emerging functions. Trends Cell Biol *16*, 351-361.

Balla, T. (2005). Inositol-lipid binding motifs: signal integrators through protein-lipid and protein-protein interactions. J Cell Sci *118*, 2093-2104.

Baude, A., Nusser, Z., Molnar, E., McIlhinney, R.A.J., and Somogyi, P. (1995). High-resolution immunogold localization of AMPA type glutamate receptor subunits at synaptic and non-synaptic sites in rat hippocampus. Neuroscience *69*, 1031-1055.

Baumert, M., Maycox, P.R., Navone, F., De Camilli, P., and Jahn, R. (1989). Synaptobrevin: an integral membrane protein of 18,000 daltons present in small synaptic vesicles of rat brain. EMBO J *8*, 379-384.

Benson, M.A., Sillitoe, R.V., and Blake, D.J. (2004). Schizophrenia genetics: dysbindin under the microscope. Trends Neurosci *27*, 516-519.
Boehm, M., and Bonifacino, J.S. (2001). Adaptins: the final recount. Mol Biol Cell *12*, 2907-2920.

Bogdanovic, A., Bennett, N., Kieffer, S., Louwagie, M., Morio, T., Garin, J., Satre, M., and Bruckert, F. (2002). Syntaxin 7, syntaxin 8, Vti1 and VAMP7 (vesicle-associated membrane protein 7) form an active SNARE complex for early macropinocytic compartment fusion in Dictyostelium discoideum. Biochem J *368*, 29-39.

Bonifacino, J.S., and Glick, B.S. (2004). The mechanisms of vesicle budding and fusion. Cell *116*, 153-166.

Bonifacino, J.S., and Traub, L.M. (2003). Signals for sorting of transmembrane proteins to endosomes and lysosomes. Annu Rev Biochem *72*, 395-447.

Borner, G.H., Harbour, M., Hester, S., Lilley, K.S., and Robinson, M.S. (2006). Comparative proteomics of clathrin-coated vesicles. J Cell Biol *175*, 571-578.

Bray, N.J., Preece, A., Williams, N.M., Moskvina, V., Buckland, P.R., Owen, M.J., and O'Donovan, M.C. (2005). Haplotypes at the dystrobrevin binding protein 1 (DTNBP1) gene locus mediate risk for schizophrenia through reduced DTNBP1 expression. Hum Mol Genet *14*, 1947-1954.

Breen, G., Prata, D., Osborne, S., Munro, J., Sinclair, M., Li, T., Staddon, S., Dempster, D., Sainz, R., Arroyo, B., Kerwin, R.W., St Clair, D., and Collier, D. (2006). Association of the dysbindin gene with bipolar affective disorder. Am J Psychiatry *163*, 1636-1638.

Burre, J., and Volknandt, W. (2007). The synaptic vesicle proteome. J Neurochem *101*, 1448-1462.

Camargo, L.M., Collura, V., Rain, J.C., Mizuguchi, K., Hermjakob, H., Kerrien, S., Bonnert, T.P., Whiting, P.J., and Brandon, N.J. (2007). Disrupted in Schizophrenia 1 Interactome: evidence for the close connectivity of risk genes and a potential synaptic basis for schizophrenia. Mol Psychiatry *12*, 74-86.

Chen, X.-W., Feng, Y.-Q., Hao, C.-J., Guo, X.-L., He, X., Zhou, Z.-Y., Guo, N., Huang, H.-P., Xiong, W., Zheng, H., Zuo, P.-L., Zhang, C.X., Li, W., and Zhou, Z. (2008). DTNBP1, a schizophrenia susceptibility gene, affects kinetics of transmitter release. J. Cell Biol. *181*, 791-801.

Chu, P.-J., Rivera, J.F., and Arnold, D.B. (2006). A Role for Kif17 in Transport of Kv4.2. J. Biol. Chem. *281*, 365-373.

Ciciotte, S.L., Gwynn, B., Moriyama, K., Huizing, M., Gahl, W.A., Bonifacino, J.S., and Peters, L.L. (2003). Cappuccino, a mouse model of Hermansky-Pudlak syndrome, encodes a novel protein that is part of the pallidin-muted complex (BLOC-1). Blood *101*, 4402-4407.

Clift-O'Grady, L., Desnos, C., Lichtenstein, Y., Faundez, V., Horng, J.T., and Kelly, R.B. (1998). Reconstitution of synaptic vesicle biogenesis from PC12 cell membranes. Methods *16*, 150-159.

Clift-O'Grady, L., Linstedt, A.D., Lowe, A.W., Grote, E., and Kelly, R.B. (1990). Biogenesis of synaptic vesicle-like structures in a pheochromocytoma cell line PC-12. J Cell Biol *110*, 1693-1703.

Cole, T.B., Wenzel, H.J., Kafer, K.E., Schwartzkroin, P.A., and Palmiter, R.D. (1999). Elimination of zinc from synaptic vesicles in the intact mouse brain by disruption of the ZnT3 gene. Proc Natl Acad Sci U S A *96*, 1716-1721.

Conti, F., Defelipe, J., Farinas, I., and Manzoni, T. (1989). Glutamate-positive neurons and axon terminals in cat sensory cortex: A correlative light and electron microscopic study. The Journal of Comparative Neurology *290*, 141-153.

Craige, B., Salazar, G., and Faundez, V. (2004). Isolation of synaptic vesicles. Curr Protoc Cell Biol *Chapter 3*, Unit 3 12.

Craige, B., Salazar, G., and Faundez, V. (2008). Phosphatidylinositol-4-Kinase Type II Alpha Contains an AP-3-sorting Motif and a Kinase Domain That Are Both Required for Endosome Traffic. Mol Biol Cell *19*, 1415-1426.

Daly, C., and Ziff, E.B. (2002). Ca2+-dependent formation of a dynamin-synaptophysin complex: potential role in synaptic vesicle endocytosis. J Biol Chem *277*, 9010-9015.

Danglot, L., and Galli, T. (2007). What is the function of neuronal AP-3? Biol Cell *99*, 349-361.

de Wit, H., Lichtenstein, Y., Geuze, H.J., Kelly, R.B., van der Sluijs, P., and Klumperman, J. (1999). Synaptic vesicles form by budding from tubular extensions of sorting endosomes in PC12 cells. Mol Biol Cell *10*, 4163-4176.

Deinhardt, K., Salinas, S., Verastegui, C., Watson, R., Worth, D., Hanrahan, S., Bucci, C., and Schiavo, G. (2006). Rab5 and Rab7 control endocytic sorting along the axonal retrograde transport pathway. Neuron *52*, 293-305.

Dell'Angelica, E.C., Ohno, H., Ooi, C.E., Rabinovich, E., Roche, K.W., and Bonifacino, J.S. (1997). AP-3: an adaptor-like protein complex with ubiquitous expression. EMBO J *16*, 917-928.

Dell'Angelica, E.C., Shotelersuk, V., Aguilar, R.C., Gahl, W.A., and Bonifacino, J.S. (1999). Altered trafficking of lysosomal proteins in Hermansky-Pudlak syndrome due to mutations in the beta 3A subunit of the AP-3 adaptor. Mol Cell *3*, 11-21.

Di Paolo, G., and De Camilli, P. (2006). Phosphoinositides in cell regulation and membrane dynamics. Nature *443*, 651-657.

Di Pietro, S.M., and Dell'Angelica, E.C. (2005). The cell biology of Hermansky-Pudlak syndrome: recent advances. Traffic *6*, 525-533.

Di Pietro, S.M., Falcon-Perez, J.M., Tenza, D., Setty, S.R., Marks, M.S., Raposo, G., and Dell'Angelica, E.C. (2006). BLOC-1 interacts with BLOC-2 and the AP-3

complex to facilitate protein trafficking on endosomes. Mol Biol Cell *17*, 4027-4038.

Dong, X., Li, H., Derdowski, A., Ding, L., Burnett, A., Chen, X., Peters, T.R., Dermody, T.S., Woodruff, E., Wang, J.J., and Spearman, P. (2005). AP-3 directs the intracellular trafficking of HIV-1 Gag and plays a key role in particle assembly. Cell *120*, 663-674.

Edwards, R.H. (2007). The neurotransmitter cycle and quantal size. Neuron *55*, 835-858.

Falcon-Perez, J.M., Starcevic, M., Gautam, R., and Dell'Angelica, E.C. (2002). BLOC-1, a Novel Complex Containing the Pallidin and Muted Proteins Involved in the Biogenesis of Melanosomes and Platelet-dense Granules. J. Biol. Chem. *277*, 28191-28199.

Faundez, V., Horng, J.T., and Kelly, R.B. (1998). A function for the AP3 coat complex in synaptic vesicle formation from endosomes. Cell *93*, 423-432.

Faundez, V.V., and Kelly, R.B. (2000). The AP-3 complex required for endosomal synaptic vesicle biogenesis is associated with a casein kinase Ialpha-like isoform. Mol Biol Cell *11*, 2591-2604.

Feng, L., Seymour, A.B., Jiang, S., To, A., Peden, A.A., Novak, E.K., Zhen, L., Rusiniak, M.E., Eicher, E.M., Robinson, M.S., Gorin, M.B., and Swank, R.T. (1999). The beta3A subunit gene (Ap3b1) of the AP-3 adaptor complex is altered in the mouse hypopigmentation mutant pearl, a model for Hermansky- Pudlak syndrome and night blindness. Hum. Mol. Genet. *8*, 323-330.

Feng, Y.-Q., Zhou, Z.-Y., He, X., Wang, H., Guo, X.-L., Hao, C.-J., Guo, Y., Zhen, X.-C., and Li, W. (2008). Dysbindin deficiency in sandy mice causes reduction of snapin and displays behaviors related to schizophrenia. Schizophrenia Research *106*, 218-228.

Folsch, H., Ohno, H., Bonifacino, J.S., and Mellman, I. (1999). A novel clathrin adaptor complex mediates basolateral targeting in polarized epithelial cells. Cell *99*, 189-198.

Folsch, H., Pypaert, M., Maday, S., Pelletier, L., and Mellman, I. (2003). The AP-1A and AP-1B clathrin adaptor complexes define biochemically and functionally distinct membrane domains. J Cell Biol *163*, 351-362.

Folsch, H., Pypaert, M., Schu, P., and Mellman, I. (2001). Distribution and function of AP-1 clathrin adaptor complexes in polarized epithelial cells. J Cell Biol *152*, 595-606.

Funke, B., Finn, C.T., Plocik, A.M., Lake, S., DeRosse, P., Kane, J.M., Kucherlapati, R., and Malhotra, A.K. (2004). Association of the DTNBP1 locus with schizophrenia in a U.S. population. Am J Hum Genet *75*, 891-898.

Garner, C.C., and Kindler, S. (1996). Synaptic proteins and the assembly of synaptic junctions. Trends in Cell Biology *6*, 429-433.

Gautam, R., Novak, E.K., Tan, J., Wakamatsu, K., Ito, S., and Swank, R.T. (2006). Interaction of Hermansky-Pudlak Syndrome genes in the regulation of lysosome-related organelles. Traffic *7*, 779-792.

González-Gaitán, M., and Jäckle, H. (1997). Role of Drosophila [alpha]-Adaptin in Presynaptic Vesicle Recycling. Cell *88*, 767-776.

Grill, B., Bienvenut, W.V., Brown, H.M., Ackley, B.D., Quadroni, M., and Jin, Y. (2007). C. elegans RPM-1 regulates axon termination and synaptogenesis through the Rab GEF GLO-4 and the Rab GTPase GLO-1. Neuron *55*, 587-601.

Grote, E., Hao, J.C., Bennett, M.K., and Kelly, R.B. (1995). A targeting signal in VAMP regulating transport to synaptic vesicles. Cell *81*, 581-589.

Guo, J., Wenk, M.R., Pellegrini, L., Onofri, F., Benfenati, F., and De Camilli, P. (2003). Phosphatidylinositol 4-kinase type IIalpha is responsible for the phosphatidylinositol 4-kinase activity associated with synaptic vesicles. Proc Natl Acad Sci U S A *100*, 3995-4000.

Halim, N.D., Weickert, C.S., McClintock, B.W., Hyde, T.M., Weinberger, D.R., Kleinman, J.E., and Lipska, B.K. (2003). Presynaptic proteins in the prefrontal cortex of patients with schizophrenia and rats with abnormal prefrontal development. Mol Psychiatry *8*, 797-810.

Hayashi, M., Raimondi, A., O'Toole, E., Paradise, S., Collesi, C., Cremona, O., Ferguson, S.M., and De Camilli, P. (2008). Cell- and stimulus-dependent heterogeneity of synaptic vesicle endocytic recycling mechanisms revealed by studies of dynamin 1-null neurons. Proceedings of the National Academy of Sciences *105*, 2175-2180.

Heerssen, H., Fetter, R.D., and Davis, G.W. (2008). Clathrin Dependence of Synaptic-Vesicle Formation at the Drosophila Neuromuscular Junction. Current Biology *18*, 401-409.

Heuser, J.E., and Reese, T.S. (1973). Evidence for recycling of synaptic vesicle membrane during transmitter release at the frog neuromuscular junction. J Cell Biol *57*, 315-344.

Honer, W.G., and Young, C.E. (2004). Presynaptic proteins and schizophrenia. Int Rev Neurobiol *59*, 175-199.

Horikawa, H.P., Kneussel, M., El Far, O., and Betz, H. (2002). Interaction of synaptophysin with the AP-1 adaptor protein gamma-adaptin. Mol Cell Neurosci *21*, 454-462.

Howe, C.L., and Mobley, W.C. (2005). Long-distance retrograde neurotrophic signaling. Curr Opin Neurobiol *15*, 40-48.

Hsu, S., Raine, L., and Fanger, H. (1981). Use of avidin-biotin-peroxidase complex (ABC) in immunoperoxidase techniques: a comparison between ABC and unlabeled antibody (PAP) procedures. J. Histochem. Cytochem. *29*, 577-580.

Huang, L., Kuo, Y.-M., and Gitschier, J. (1999). The pallid gene encodes a novel, syntaxin 13-interacting protein involved in platelet storage pool deficiency. Nat Genet *23*, 329-332.

Hunt, J.M., Bommert, K., Charlton, M.P., Kistner, A., Habermann, E., Augustine, G.J., and Betzt, H. (1994). A post-docking role for synaptobrevin in synaptic vesicle fusion. Neuron *12*, 1269-1279.

Ilardi, J.M., Mochida, S., and Sheng, Z.-H. (1999). Snapin: a SNARE-associated protein implicated in synaptic transmission. Nat Neurosci *2*, 119-124.

Kantheti, P., Diaz, M.E., Peden, A.E., Seong, E.E., Dolan, D.F., Robinson, M.S., Noebels, J.L., and Burmeister, M.L. (2003). Genetic and phenotypic analysis of the mouse mutant mh2J, an Ap3d allele caused by IAP element insertion. Mamm Genome *14*, 157-167.

Kantheti, P., Qiao, X., Diaz, M.E., Peden, A.A., Meyer, G.E., Carskadon, S.L., Kapfhamer, D., Sufalko, D., Robinson, M.S., Noebels, J.L., and Burmeister, M. (1998). Mutation in AP-3 [delta] in the mocha Mouse Links Endosomal Transport to Storage Deficiency in Platelets, Melanosomes, and Synaptic Vesicles. Neuron *21*, 111-122.

Karten, B., Campenot, R.B., Vance, D.E., and Vance, J.E. (2006). The Niemann-Pick C1 protein in recycling endosomes of presynaptic nerve terminals. J Lipid Res *47*, 504-514.

Karunanithi, S., Marin, L., Wong, K., and Atwood, H.L. (2002). Quantal Size and Variation Determined by Vesicle Size in Normal and Mutant Drosophila Glutamatergic Synapses. J. Neurosci. *22*, 10267-10276.

Kasprowicz, J., Kuenen, S., Miskiewicz, K., Habets, R.L.P., Smitz, L., and Verstreken, P. (2008). Inactivation of clathrin heavy chain inhibits synaptic recycling but allows bulk membrane uptake. J. Cell Biol. *182*, 1007-1016.

Knable, M.B., Barci, B.M., Webster, M.J., Meador-Woodruff, J., and Torrey, E.F. (2004). Molecular abnormalities of the hippocampus in severe psychiatric illness:

postmortem findings from the Stanley Neuropathology Consortium. Mol Psychiatry *9*, 609-620, 544.

Kobayashi, T., Stang, E., Fang, K.S., de Moerloose, P., Parton, R.G., and Gruenberg, J. (1998). A lipid associated with the antiphospholipid syndrome regulates endosome structure and function. Nature *392*, 193-197.

Krizkova, A., and Vozeh, F. (2004). Development of early motor learning and topical motor skills in a model of cerebellar degeneration. Behavioural Brain Research *150*, 65-72.

Lalli, G., Bohnert, S., Deinhardt, K., Verastegui, C., and Schiavo, G. (2003). The journey of tetanus and botulinum neurotoxins in neurons. Trends Microbiol *11*, 431-437.

Le Borgne, R., Alconada, A., Bauer, U., and Hoflack, B. (1998). The mammalian AP-3 adaptor-like complex mediates the intracellular transport of lysosomal membrane glycoproteins. J Biol Chem *273*, 29451-29461.

Lebrand, C., Corti, M., Goodson, H., Cosson, P., Cavalli, V., Mayran, N., Faure, J., and Gruenberg, J. (2002). Late endosome motility depends on lipids via the small GTPase Rab7. EMBO J *21*, 1289-1300.

Li, W., Rusiniak, M.E., Chintala, S., Gautam, R., Novak, E.K., and Swank, R.T. (2004). Murine Hermansky-Pudlak syndrome genes: regulators of lysosome-related organelles. BioEssays *26*, 616-628.

Li, W., Zhang, Q., Oiso, N., Novak, E.K., Gautam, R., O'Brien, E.P., Tinsley, C.L., Blake, D.J., Spritz, R.A., Copeland, N.G., Jenkins, N.A., Amato, D., Roe, B.A., Starcevic, M., Dell'Angelica, E.C., Elliott, R.W., Mishra, V., Kingsmore, S.F., Paylor, R.E., and Swank, R.T. (2003). Hermansky-Pudlak syndrome type 7 (HPS-7) results from mutant dysbindin, a member of the biogenesis of lysosome-related organelles complex 1 (BLOC-1). Nat Genet *35*, 84-89.

Lichtenstein, Y., Desnos, C., Faundez, V., Kelly, R.B., and Clift-O'Grady, L. (1998). Vesiculation and sorting from PC12-derived endosomes in vitro. Proc Natl Acad Sci U S A *95*, 11223-11228.

Martinez-Arca, S., Rudge, R., Vacca, M., Raposo, G., Camonis, J., Proux-Gillardeaux, V., Daviet, L., Formstecher, E., Hamburger, A., Filippini, F., D'Esposito, M., and Galli, T. (2003). A dual mechanism controlling the localization and function of exocytic v-SNAREs. Proc Natl Acad Sci U S A *100*, 9011-9016.

Masafumi Matsushita, S.T., Norihiro Nakamura, Hiroki Inoue, Hiroshi Kanazawa,. (2004). A Novel Kinesin-Like Protein, KIF1Bβ3 Is Involved

in the Movement of Lysosomes to the Cell Periphery in Non-Neuronal Cells. Traffic *5*, 140-151.

Mirnics, K., Middleton, F.A., Marquez, A., Lewis, D.A., and Levitt, P. (2000). Molecular characterization of schizophrenia viewed by microarray analysis of gene expression in prefrontal cortex. Neuron *28*, 53-67.

Moriyama, K., and Bonifacino, J.S. (2002). Pallidin is a component of a multi-protein complex involved in the biogenesis of lysosome-related organelles. Traffic *3*, 666-677.

Motley, A., Bright, N.A., Seaman, M.N., and Robinson, M.S. (2003). Clathrin-mediated endocytosis in AP-2-depleted cells. J Cell Biol *162*, 909-918.

Mukaetova-Ladinska, E.B., Hurt, J., Honer, W.G., Harrington, C.R., and Wischik, C.M. (2002). Loss of synaptic but not cytoskeletal proteins in the cerebellum of chronic schizophrenics. Neurosci Lett *317*, 161-165.

Mullock, B.M., Smith, C.W., Ihrke, G., Bright, N.A., Lindsay, M., Parkinson, E.J., Brooks, D.A., Parton, R.G., James, D.E., Luzio, J.P., and Piper, R.C. (2000). Syntaxin 7 is localized to late endosome compartments, associates with Vamp 8, and Is required for late endosome-lysosome fusion. Mol Biol Cell *11*, 3137-3153.

Murthy, V.N., and De Camilli, P. (2003). Cell biology of the presynaptic terminal. Annu Rev Neurosci *26*, 701-728.

Nagy, A., and Delgado-Escueta, A. (1984). Rapid preparation of synaptosomes from mammalian brain using nontoxic isoosmotic gradient material (Percoll). J. Neurochem. *43*, 1114-1123.

Nakatsu, F., Okada, M., Mori, F., Kumazawa, N., Iwasa, H., Zhu, G., Kasagi, Y., Kamiya, H., Harada, A., Nishimura, K., Takeuchi, A., Miyazaki, T., Watanabe, M., Yuasa, S., Manabe, T., Wakabayashi, K., Kaneko, S., Saito, T., and Ohno, H. (2004). Defective function of GABA-containing synaptic vesicles in mice lacking the AP-3B clathrin adaptor. J. Cell Biol. *167*, 293-302.

Narayanan, R., Kramer, H., and Ramaswami, M. (2000). Drosophila endosomal proteins hook and deep orange regulate synapse size but not synaptic vesicle recycling. J Neurobiol *45*, 105-119.

Newell-Litwa, K., Salazar, G., Smith, Y., and Faundez, V. (2009). Roles of BLOC-1 and adaptor protein-3 complexes in cargo sorting to synaptic vesicles. Mol Biol Cell *20*, 1441-1453.

Newell-Litwa, K., Seong, E., Burmeister, M., and Faundez, V. (2007). Neuronal and non-neuronal functions of the AP-3 sorting machinery. J Cell Sci *120*, 531-541.

Nie, Z., and Randazzo, P.A. (2006). Arf GAPs and membrane traffic. J Cell Sci *119*, 1203-1211.

Nixon, R.A., Cataldo, A.M., and Mathews, P.M. (2000). The endosomal-lysosomal system of neurons in Alzheimer's disease pathogenesis: a review. Neurochem Res *25*, 1161-1172.

Nonet, M.L., Holgado, A.M., Brewer, F., Serpe, C.J., Norbeck, B.A., Holleran, J., Wei, L., Hartwieg, E., Jorgensen, E.M., and Alfonso, A. (1999). UNC-11, a Caenorhabditis elegans AP180 Homologue, Regulates the Size and Protein Composition of Synaptic Vesicles. Mol. Biol. Cell *10*, 2343-2360.

Norton, N., Williams, H.J., and Owen, M.J. (2006). An update on the genetics of schizophrenia. Curr Opin Psychiatry *19*, 158-164.

Numakawa, T., Yagasaki, Y., Ishimoto, T., Okada, T., Suzuki, T., Iwata, N., Ozaki, N., Taguchi, T., Tatsumi, M., Kamijima, K., Straub, R.E., Weinberger, D.R., Kunugi, H., and Hashimoto, R. (2004). Evidence of novel neuronal functions of dysbindin, a susceptibility gene for schizophrenia. Hum Mol Genet *13*, 2699-2708.

Ohno, H. (2006a). Clathrin-associated adaptor protein complexes. J Cell Sci *119*, 3719-3721.

Ohno, H. (2006b). Physiological roles of clathrin adaptor AP complexes: lessons from mutant animals. J Biochem *139*, 943-948.

Ohno, H., Tomemori, T., Nakatsu, F., Okazaki, Y., Aguilar, R.C., Foelsch, H., Mellman, I., Saito, T., Shirasawa, T., and Bonifacino, J.S. (1999). Mu1B, a novel adaptor medium chain expressed in polarized epithelial cells. FEBS Lett *449*, 215-220.

Ooi, C.E., Dell'Angelica, E.C., and Bonifacino, J.S. (1998). ADP-Ribosylation factor 1 (ARF1) regulates recruitment of the AP-3 adaptor complex to membranes. J Cell Biol *142*, 391-402.

Overly, C.C., and Hollenbeck, P.J. (1996). Dynamic organization of endocytic pathways in axons of cultured sympathetic neurons. J Neurosci *16*, 6056-6064.
Owen, M.J., Craddock, N., and O'Donovan, M.C. (2005). Schizophrenia: genes at last? Trends Genet *21*, 518-525.

Parton, R.G., Simons, K., and Dotti, C.G. (1992). Axonal and dendritic endocytic pathways in cultured neurons. J Cell Biol *119*, 123-137.

Peden, A.A., Oorschot, V., Hesser, B.A., Austin, C.D., Scheller, R.H., and Klumperman, J. (2004). Localization of the AP-3 adaptor complex defines a

novel endosomal exit site for lysosomal membrane proteins. J Cell Biol *164*, 1065-1076.

Pevsner, J., Volknandt, W., Wong, B.R., and Scheller, R.H. (1994). Two rat homologs of clathrin-associated adaptor proteins. Gene *146*, 279-283.

Pryor, P.R., Mullock, B.M., Bright, N.A., Lindsay, M.R., Gray, S.R., Richardson, S.C., Stewart, A., James, D.E., Piper, R.C., and Luzio, J.P. (2004). Combinatorial SNARE complexes with VAMP7 or VAMP8 define different late endocytic fusion events. EMBO Rep *5*, 590-595.

Raiborg, C., Bache, K.G., Gillooly, D.J., Madshus, I.H., Stang, E., and Stenmark, H. (2002). Hrs sorts ubiquitinated proteins into clathrin-coated microdomains of early endosomes. Nat Cell Biol *4*, 394-398.

Raiborg, C., Wesche, J., Malerod, L., and Stenmark, H. (2006). Flat clathrin coats on endosomes mediate degradative protein sorting by scaffolding Hrs in dynamic microdomains. J Cell Sci *119*, 2414-2424.

Ramirez, A., Heimbach, A., Grundemann, J., Stiller, B., Hampshire, D., Cid, L.P., Goebel, I., Mubaidin, A.F., Wriekat, A.L., Roeper, J., Al-Din, A., Hillmer, A.M., Karsak, M., Liss, B., Woods, C.G., Behrens, M.I., and Kubisch, C. (2006). Hereditary parkinsonism with dementia is caused by mutations in ATP13A2, encoding a lysosomal type 5 P-type ATPase. Nat Genet *38*, 1184-1191.

Raposo, G., and Marks, M.S. (2007). Melanosomes--dark organelles enlighten endosomal membrane transport. Nat Rev Mol Cell Biol *8*, 786-797.

Reist, N.E., Buchanan, J., Li, J., DiAntonio, A., Buxton, E.M., and Schwarz, T.L. (1998). Morphologically Docked Synaptic Vesicles Are Reduced in synaptotagmin Mutants of Drosophila. J. Neurosci. *18*, 7662-7673.

Robinson, M.S. (2004). Adaptable adaptors for coated vesicles. Trends Cell Biol *14*, 167-174.

Roos, J., and Kelly, R.B. (1998). Dap160, a neural-specific Eps15 homology and multiple SH3 domain-containing protein that interacts with Drosophila dynamin. J Biol Chem *273*, 19108-19119.

Rous, B.A., Reaves, B.J., Ihrke, G., Briggs, J.A., Gray, S.R., Stephens, D.J., Banting, G., and Luzio, J.P. (2002). Role of adaptor complex AP-3 in targeting wild-type and mutated CD63 to lysosomes. Mol Biol Cell *13*, 1071-1082.

Rubinsztein, D.C. (2006). The roles of intracellular protein-degradation pathways in neurodegeneration. Nature *443*, 780-786.

Ruder, C., Reimer, T., Delgado-Martinez, I., Hermosilla, R., Engelsberg, A., Nehring, R., Dorken, B., and Rehm, A. (2005). EBAG9 Adds a New Layer of Control on Large Dense-Core Vesicle Exocytosis via Interaction with Snapin. Mol. Biol. Cell *16*, 1245-1257.

Sagne, C., and Gasnier, B. (2008). Molecular physiology and pathophysiology of lysosomal membrane transporters. Journal of inherited metabolic disease.

Salazar, G., Craige, B., Love, R., Kalman, D., and Faundez, V. (2005a). Vglut1 and ZnT3 co-targeting mechanisms regulate vesicular zinc stores in PC12 cells. J Cell Sci *118*, 1911-1921.

Salazar, G., Craige, B., Styers, M.L., Newell-Litwa, K.A., Doucette, M.M., Wainer, B.H., Falcon-Perez, J.M., Dell'Angelica, E.C., Peden, A.A., Werner, E., and Faundez, V. (2006). BLOC-1 Complex Deficiency Alters the Targeting of Adaptor Protein Complex-3 Cargoes. Mol. Biol. Cell *17*, 4014-4026.

Salazar, G., Craige, B., Wainer, B.H., Guo, J., De Camilli, P., and Faundez, V. (2005b). Phosphatidylinositol-4-kinase type II alpha is a component of adaptor protein-3-derived vesicles. Mol Biol Cell *16*, 3692-3704.

Salazar, G., Love, R., Styers, M.L., Werner, E., Peden, A., Rodriguez, S., Gearing, M., Wainer, B.H., and Faundez, V. (2004a). AP-3-dependent mechanisms control the targeting of a chloride channel (ClC-3) in neuronal and non-neuronal cells. J Biol Chem *279*, 25430-25439.

Salazar, G., Love, R., Werner, E., Doucette, M.M., Cheng, S., Levey, A., and Faundez, V. (2004b). The zinc transporter ZnT3 interacts with AP-3 and it is preferentially targeted to a distinct synaptic vesicle subpopulation. Mol Biol Cell *15*, 575-587.

Salazar, G., Zlatic, S., Craige, B., Peden, A.A., Pohl, J., and Faundez, V. (2009). Hermansky-Pudlak syndrome protein complexes associate with phosphatidylinositol 4-kinase type II alpha in neuronal and non-neuronal cells. J Biol Chem *284*, 1790-1802.

Salem, N., Faundez, V., Horng, J.T., and Kelly, R.B. (1998). A v-SNARE participates in synaptic vesicle formation mediated by the AP3 adaptor complex. Nat Neurosci *1*, 551-556.

Sato, K., Ernstrom, G.G., Watanabe, S., Weimer, R.M., Chen, C.-H., Sato, M., Siddiqui, A., Jorgensen, E.M., and Grant, B.D. (2009). Differential requirements for clathrin in receptor-mediated endocytosis and maintenance of synaptic vesicle pools. Proceedings of the National Academy of Sciences *106*, 1139-1144.

Saxena, S., Bucci, C., Weis, J., and Kruttgen, A. (2005). The small GTPase Rab7 controls the endosomal trafficking and neuritogenic signaling of the nerve growth factor receptor TrkA. J Neurosci *25*, 10930-10940.

Scheuber, A., Rudge, R., Danglot, L., Raposo, G., Binz, T., Poncer, J.C., and Galli, T. (2006). Loss of AP-3 function affects spontaneous and evoked release at hippocampal mossy fiber synapses. Proc Natl Acad Sci U S A *103*, 16562-16567.

Schiavo, G., Benfenati, F., Poulain, B., Rossetto, O., Polverino de Laureto, P., DasGupta, B.R., and Montecucco, C. (1992). Tetanus and botulinum-B neurotoxins block neurotransmitter release by proteolytic cleavage of synaptobrevin. Nature *359*, 832-835.

Schikorski, T., and Stevens, C.F. (1997). Quantitative Ultrastructural Analysis of Hippocampal Excitatory Synapses. J. Neurosci. *17*, 5858-5867.

Schmidt, A., Hannah, M.J., and Huttner, W.B. (1997). Synaptic-like microvesicles of neuroendocrine cells originate from a novel compartment that is continuous with the plasma membrane and devoid of transferrin receptor. J Cell Biol *137*, 445-458.

Seong, E., Wainer, B.H., Hughes, E.D., Saunders, T.L., Burmeister, M., and Faundez, V. (2005). Genetic Analysis of the Neuronal and Ubiquitous AP-3 Adaptor Complexes Reveals Divergent Functions in Brain. Mol. Biol. Cell *16*, 128-140.

Setty, S.R., Tenza, D., Truschel, S.T., Chou, E., Sviderskaya, E.V., Theos, A.C., Lamoreux, M.L., Di Pietro, S.M., Starcevic, M., Bennett, D.C., Dell'Angelica, E.C., Raposo, G., and Marks, M.S. (2007). BLOC-1 is required for cargo-specific sorting from vacuolar early endosomes toward lysosome-related organelles. Mol Biol Cell *18*, 768-780.

Setty, S.R.G., Tenza, D., Sviderskaya, E.V., Bennett, D.C., Raposo, G., and Marks, M.S. (2008). Cell-specific ATP7A transport sustains copper-dependent tyrosinase activity in melanosomes. Nature *454*, 1142-1146.

Skibinski, G., Parkinson, N.J., Brown, J.M., Chakrabarti, L., Lloyd, S.L., Hummerich, H., Nielsen, J.E., Hodges, J.R., Spillantini, M.G., Thusgaard, T., Brandner, S., Brun, A., Rossor, M.N., Gade, A., Johannsen, P., Sorensen, S.A., Gydesen, S., Fisher, E.M., and Collinge, J. (2005). Mutations in the endosomal ESCRTIII-complex subunit CHMP2B in frontotemporal dementia. Nat Genet *37*, 806-808.

Sorkin, A. (2004). Cargo recognition during clathrin-mediated endocytosis: a team effort. Curr Opin Cell Biol *16*, 392-399.

Stepp, J.D., Huang, K., and Lemmon, S.K. (1997). The yeast adaptor protein complex, AP-3, is essential for the efficient delivery of alkaline phosphatase by the alternate pathway to the vacuole. J Cell Biol *139*, 1761-1774.

Stobrawa, S.M., Breiderhoff, T., Takamori, S., Engel, D., Schweizer, M., Zdebik, A.A., Bosl, M.R., Ruether, K., Jahn, H., Draguhn, A., Jahn, R., and Jentsch, T.J. (2001). Disruption of ClC-3, a chloride channel expressed on synaptic vesicles, leads to a loss of the hippocampus. Neuron *29*, 185-196.

Straub, R.E., Mayhew, M., Vakkalanka, R., Kolachana, B., Goldberg, T.E., Egan, M.F., and Weinberger, D.R. (2005). MUTED (6p24.3), a protein that binds to dysbindin (DTNBP1, 6p22.3), is strongly associated with schizophrenia and exhibits statistical epistasis with COMT. *Neuropsychopharmacology*, S1-S270.

Styers, M.L., Salazar, G., Love, R., Peden, A.A., Kowalczyk, A.P., and Faundez, V. (2004). The endo-lysosomal sorting machinery interacts with the intermediate filament cytoskeleton. Mol Biol Cell *15*, 5369-5382.

Südhof, T.C. (2006). Synaptic Vesicles: An Organelle Comes of Age. Cell *127*, 671-673.

Sugimoto, H., Sugahara, M., Folsch, H., Koide, Y., Nakatsu, F., Tanaka, N., Nishimura, T., Furukawa, M., Mullins, C., Nakamura, N., Mellman, I., and Ohno, H. (2002). Differential recognition of tyrosine-based basolateral signals by AP-1B subunit mu1B in polarized epithelial cells. Mol Biol Cell *13*, 2374-2382.

Swedlow, J.R., Sedat, J.W., and Agard, D.A. (eds.) (1997). Deconvolution in optical microscopy. Academic Press: San Diego, CA.

Sweeney, N.T., Brenman, J.E., Jan, Y.N., and Gao, F.B. (2006). The coiled-coil protein shrub controls neuronal morphogenesis in Drosophila. Curr Biol *16*, 1006-1011.

Takamori, S., Holt, M., Stenius, K., Lemke, E.A., Gronborg, M., Riedel, D., Urlaub, H., Schenck, S., Brugger, B., Ringler, P., Muller, S.A., Rammner, B., Grater, F., Hub, J.S., De Groot, B.L., Mieskes, G., Moriyama, Y., Klingauf, J., Grubmuller, H., Heuser, J., Wieland, F., and Jahn, R. (2006). Molecular anatomy of a trafficking organelle. Cell *127*, 831-846.

Talbot, K., Cho, D.S., Ong, W.Y., Benson, M.A., Han, L.Y., Kazi, H.A., Kamins, J., Hahn, C.G., Blake, D.J., and Arnold, S.E. (2006). Dysbindin-1 is a synaptic and microtubular protein that binds brain snapin. Hum Mol Genet *15*, 3041-3054.

Talbot, K., Eidem, W.L., Tinsley, C.L., Benson, M.A., Thompson, E.W., Smith, R.J., Hahn, C.G., Siegel, S.J., Trojanowski, J.Q., Gur, R.E., Blake, D.J., and Arnold, S.E. (2004). Dysbindin-1 is reduced in intrinsic, glutamatergic terminals of the hippocampal formation in schizophrenia. J Clin Invest *113*, 1353-1363.

Theos, A.C., Tenza, D., Martina, J.A., Hurbain, I., Peden, A.A., Sviderskaya, E.V., Stewart, A., Robinson, M.S., Bennett, D.C., Cutler, D.F., Bonifacino, J.S., Marks, M.S., and Raposo, G. (2005). Functions of adaptor protein (AP)-3 and AP-1 in tyrosinase sorting from endosomes to melanosomes. Mol Biol Cell *16*, 5356-5372.

Thiele, C., Hannah, M.J., Fahrenholz, F., and Huttner, W.B. (2000). Cholesterol binds to synaptophysin and is required for biogenesis of synaptic vesicles. Nat Cell Biol *2*, 42-49.

Tian, J.-H., Wu, Z.-X., Unzicker, M., Lu, L., Cai, Q., Li, C., Schirra, C., Matti, U., Stevens, D., Deng, C., Rettig, J., and Sheng, Z.-H. (2005). The Role of Snapin in Neurosecretion: Snapin Knock-Out Mice Exhibit Impaired Calcium-Dependent Exocytosis of Large Dense-Core Vesicles in Chromaffin Cells. J. Neurosci. *25*, 10546-10555.

Tippens, A.L., and Lee, A. (2007). Caldendrin, a neuron-specific modulator of Cav/1.2 (L-type) Ca2+ channels. J Biol Chem *282*, 8464-8473.
Toshio Kosaka, K.I. (1983). Possible temperature-dependent blockage of synaptic vesicle recycling induced by a single gene mutation in <I>drosophila</I>. Journal of Neurobiology *14*, 207-225.

Traub, L.M. (2003). Sorting it out: AP-2 and alternate clathrin adaptors in endocytic cargo selection. J Cell Biol *163*, 203-208.

Voglmaier, S.M., Kam, K., Yang, H., Fortin, D.L., Hua, Z., Nicoll, R.A., and Edwards, R.H. (2006). Distinct endocytic pathways control the rate and extent of synaptic vesicle protein recycling. Neuron *51*, 71-84.

Vogt, K., Mellor, J., Tong, G., and Nicoll, R. (2000). The actions of synaptically released zinc at hippocampal mossy fiber synapses. Neuron *26*, 187-196.

Wade, N., Bryant, N.J., Connolly, L.M., Simpson, R.J., Luzio, J.P., Piper, R.C., and James, D.E. (2001). Syntaxin 7 complexes with mouse Vps10p tail interactor 1b, syntaxin 6, vesicle-associated membrane protein (VAMP)8, and VAMP7 in b16 melanoma cells. J Biol Chem *276*, 19820-19827.

Ward, D.M., Pevsner, J., Scullion, M.A., Vaughn, M., and Kaplan, J. (2000). Syntaxin 7 and VAMP-7 are soluble N-ethylmaleimide-sensitive factor attachment protein receptors required for late endosome-lysosome and homotypic lysosome fusion in alveolar macrophages. Mol Biol Cell *11*, 2327-2333.

White, I.J., Bailey, L.M., Aghakhani, M.R., Moss, S.E., and Futter, C.E. (2006). EGF stimulates annexin 1-dependent inward vesiculation in a multivesicular endosome subpopulation. EMBO J *25*, 1-12.

Yang, W., Li, C., Ward, D.M., Kaplan, J., and Mansour, S.L. (2000). Defective organellar membrane protein trafficking in Ap3b1-deficient cells. J Cell Sci *113*, 4077-4086.

Zhang, B., Ganetzky, B., Bellen, H.J., and Murthy, V.N. (1999). Tailoring Uniform Coats for Synaptic Vesicles during Endocytosis. Neuron *23*, 419-422.

Zhang, B., Koh, Y.H., Beckstead, R.B., Budnik, V., Ganetzky, B., and Bellen, H.J. (1998). Synaptic Vesicle Size and Number Are Regulated by a Clathrin Adaptor Protein Required for Endocytosis. Neuron *21*, 1465-1475.

Zhang, Q., Li, W., Novak, E.K., Karim, A., Mishra, V.S., Kingsmore, S.F., Roe, B.A., Suzuki, T., and Swank, R.T. (2002). The gene for the muted (mu) mouse, a model for Hermansky-Pudlak syndrome, defines a novel protein which regulates vesicle trafficking. Hum. Mol. Genet. *11*, 697-706.

Zhao, C., Takita, J., Tanaka, Y., Setou, M., Nakagawa, T., Takeda, S., Yang, H.W., Terada, S., Nakata, T., Takei, Y., Saito, M., Tsuji, S., Hayashi, Y., and Hirokawa, N. (2001). Charcot-Marie-Tooth Disease Type 2A Caused by Mutation in a Microtubule Motor KIF1B[beta]. Cell *105*, 587-597.

Zhen, L., Jiang, S., Feng, L., Bright, N.A., Peden, A.A., Seymour, A.B., Novak, E.K., Elliott, R., Gorin, M.B., Robinson, M.S., and Swank, R.T. (1999). Abnormal expression and subcellular distribution of subunit proteins of the AP-3 adaptor complex lead to platelet storage pool deficiency in the pearl mouse. Blood *94*, 146-155.

Zimmermann, H., and Denston, C.R. (1977). Recycling of synaptic vesicles in the cholinergic synapses of the torpedo electric organ during induced transmitter release. Neuroscience *2*, 695-714.